TÉCNICO LISBOA

Recycling of Li-ion batteries from Electric Vehicles

Melissa Bacatelo Guerra Martins Costa

Thesis to obtain the Master of Science Degree in

Materials Engineering

Supervisor: Prof. Dr. Fernanda Maria Ramos da Cruz Margarido

Co-Supervisor: Dr. Carlos Alberto Gonçalves Nogueira

Examination Committee

Chairperson: Prof. Pedro Miguel Gomes Abrunhosa Amaral

Supervisor: Prof. Dr. Fernanda Maria Ramos da Cruz Margarido

Members of the Committee: Prof Rui Costa Neto

November 2018

Page intentionally left blank

Acknowledgements

I am grateful to everyone who has directly or indirectly contributed to the development of this work.

First of all, I would like to express my gratitude to my supervisor Professor Fernanda Margarido, for her guidance that began even before I started to work on this thesis and for being always available to help me every step of the way with her knowledge and support.

To my co-supervisor, Professor Carlos Nogueira, for his active participation in the experimental work and help throughout the interpretation of the results.

To Professor Rui Neto, for guiding me specially in the initial stage of the practical work, when I needed the most, and for his careful revision and availability throughout this thesis.

To Professor Manuel Francisco, for his knowledge, availability and interest in this study.

To the entire team from the Center for Innovation, Technology and Policy Research–IN+ and Laboratório Nacional de Energia e Geologia (LNEG), for they have provided a friendly and supportive working atmosphere.

To Valorcar, for providing the lithium-ion batteries used in this study.

I would also like to thank my thesis companion, Francisco Capucha, for his constant support throughout the entire work and to Francisco Paulo for helping me with a technical design.

Finally, I would like to thank my mom and Fernando for everything, because that is the only word that could sum it all.

Page intentionally left blank

Resumo

A reciclagem de baterias de iões de lítio (iões-Li) tem atraído atenção por motivos económicos e ambientais devido ao crescimento do número de veículos elétricos, o que contribui para um aumento da quantidade destas baterias. O objetivo deste trabalho foi caracterizar físico-quimicamente as baterias de iões-Li usadas num veículo elétrico híbrido, contribuindo para uma melhor definição do seu processo de reciclagem. Foi proposto um procedimento para efetuar o descarregamento e desmantelamento seguro de um módulo destas baterias. A caracterização das células incluiu o balanço mássico dos componentes e a análise elementar, identificação de fases e morfologia dos elétrodos. Efetuou-se também o processamento hidrometalúrgico das baterias e a receita orçamental dos metais recuperados foi avaliada. Os elétrodos, constituídos por Li (1.1%), Ni (5.7%), Co (1.0%), Cu (17.1%) e Al (6.1%), correspondem a 60% do peso das células. Os restantes componentes são peças metálicas (21%), componentes plásticos (11%) e eletrólito (9%). A difração de raios-X permitiu identificar a grafite no material anódico e, juntamente com a análise elementar, a bateria foi classificada como óxido de lítio níquel cobalto alumínio (NCA). A morfologia do material ativo do ânodo e cátodo mostrou uma morfologia das partículas do tipo euédrico e esférico, respetivamente. As melhores condições de lixiviação, para um rácio L/S de 20L/Kg e uma temperatura de 60ºC, foram atingidas após 1 h de lixiviação, utilizando 0.5 M H_2SO_4 com $Na_2S_2O_5$ visto que se obteve uma recuperação total dos metais Li, Ni e Co, minimizando a solubilização do Al e Cu (15% e 0.005% respetivamente). A receita orçamental foi de 678 €/tonelada.

Palavras-chave: Baterias de iões de lítio, reciclagem, lixiviação, procedimento de descarga

Page intentionally left blank

Abstract

Recycling of spent lithium-ion batteries (LIBs) has attracted significant attention from an economical and environmental perspective due to the increasing number of electric vehicles, contributing to a growing amount of LIBs entering the waste stream. The present work aimed at the physicochemical characterization of spent LIBs, contributing for a better definition of their recycling process. A procedure for a safe discharge and disassembly of a LIB module used in a hybrid electric vehicle was proposed. The characterization of the battery's cells included the components' mass balance and the elemental analysis, phase identification and morphology of the electrodes. Additionally, the hydrometallurgical extraction of metals and revenue of the recovered elements was evaluated. The electrodes containing Li (1.1%), Ni (5.7%), Co (1.0%), Cu (17.1%) and Al (6.1%) correspond to 60% of the cell's weight. The remaining components are the metallic parts (21%), the plastic components (11%) and the electrolyte (9%). In the X-ray powder diffraction, the graphite phase was identified in the anodic material and together with the elemental analyses, the battery was categorized as lithium nickel cobalt aluminium oxide (NCA). The morphology of the anodic and cathodic active material showed an euedric and spherical morphology of the particles, respectively. The best leaching conditions with a fixed L/S ratio of 20 L/kg and a leaching temperature of 60ºC were achieved after 1 h of leaching using 0.5M H_2SO_4 with 0.1M $Na_2S_2O_5$ as the recovery of Li, Ni and Co was about 100% while the Al and Cu yield was around 15% and 0.005%, respectively. The expected revenue was 678 €/ton.

Keywords: lithium-ion batteries, recycling, leaching, discharge procedure

Page intentionally left blank

Table of Contents

Acknowledgements ... **iii**

Resumo ... **v**

Abstract ... **vii**

Table of Contents ... **ix**

List of figures ... **xii**

List of Tables ... **xv**

List of Acronyms ... **xvii**

Chapter 1. Introduction ... **1**

1.1. Context and problem definition ... 1

1.2. Solution objectives and research questions ... 2

1.3. Publications ... 3

1.4. Document structure ... 3

Chapter 2. State of the Art ... **5**

2.1. Fossil fuel vehicles - Issues ... 5

2.2. Electric vehicles – Solution? ... 8

2.2.1. EVs mechanism ... 9

2.2.2. Types of Electric Vehicles ... 9

2.2.2.1. Hybrid Electric Vehicles ... 10

2.2.2.2. Plug-in Hybrid Electric Vehicles ... 13

2.2.2.3. Full Electric Vehicles ... 15

2.2.2.4. Comparative assessment ... 16

2.3. Battery requirements in EVs ... 17

2.4. Expected LIB growth in the market demand and need for recycling ... 19

2.5. Review of LIB ... 20

2.5.1. Basic operation in a Li-ion rechargeable battery ... 21

2.5.2. Constitution of LIB ... 23

2.5.2.1. Chemically active compounds of LIBs ... 25

2.5.2.2. Elements present in a typical LIB ... 27

2.6. Recycling techniques for LIBs ... 29

2.6.1. Deactivation ... 31

2.6.1.1. Discharge 31
2.6.1.2. Thermal pre-treatment 32
2.6.1.3. Freezing of the electrolyte 33
2.6.2. Dismantling and mechanical treatment 33
2.6.2.1. Disassembly 33
2.6.2.2. Mechanical treatment 34
2.6.2.3. Problems with deactivation and dismantling of LIB 36
2.6.3. Pyrometallurgical processes 36
2.6.4. Hydrometallurgical processes 37
2.6.4.1. Leaching 37
2.6.4.2. Impurities and purification 38
2.6.4.3. Electrochemical processes 38
2.6.4.4. Solvent extraction 38
Chapter 3. Experimental Methodology 39
3.1. LIB discharge 40
3.2. LIB disassembly 42
3.3. Materials balance of components 43
3.4. Chemical characterization 43
3.4.1. Phase identification (XRPD) 43
3.4.2. Elemental chemical analysis (AAS) 44
3.4.3. Morphological and chemical characterization (SEM/EDS) 46
3.5. Leaching tests 47
Chapter 4. Results and Discussion 49
4.1. Discharge 49
4.2. Disassembly 50
4.3. Materials balance of components 53
4.4. Phase and chemical characterization 56
4.4.1. Phase identification (XRPD) 56
4.4.2. Elemental chemical analysis (AAS) 57
4.4.3. Morphological and chemical characterization (SEM/EDS) 60
4.5. Leaching tests 63
4.6. LIB recycling profitability critical analysis 67

Chapter 5. Conclusions and Future Work 71

5.1. Recommendations for future developments..... 72

References 73

Appendix A..... 81

Appendix B..... 82

Appendix C..... 83

Appendix D..... 84

List of figures

Figure 1 - Diagram of energy conversion in an internal combustion engine. Adapted from [14]. 5

Figure 2 - Fossil fuel reserves-to-production ratios at end 2015. Adapted from [23]. 6

Figure 3 – Total CO_2 emissions from 1750 to 2010. Data from [25]. 7

Figure 4 – Historical crude oil prices [28]. 7

Figure 5 – Sources of EU crude oil imports (2015) [28]. 8

Figure 6 – Rechargeable battery EV [33]. 9

Figure 7 – Types of electric vehicles. Based on [32, 35]. 9

Figure 8 – Types of electric vehicles considering performance features. Based on [32, 36]. 10

Figure 9 - Schematic diagram for series and parallel HEVs configurations [32]. 10

Figure 10 - Performance characteristics of a typical electric motor for traction [35]. 11

Figure 11 – Series PHEV design [40]. 13

Figure 12 - Parallel PHEV design [40]. 14

Figure 13 – PHEV battery SOC during operational modes, including charge, standby, charge-depletion operation, and charge-sustaining operation [32]. 15

Figure 14 - Process diagram of a typical FEV. Adapted from [35]. 16

Figure 15 – A comparison of the engine and battery capacity in electric vehicles [41]. 17

Figure 16 – Projection of total worldwide Li demand from 2017 to 2025. Based on [42]. 19

Figure 17 – Forecast consumption of lithium by first use, 2016-2031 (000t LCE) [44]. 19

Figure 18 – Projected market for LIB used in EV from 2012 to 2020. Based on [45]. 20

Figure 19 - Types of batteries and classification of the LIBs as secondary batteries. Based on [47]... 20

Figure 20 - Power (acceleration) and energy (range) by battery type [3]. 21

Figure 21 - Schematic illustration of the fundamental operating principle of a LIB in the discharged (a) and in the charged state (b) [7]. 22

Figure 22 – Schematic illustration of inside a typical LIB [47]. 23

Figure 23 – Composition of a typical LIB, in weight percentage of the total battery cell. Based on [46, 49]. 24

Figure 24 - Major innovations in material technology: past, existing and expected battery chemistries. Based on [7]. 25

Figure 25 - Comparison of the dimensions among the four principal LIB technologies for EVs. Based on [53]. 26

Figure 26 – LIB cell composition range, in weight %. 27

Figure 27 – Typical LIB module composition range, in weight %. 28

Figure 28 – Economic importance and supply risk of 2017 criticality assessment of Li, Ni, Cu, Al, Mn, Fe (non-critical raw materials represented by the blue dots) and Co (critical raw material represented by the red dot). Adapted from [43, 55] 28

Figure 29 - Schematic presentation of the circular economy. Based on [11]. 29

Figure 30 - Possible destinations for LIB waste. Based on [49]. 29

Figure 31 – Value chain for electric vehicle batteries [53]. 30

Figure 32 – Unit operations in battery recycling and their possible combinations to establish efficient recycling process routes. Based on [57]. 31

Figure 33 - Reactions and gas formation during electrolysis of a sodium chloride and a sodium hydroxide dissolution [57]. 32

Figure 34 - Components of a battery system [54]. 33

Figure 35 - Air classification in recycling processes for LIBs using a zigzag classifier; typical light and heavyweight fractions are shown [54]. 35

Figure 36 - Experimental methodology. 39

Figure 37 – Projection view of the LIB module used. 40

Figure 38 – Representation of the used electric circuit in the discharging of the LIB. 40

Figure 39 – Followed discharging procedure. 41

Figure 40 - Followed disassembly process. 42

Figure 41 - Disassembly of the battery cells. 43

Figure 42 – XRPD sample preparation followed procedure. 43

Figure 43 - Followed spectroanalytical procedure. 45

Figure 44 – Cathodic and anodic samples (“P” and “T”) analysed by SEM. 46

Figure 45 - Followed leaching procedure. 47

Figure 46 - Main components of the HEV battery system used after disassembly. 50

Figure 47 – Solvents in contact with the polymer. 52

Figure 48 – Mechanical lathe used to separate the components (4) and (4a). 53

Figure 49 - Schematic drawing of the Li-ion battery cell constitution. 53

Figure 50 - Components arrangement and details of the electrodes in the cylindrical cells. 54

Figure 51 – Average measured dimensions of the cell components B1 to B7. 55

Figure 52 - Comparison between the obtained values of weight (%) of the cell components with the referenced values. 56

Figure 53 - XRPD patterns (CuKα radiation without filter) of electrodic material and phase identification: a – anode; b – cathode 57

Figure 54 – Constitution of the studied LIB module, cell and electrodes (%w/w). 59

Figure 55 - SEM micrograph of anodic material (“T” sample type) of spent LIB, and EDS spectra of two different phases. 60

Figure 56 - SEM micrograph of anodic material (“P” sample type) of spent LIB. 61

Figure 57 - SEM micrograph of cathodic material (“T” sample type) of spent LIB, and EDS spectra of three different phases. 62

Figure 58 - SEM micrograph of cathodic material (“P” sample type) of spent LIB using BSE. 62

Figure 59 - Dissolution of different metals from spent LIBs with the leaching time using different additives. Leaching conditions: L/S: 20 L/kg; leaching temperature: 60ºC. The meaning of the defined nomenclature can be found on Figure 45. 65

Figure 60 – Acid and/or reducer nature effect on the leaching efficiency of the cathodic and anodic material. Leaching conditions: L/S: 20 L/kg; leaching time: 4 h; leaching temperature: 60ºC. 66

List of Tables

Table 1 – Research questions associated with each objective. 2

Table 2 – Balance of the chemical elements in the general combustion equation (1) [15]. 5

Table 3 - Comparison of technical characteristics of electric vehicles [35]. 16

Table 4 – Lithium-ion battery cell components and respective functions. Based on [3, 46, 49]. 24

Table 5 – Specifications of the lithium-ion batteries modules used. 39

Table 6 – Wavelength and standards concentration used in AAS for Li, Ni, Co, Cu, Al and Mn. 45

Table 7 - Measured current in the wire and operating voltage for a given oil heater power and time and comparison between the measured open circuit voltage and the calculated open circuit voltage. 49

Table 8 –Identification of the main components of the HEV battery system used. 51

Table 9 – Identification of the solvents used in an attempt to dissolve the polymer. 52

Table 10 - Materials mass balance of the main components of the cells of lithium-ion batteries. 55

Table 11 - Elemental chemical composition (%w/w) of the electrode materials. 58

Table 12 – Chemical composition (%w/w) per cell and per lithium-ion battery module and its comparison with the reported values (see Figure 26 and Figure 27). 59

Table 13 – Experimental standardized weight of Li, Ni, Co and Al elements and its conversion. 60

Table 14 – Indices information. 68

Table 15 – Revenue estimation of the recycling of a NCA battery based on the commodity market prices of the elements, the mass of each element per tonne of LIB module and the recycling efficiencies obtained from scenario 1 and 2. The prices were taken from [73, 74, 75]. 69

Table 16 - EU policy measure and description in the context of oil import dependency [28]. 81

Table 17 - Comparison of specific performance targets for HEV, PHEV and FEV. Based on [32]. 82

Table 18 – Composition of typical spent LIB cells (weight %) [52] 83

Table 19 – Reported elemental and material concentrations (mass %) in LIB modules samples (complete battery) [49]. 83

Page intentionally left blank

List of Acronyms

AAS	Atomic absorption spectrometry	**LIBs**	Lithium ion batteries
BMS	Battery management system	**LMO**	Lithium-manganese spinel
BMU	Battery management unit	**LNEG**	Laboratório Nacional de Energia e Geologia
EI	Economic importance	**NCA**	Lithium-nickel-cobalt-aluminium
EOL	End-of-life	**NiMH**	Nickel-metal hydride
EPBA	European Portable Battery Association	**NMC**	Lithium nickel-manganese-cobalt oxide
EPR	Extended Producer Responsibility	**PHEV**	Plug-in hybrid electric vehicle
EU	European Union	**SEI**	Solid electrolyte interphase
EV	Electric vehicles	**SOC**	State-of-charge
FCV	Fuel cell vehicle	**SR**	Supply risk
FEV	Full electric vehicle	**V_{oc}**	Open circuit voltage
GHG	Global greenhouse gas	**XRPD**	X-ray powder diffraction
HEV	Hybrid electric vehicle		
HVAC	Heating/ventilation/air conditioning		
ICE	Internal combustion engine		
L/S	Liquid/solid ratio		
LCE	Lithium carbonate equivalent		
LCO	Lithium cobalt oxide		
LFP	Lithium-iron phosphate		

Chemical Compounds:

C_6H_{14}	Hexane	H_2SO_4	Sulfuric acid
C_7H_8	Toluene	NaOH	Sodium hydroxide
CH_2Cl_2	Dichloromethane	NH_3	Ammonia
$CHCl_3$	Chloroform	PC	Propylene carbonate
$C_2H_4Cl_2$	1,2- Dichloroethane	PVDF	Polyvinylidene fluoride
CH_3CN	Acetonitrile		
$(C_2H_5)_2O$	Diethyl ether		
$C_4H_8O_2$	Ethyl acetate		
CH_3OH	Methanol		
C_2H_6OH	Ethanol		
C_3H_6O	Acetone		
$C_4H_8O_2$	1,4-Dioxane		
C_3H_8O	1-propanol		
C_2H_6OS	Dimethyl sulfoxide		
C_3H_8O	2-Propanol		
C_3H_7NO	Dimethylformamide		
$C_2H_5NO_3$	2-Nitroethanol		
EC	Ethylene carbonate		
EGDME	Ethylene glycol dimethyl ether		
H_3PO_4	Orthophosphoric acid		
HCl	Hydrochloric acid		
HF	Hydrofluoric acid		
HNO_3	Nitric acid		

Chapter 1. Introduction

1.1. Context and problem definition

The present economy based on fossil fuels is at risk due to several factors including the continuous increase in the oil demand and in the carbon dioxide emissions, contributing to the climate change, the depletion of non-renewable resources and the dependency on politically unstable oil producing countries. As the transport sector consumes about 27% of energy demand, mandatory emission reduction targets for new vehicles were set by the European Union (EU) legislation and the manufactures were given additional incentives to produce vehicles with extremely low emissions. A possible solution to this problem is to significantly increase the amount of clean energy sources, in particular, by replacing internal combustion engine (ICE) vehicles with ideally zero emission vehicles, i.e. electric vehicles (EVs), or at least with controlled emission vehicles such as hybrid electric vehicles (HEVs) [1, 2].

A closer look at these technologies will lead to one of the crucial components of EVs, the batteries, which are the energy source for traction and the main challenge to overcome. Currently, lithium-ion batteries (LIBs) are the most suitable technology for electric vehicles as they can output high energy and power per unit of battery mass while having a higher-energy efficiency compared to other rechargeable batteries [3].

In fact, the LIB industry has been growing exponentially due to the widespread application of these batteries in EVs and therefore the number of spent LIBs is currently increasing sharply, which creates the need to handle these batteries in a proper way. To maintain a sustainable battery production, spent LIBs must be appropriately dealt with to guarantee their safe disposal and also to recycle their valuable metals (e.g. Cu, Co, Al) and the Li they contain, which has no foreseen substitute in EV applications and might encounter supply risks, which could impact significantly the adoption of some energy technologies [4, 5].

However, the recycling of LIBs is a complex task. This is mainly due to the wide variety of materials in each cell, which makes the separation of the material mix a challenge, and because of the broad range of different cell designs and chemical compositions of the active materials, specially the cathode, which hinder the development of a standardized recycling method [6, 7, 8]. Additionally, there are safety concerns regarding the deactivation and dismantling of LIBs that must be addressed [9]. Nowadays industrial recycling processes of LIBs are mostly pyrometallurgical and as such energy and cost intensive [10]. The challenge is to recover the mentioned metals without sacrificing the economics of the recycling process and hence move towards a circular economy [11].

A procedure for a safe discharge and disassembly of LIBs used in HEVs will be studied, followed by a physical and chemical characterization of the battery cells, and more thoroughly of the electrodes as they contain the elements with a higher economical metal value, which revenue will also be calculated. Finally, the hydrometallurgical extraction of metals from spent LIBs will be investigated.

1.2. Solution objectives and research questions

This thesis has four main objectives:

1. Propose a safe discharge and dismantling procedure for spent LIBs for EVs since safety is a crucial issue when handling end-of-life management of these batteries;
2. Obtain a physical and chemical characterization of spent LIBs in order to contribute for a better definition of the recycling process of these spent products;
3. Compare alternative leaching approaches of the metals contained in the electrode materials, namely using different acids and reducing agents in order to evaluate the leaching behaviour aiming at the development of hydrometallurgical recycling solutions;
4. Estimate the revenue of the recovered materials present in the electrodes to have a preliminary indication of the economic impact of the recycling process.

The experimental work was developed in Instituto Superior Técnico (IST) and in cooperation with Laboratório Nacional de Energia e Geologia (LNEG), using as a case study spent lithium-ion battery modules from a hybrid electric vehicle provided by Valorcar, a non-profit private organization licensed to manage the integrated system of end-of-life vehicles management, in line with the Extended Producer Responsibility (EPR) goals.

Considering the main objectives, the development of the work presented in this thesis was guided by the following research questions presented in Table 1.

Table 1 – Research questions associated with each objective.

Objective Number	Related Research Questions
1	**a)** Which are the main safety problems associated with the discharge of LIBs and what causes them? **b)** Which are the possible solutions to these problems? **c)** How can the solutions found be implemented in the industrial recycling process?
2	**a)** What is the weight contribution of each cell component? **b)** Which phases are present in the electrodic material of the LIB? **c)** Which metals are present in the electrodic material and what is their weight percentage? **d)** What type of battery was provided? **e)** What is the morphology of the active electrode materials?
3	**a)** Which are the conditions that maximize the extraction of metals from the LIBs?
4	**a)** Is it profitable to recycle the LIBs at an industrial scale?

1.3. Publications

The work developed in this thesis resulted in a publication, indicated below, which is in submission.

M. Bacatelo, R. Costa Neto, C.A.Nogueira, F.Margarido, M.F.C. Pereira. “Safe disassembly procedure and characterisation of spent lithium-ion batteries from hybrid electric vehicles”, *Waste Management*, 2018.

1.4. Document structure

This thesis is composed of five chapters.

In Chapter 1, the introduction to the topic addressed is presented and the main objectives of this thesis are listed.

In Chapter 2, a literature review is presented in order to contextualize the theme and introduce the studies and conclusions already done. It starts by presenting the problems associated with fossil fuel vehicles and addresses the reasons behind the use of electric vehicles as a potential solution to these issues. The strict battery requirements are listed and associated with the increasing market demand of LIBs, and therefore the need for recycling these batteries. A brief review of LIBs is done, followed by the recycling techniques used for processing these batteries and the associated issues.

In Chapter 3, the experimental methodology followed is described, in particular the procedure for a safe discharge and disassembly is proposed. Additionally, the dismantling procedures and preparation of the electrode materials are presented, as well as the characterization techniques used such as X-ray powder diffraction (XRPD), flame atomic absorption spectroscopy (AAS) and scanning electron microscopy (SEM). Finally, the leaching tests methodology is described.

In Chapter 4, the results obtained are presented followed by a discussion regarding their meaning and possible impact.

In Chapter 5, the main conclusions of this thesis are stated. Moreover, the challenges and limitations encountered during the development of this study, as well as some recommendations for future development, are presented.

Page intentionally left blank

Chapter 2. State of the Art

2.1. Fossil fuel vehicles - Issues

Fossil fuels are mineral fuels that were formed in an earlier geological period from fossilized remains of dead plants and animals and are still being created today by underground heat and pressure. However, they are being consumed much more rapidly than they are created. As the oil is formed in the time scale of million years and consumed the last 130 years, fossil fuels are considered non-renewable [12].

The development of internal combustion engine (ICE) automobiles was considered one of the greatest achievements of modern technology [13]. The chemical energy bound in the hydrocarbon fuel is transformed into thermal energy in the combustion space or chamber [14]. The combustion of fuels involves both physical and chemical processes that can be summarized by the exothermic chemical equation (1) since generally any hydrocarbon fuel will burn in the presence of air and dissociates to carbon monoxide (CO) and free hydrogen and oxygen [15].

$$C_xH_y + \mathrm{m}(O_2 + 3.76N_2) \longrightarrow n_1CO_2 + n_2H_2O + n_3CO + n_4H_2 + n_5O_2 + n_6N_2 + Heat \quad (1)$$

However, the equation (1) can be modified since the nitrogen contained in the fuels can react with the oxygen forming NO_x [16]. The balance of carbon, hydrogen, oxygen and nitrogen can be represented in Table 2 [15].

Table 2 – Balance of the chemical elements in the general combustion equation (1) [15].

Chemical Element	Balance
Carbon	$n_1 + n_3 = x$
Hydrogen	$n_2 + n_4 = 0.5y$
Oxygen	$n_1 + 0.5n_2 + 0.5n_3 + n_4 = m$
Nitrogen	$n_5 = 3.76\,m$

Finally, in ICE vehicles, the heat energy released by the fuel is converted into mechanical energy in the engine, with an average efficiency of 20%, which is transferred to other moving parts such as wheels and propellers as kinetic energy [14, 17]. This process is summarized in Figure 1, in which is possible to understand that the conversion of energy stored in the fossil fuel to electricity is only around 16% [14].

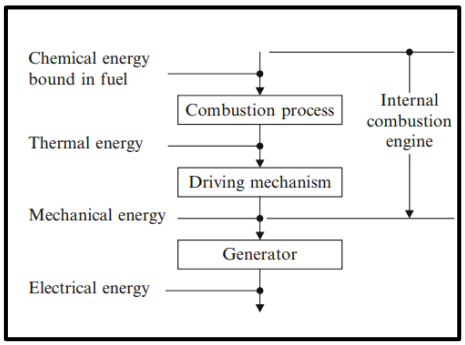

Figure 1 - Diagram of energy conversion in an internal combustion engine. Adapted from [14].

The main automotive fuels are gasoline and diesel, which are produced in oil refineries from crude oil [15, 18]. However, the increasingly large number of automobiles in use around the world is causing serious problems for the environment and hydrocarbon resources [13, 19]. The main risk factors to the present economy based on fossil fuels are the following:

1. Increase in oil demand

According to the OECD[1], in 2009 the transportation sector accounted for 53% of the world's oil consumption and is expected to increase this value by 60% in 2035 [20]. Particularly, in 2014, the road transportation represented 44% of global oil demand [21].

2. Depletion of non-renewable resources

All fossil fuels are finite and non-renewable on a human scale. These resources are thus limited physically and, more stringently, economically. However, different views about this phenomenon exist in the scientific discussion [22]. The hydrocarbons reserves-to-production ratios at end of 2015, according to the BP Statistical Review of World Energy, are shown in Figure 2 [23].

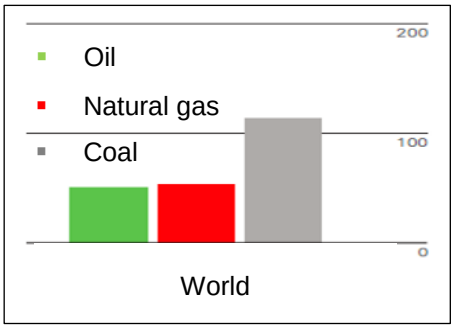

Figure 2 - Fossil fuel reserves-to-production ratios at end 2015. Adapted from [23].

The depletion dates of oil, natural gas and coal, assuming no future discoveries, is 2066, 2068 and 2126, respectively [23]. Nonetheless, since the reserves are on the rise today and that the rate of rise is declining, the depletion dates can easily be altered. There is neither any imminent end of oil nor any looming gas crisis in next several decades, yet it may be the beginning of a breakpoint sometime in a distant future [22].

3. Increase of CO_2 emissions and climate change

Global carbon emissions from fossil fuels have significantly increased since 1900. From 1970 to 2010, the total amount of CO_2 emissions have more than doubled, as shown in Figure 3, with emissions from fossil fuel combustion and industrial processes contributing to about 78% of the global greenhouse gas (GHG) emissions [24].

[1] The Organization for Economic Co-operation and Development (OECD) is an international economic organization of 31 countries that defines itself as a forum of countries committed to democracy and the market economy, providing a setting to compare policy experiences, seeking answers to common problems, identifying good practices, and coordinating domestic and international policies of its members. For more information, see http://www.oecd.org/.

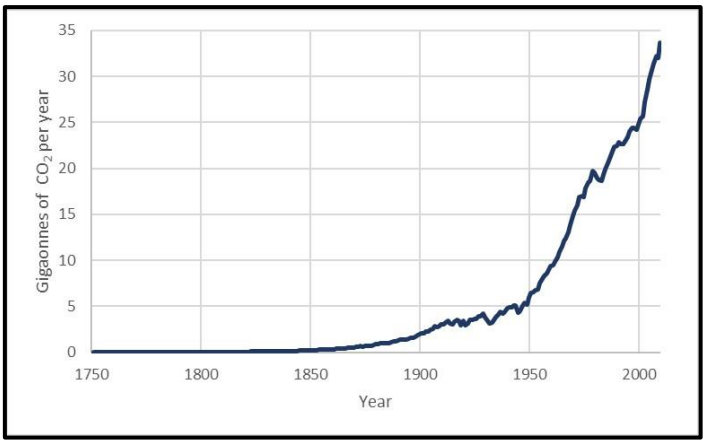

Figure 3 – Total CO_2 emissions from 1750 to 2010. Data from [25].

Considering that CO_2 has a greenhouse effect, it contributes to a rise in global temperature with associated series of dramatic climate changes. In fact, if its emissions continue at high level, models predict a temperature rise between 1.8 and 4.0 ºC in 2100 [26].

4. Emission of NO_x

The increased combustion of fossil fuels since the last century has been a primary source of NO_x, leading to the increase of pollutants concentration in the atmosphere [27].

5. Increase trend and high volatility of oil prices

Oil prices are inherently volatile. As shown in Figure 4, over the past eight years alone, oil prices have risen until 2008 and then declined with some fluctuations until 2016. Large fluctuations in the oil price can lead to economic and financial uncertainty [28].

Figure 4 – Historical crude oil prices [28].

6. Dependency on politically unstable oil producing countries

In 2015, around 30% of EU crude oil imports came from Russia, 16% from Nigeria and sub-Saharan Africa, 16% from the Middle East and 8% from North Africa, as shown in Figure 5. A high proportion of these regions are from geopolitically unstable regions that have seen increases in terrorism, internal

and border conflicts, or wars. Knowing that the EU does not have significant oil reserves, its economy, particularly the transport sector, is facing an increased risk of oil supply interruptions and shortages [28].

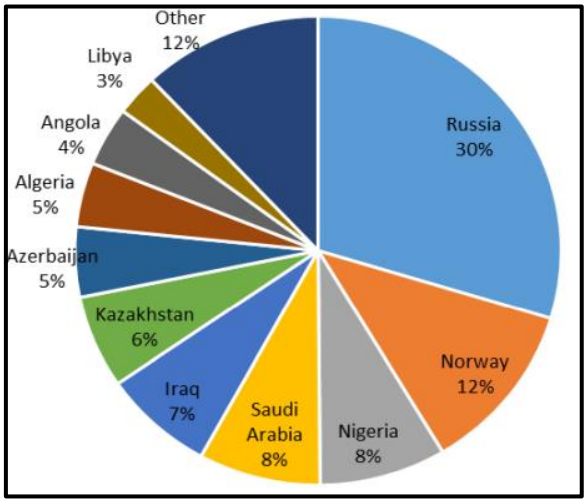

Figure 5 – Sources of EU crude oil imports (2015) [28].

7. EU policies

As the EU has become increasingly dependent on imported sources of oil, the energy policy in the EU considers the risks associated with high dependence on oil imports. Appendix A shows the key policies that the EU has put in place to reduce the oil import dependency [28].

2.2. Electric vehicles – Solution?

As discussed in the previous sub-chapter, the deteriorating air quality, climate change issues and depleting petroleum resources are becoming serious threats to modern life. Considering that the transport sector consumes about 27% of energy demand and is roughly responsible for 14% of GHG emissions there has been progressively more rigorous emissions and fuel efficiency standards to stimulate the development of safer, cleaner and more efficient vehicles [29, 30]. These goals might be met by replacing ICE vehicles with ideally, zero emission vehicles, i.e. electric vehicles [1].

In fact, it is expected that an increased uptake of electric mobility will decrease the environmental impacts caused by the tailpipe emissions from ICE vehicles significantly. In addition, EVs might contribute to reducing the amount of GHG emissions during their life cycle, if powered with low carbon intensity energy sources, therefore, diminishing their contribution to climate change [7]. In the near future, electric vehicles (EVs) are expected to dominate the clean vehicle market. Particularly, five years ago it was predictable that by 2020, more than 50% of new vehicle sales would be EV models[2] [30, 31].

However, to enable this revolutionary change, the key technology is the battery since it is the energy source for traction [30].

[2] Though fuel cell vehicle (FCV) is one of the technologies under consideration of electric-drive vehicles, the durability, high cost, and production and distribution of hydrogen have hindered its development. The US Department of Energy (DOE) dropped its research support for FCV in its budget of fiscal year of 2010 [31]. For that reason, FCVs are not considered in this chapter.

2.2.1. EVs mechanism

EVs consist of a rechargeable electric battery to power electric motors for propulsion, an electric motor and a controller. The battery is mainly recharged from external power sources, such as the electrical grid using a charger than can be either on-board or off-board the electric vehicle, but the electric motors can also be operated in reverse as a generator to partially recharge the battery through regenerative braking [32, 33].

The controller manages the power supplied to the motor, and therefore the vehicle speed, in forward and reverse. This is usually known as a “two-quadrant controller” — forwards and backwards. It is usually desirable to use regenerative braking both to recover energy and as a convenient form of frictionless braking. When the controller also allows regenerative braking in forward and reverse directions, it is known as a “four-quadrant controller”. The concept of an EV is summarized in Figure 6 [33].

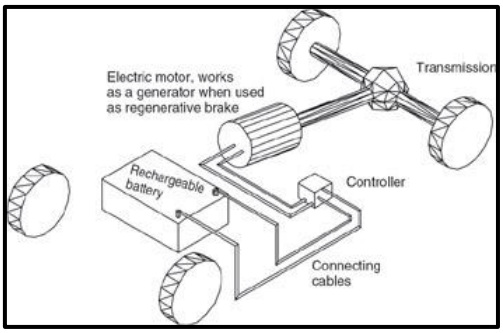

Figure 6 – Rechargeable battery EV [33].

2.2.2. Types of Electric Vehicles

While the definition of EV types are not entirely consistent, it is useful to classify them in three main categories, which are plug-in hybrid electric vehicle (PHEV), hybrid electric vehicle (HEV) and full electric vehicle (FEV) that have passed to the production stage, shown in Figure 7 [34].

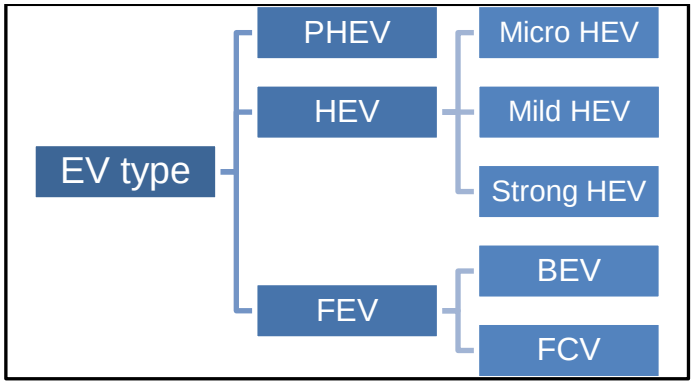

Figure 7 – Types of electric vehicles. Based on [32, 35].

According to the degree of electrification and performance features of EVs, the main differences between the different types can be shown in Figure 8 [32].

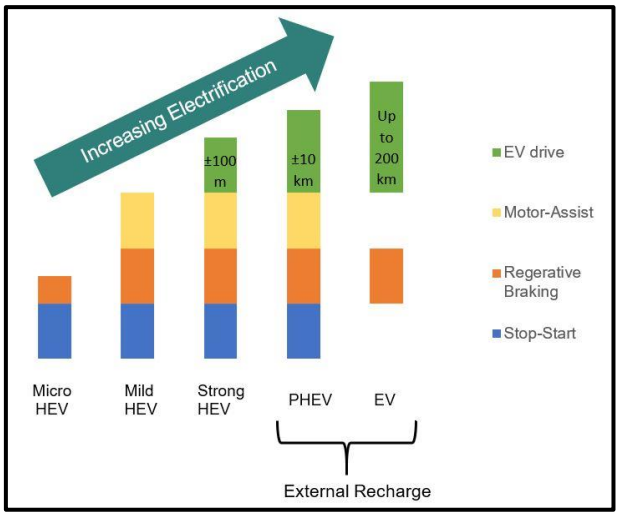

Figure 8 – Types of electric vehicles considering performance features. Based on [32, 36].

2.2.2.1. Hybrid Electric Vehicles

A HEV is a vehicle with two or more energy storage systems both of which must provide propulsion power – either together or independently [37]. In HEVs, the propulsion energy is available from a combination of two or more power sources or converters, in each at least one of them is electric. The development of HEVs has been mainly focused on vehicles powered by the conventional ICE combined with a battery electric drivetrain [35, 32].

The purpose of the presence of both, the battery and the electric motor system, is to achieve either better vehicle fuel economy or performance than a conventional ICE since the battery serves as an electrochemical "flywheel"/energy buffer that improves the efficiency of operation by allowing the ICE to operate closer to its optimal efficiency [35, 32]. Additionally, in regenerative braking the HEV electric motor operates in reverse as a generator and charges the battery, providing energy for subsequent accelerations [32].

A) HEV designs

Currently, there is a variety of HEV designs with varying size of the drivetrains and different combination between them. In fact, the ICE and electric drivetrains can be combined in series and/or parallel, as shown in Figure 9 [32].

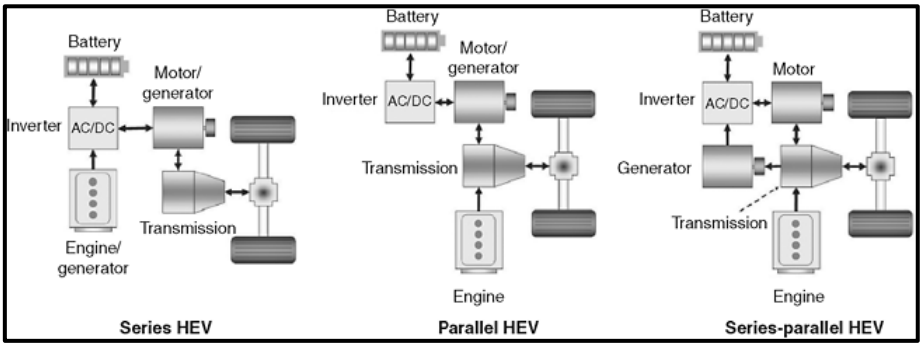

Figure 9 - Schematic diagram for series and parallel HEVs configurations [32].

An essential feature of the HEVs is the electric motor/generator system, which when used as a:

- Generator, it generates electrical power to charge the battery and start the vehicle's ICE when needed;
- Motor, it drives the vehicle by turning the vehicles wheels [35].

In the series configuration, the ICE drives the generator to recharge the battery, which powers the electric motor to turn the wheels. This case can be seen as an EV that uses a gasoline-powered ICE and a generator as a range extender, i.e., the ICE operates at its maximum efficiency, but it is not able to dissociate the driving conditions in a highway or in the city. On the other hand, in the parallel configuration, both the electric and ICE drivetrains power the wheels through the transmission connection and so either drivetrain or both can propel the vehicle, allowing the vehicle to adapt to the driving conditions and increasing its overall efficiency. Additionally, there are more complex designs that combine series and parallel hybrid features by using power-split transmissions to take advantage of both efficiency conversions [32].

Generally, HEVs maintain their batteries at an approximately constant state-of-charge (SOC) while driving and recharging occurs only through on-board electricity generation, generated either from the ICE coupled to the motor/generator or from the recapture of kinetic energy through regenerative braking [35].

In a typical electric mode operation, at start-up and at low vehicle speeds and acceleration, the electric motor/generator uses power from the battery pack and acts as a motor to drive the vehicle where it offers high torque. At higher speeds, faster acceleration or, when more power for charging the batteries is required, the ICE is engaged and it is automatically started by the motor/generator acting as a starter. This mechanism can be shown in Figure 10 [35].

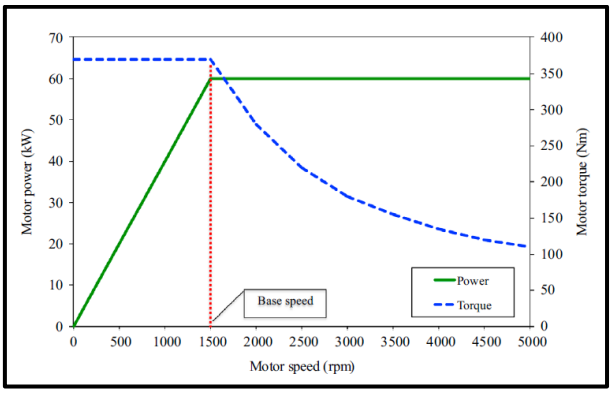

Figure 10 - Performance characteristics of a typical electric motor for traction [35].

This combined mode of vehicle operation allows the ICE to be used only at high efficiencies and to be normally switched off at traffic stops. In the latter case, any accessory power requirements, like air conditioning is provided by the battery pack. This limitation of ICE use results in an improved vehicle efficiency, performance optimization and lower emissions compared to conventional gasoline vehicles [38].

B) HEV battery charging

In an HEV, the battery can be charged in two ways:

- Using the motor/generator system, acting as a generator either while driving or when the vehicle is stationary [35].
- Via regenerative braking. During the vehicle's deceleration, the regenerative brakes set the electric motor into reverse mode, thus running back-wards and the car's wheels slow down. While running back-wards, the motor also acts as a generator producing electricity using the kinetic energy to charge the battery instead of turning it into heat as it happens on a conventional vehicle. The regenerative braking technology is more effective at lower speeds or in stop-and-go driving situations, i.e. city traffic. In the case that regenerative braking power is not enough to fully stop the vehicle, HEV can also employ friction brakes [35].

C) Types of HEVs

Currently, there is a variety of HEV types in the automotive market that can be divided in three according to the battery requirements:

1) Micro HEV

The vehicle efficiency in micro hybrids, also referred to as stop-start, is improved by turning off the ICE during inactive periods. During the engine-off time, the vehicle's electrical system is powered by the vehicle starter-lighting-ignition battery. At idle, the battery powers auxiliary loads, including, most significantly, the heating/ventilation/air conditioning (HVAC) system. When the driver's control command prompts a shift into drive, the HEV's starter/generator restarts the ICE to provide the required traction power. Extended idle periods can also trigger engine starts, particularly during HVAC operation, which can consume several kilowatts of power [32].

The aim of the stop-start HEV systems is to provide a seamless engine to motor transitions, offering their greatest benefits in urban driving due to the frequent stops. Although these vehicles offer a minimal fuel economy improvement of around 5%, depending on design and driving conditions, they have the least expensive hybridization strategy [32].

2) Mild HEV

Mild HEV are the lower-power subset of power-assist hybrid vehicles that are capable of motor-assist, but not all-electric propulsion. These vehicles offer an alternative lower-cost design compared to the strong HEV and still provide substantial fuel economy and emissions reduction advantages. The power capability and torque of the electric drivetrain are significantly less than that of the ICE [32].

3) Strong HEV

Strong HEV or full HEVs are a subset of power-assist hybrid vehicles which are not only capable of motor-assist but also all-electric propulsion which may include electric launch. In these vehicles, the power capability and torque of the electric drivetrain is comparable to that of the ICE [32].

Strong HEVs use petroleum-based fuels in ICEs as the source of energy and batteries to improve the efficiency of operation by maximizing the operation of the internal combustion engine at its maximum efficiency operational conditions, which also reduces the emissions of noxious pollutants and GHGs. Thus, these vehicles provide a high fuel-economy improvement of 50% or more in city driving and large emission reduction opportunities [32].

2.2.2.2. Plug-in Hybrid Electric Vehicles

A plug-in hybrid electric vehicle can be defined as a HEV that:

- Has a battery storage system of at least 4 kW h;
- Can recharge the battery from an external source;
- Can drive at least 10 km in electric mode [39].

Comparing to HEV, plug-in hybrid vehicles may offer a reduction of:

- 25-55% in NO_x emissions;
- 40-80% in gasoline consumption;
- 35-65% in GHG emissions. In fact, just like a FEV, if the electricity used to power the vehicle comes from a combination of energy sources including zero emission renewable energy sources such as hydropower, solar or wind, the PHEVs GHG emissions are close to zero [35].

These vehicles can run on fossil fuels and on electricity or a combination of both, allowing them to have the potential to provide most of the benefits of FEVs without the disadvantages in terms of range and refuelling time combined with a lower cost. The key feature of PHEVs is the ability to recharge the battery by plugging into the electrical grid. PHEVs use both grid electricity and on-board petroleum-based fuel as energy sources, with the electrical energy fraction depending on the size of the battery and the operating strategy [32, 35].

A) PHEV designs

Currently, there are three main designs of PHEV: the series, parallel and series/parallel. In the series design, shown in Figure 11, the vehicle's wheels are only rotated by the electric motor and not the ICE. The ICE is used to turn the generator, which will supply electric power to the electric motor system providing driving power. Any excess charge produced by the engine can be stored by the battery [35].

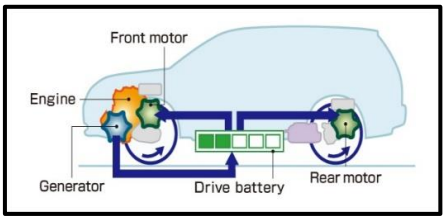

Figure 11 – Series PHEV design [40].

In the parallel design, shown in Figure 12, both the electric motor and the ICE can drive the vehicle's wheels independently or even simultaneously through mechanical coupling [35].

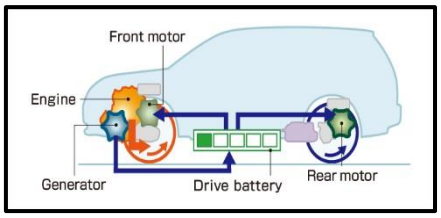

Figure 12 - Parallel PHEV design [40].

Finally, in the series/parallel design the vehicle can operate in either series or parallel mode [35].

B) PHEV modes

Regardless of the design, PHEVs may offer two basic modes of operation that manage the vehicle's battery discharge strategy: charge-depleting and charge-sustaining. The variations or combinations of these two modes are called blended and mixed mode, respectively. The size and type of battery required will be affected by the use of these modes [35].

In the charge depleting mode, also used in FEVs, a fully charged PHEV is allowed to operate only on electric power until its battery SOC is depleted to a predetermined level, at which time the vehicle's ICE is engaged [35].

In the blended mode, the ICE is engaged before the battery depletion level is reached to increase the distance travelled by a fully charged PHEV compared to charge-depleting mode alone. This is employed in PHEVs, which do not have enough power to sustain high speeds or speeds above a certain value, without using the ICE [35].

In charge-sustaining operation, the SOC is maintained at a predetermined narrow band by combining the vehicle's two power sources, balancing the discharge of the battery with charge from regenerative braking as in the power-assist hybrid. This operation can be compared to the operational mode for the power-assist HEV, but typically at a lower SOC [35].

In the usual operating strategy, which is the mixed mode, the HEV charge-depletion operation is firstly used after recharge of the battery pack from the grid connection. Unless the ICE drivetrain is needed to meet power demands, this consists of an all-electric operation with the electric drivetrain providing full-traction. The charge-depletion operation continues until the battery pack is substantially depleted, at which point charge-sustaining HEV operation starts [32].

The PHEV operation modes are illustrated by the plot of SOC in Figure 13 [32, 35].

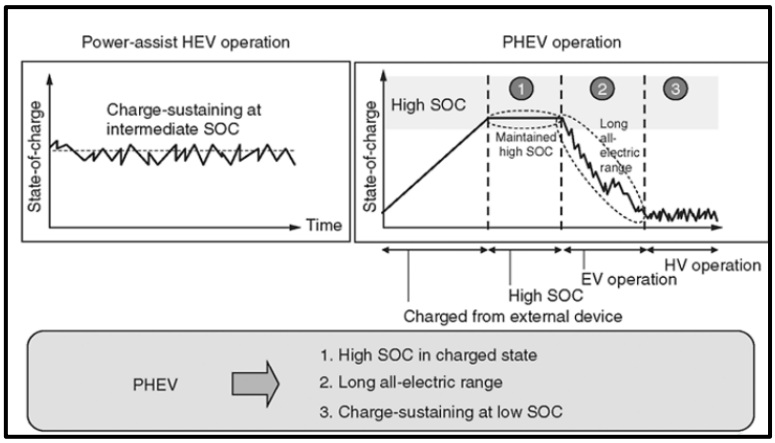

Figure 13 – PHEV battery SOC during operational modes, including charge, standby, charge-depletion operation, and charge-sustaining operation [32].

C) PHEV battery charging

In a PHEV, the battery can be charged in three ways:

1. Using the electric grid by plugging the vehicle into a standard electrical outlet of 120/249 AC [35].
2. Via regenerative braking [35].
3. Using the ICE when residual charge in the battery is low or when accelerating and other times when higher motor output is needed [35].

2.2.2.3. Full Electric Vehicles

FEVs are powered only by an electric motor instead of a gasoline ICE. The electricity is usually generated by on-board rechargeable battery packs, but it can also be by flywheels or capacitors. The battery can be charged either in standard home electricity outlets or in external dedicated charging stations, similarly to the PHEVs [35].

These vehicles have the potential to decrease significantly the harmful GHG emissions of the transport sector compared to conventional ICE vehicles, and the level of emission reductions from FEVs is potentially much higher than PHEVs, depending on the efficiency and emissions intensity of the electricity generation system in the specific region where the vehicle will recharge its battery pack [35].

Additionally, FEVs have certain performance advantages over conventional gasoline vehicles due to their built-in high-power battery packs. These battery packs drive electric motors with inherently higher torque in lower vehicle speeds than ICE, i.e. FEVs can be much quicker and accelerate from rest faster than conventional vehicles without using any transmission or clutch systems. However, the absence of an ICE minimizes the available heating capability of the vehicle's internal heating system, which is especially significant in colder climates [35].

There are several FEVs available today in the automotive market but the most recently manufactured FEVs use Li-ion battery packs that have an improved performance compared to NiMH (nickel-metal hydride) vehicles [35].

A) FEVs mode of operation

The basic systems of a FEV include the battery pack, the electric motor controller and the electric motor as shown in Figure 14. Under normal operation, the battery pack powers the motor controller, which delivers regulated and controlled power to the electric motor to turn the vehicle's wheels. The amount of power or voltage that the controller delivers to the motor is determined by the position of the accelerator pedal, which is connected to a pair of variable resistors. At any given instance, the relative resistance of these resistors gives the signal to the controller of how much electric power should be delivered to the electric motor [35].

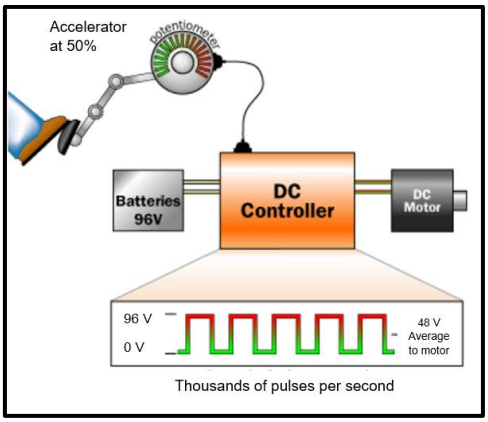

Figure 14 - Process diagram of a typical FEV. Adapted from [35].

When the vehicle is stopped, and the accelerator is not pressed, the controller can deliver zero power or zero voltage whereas when the driver fully presses the pedal, it delivers full power or full battery voltage. In between these two situations, the controller delivers any intermediate power level [35].

2.2.2.4. Comparative assessment

A comparison of the technical characteristics of the three types of electric vehicles is shown in Table 3. FEVs operate only on battery charge and therefore employ the charge depleting mode of operation while PHEVs offer the possibility of on-board battery charge sustaining modes of operation. Finally, HEVs offer higher range compared to PHEVs and FEVs [35].

Table 3 - Comparison of technical characteristics of electric vehicles [35].

Vehicle type	Mode of operation	Maximum driving range (km)	Top speed(km/h)
HEV	Charge-sustaining	900-1200 (hybrid)	170
PHEV	Charge-sustaining	20-60 (electric)	160
	Charge-depleting Mixed Mode	900 (hybrid)	
FEV	Charge-depleting	120-390	80-200

A comparison of engine and battery capacity of the different types of electric vehicles can be illustrated in Figure 15 [41].

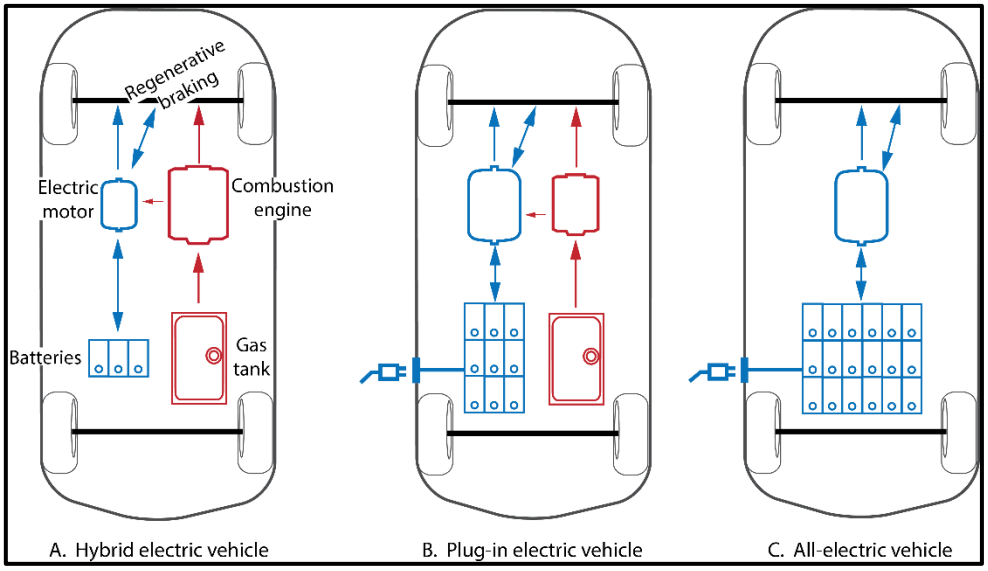

Figure 15 – A comparison of the engine and battery capacity in electric vehicles [41].

2.3. Battery requirements in EVs

The batteries in the EVs are one of the main challenges to overcome. The battery packs must be contained physically within the vehicle in a safe way in the event of crashes while being electrically isolated from the vehicle [32]. The main problem regarding the batteries of the EVs is that they are required to handle high power (up to a hundred kW) and high energy capacity (up to tens of kWh) within a limited amount of weight (less than one-third of the vehicle weight) and volume (even a smaller fraction of the vehicle volume) at an affordable price [30, 32].

The first EV was seen on the road shortly after the invention of rechargeable lead–acid batteries and electric motors in the late 1800s [30]. In the beginning of 1900, the number of EVs was almost double than that of gasoline power cars. In the development of EVs in the 20th century, a variety of batteries were used including lead-acid, nickel-iron, nickel-cadmium, nickel-zinc, sodium-sulphur, sodium-metal chloride, zinc-bromine and zinc-chloride [32].

However, until near the end of the 20th century, the lead-acid battery was the most commercially viable battery since the other batteries were significantly more expensive and also because several battery types raised significant toxicity and/or safety issues despite providing higher specific energy and energy density as well as longer life compared to lead-acid batteries [32].

In the 1990s, the NiMH batteries were being developed. However, its cost per unit energy was not commercially sustainable for EV applications unless it was for small, high-power battery packs for HEVs.

By 1920, due to the limitations of heavy weight, long charging time, short trip range and low durability of batteries at that time, EVs almost disappeared, giving the whole market to ICE vehicles [30].

More recently, renewed interest in EVs has been stimulated by the development of high energy density lithium-ion cells. Large LIBs were developed in the early 1990s by Sony and Hitachi for EVs due to their strong potential of high energy density. However, they had low power performance and serious safety issues, which were improved by the evolution of the thin electrode designs and enhanced manufacturing techniques and cell designs, as well as chemistries with greatly reduced volatility [32].

It is useful to compare the battery performance requirements of the different types of vehicles and draw some general conclusions, regarding the suitable battery types for each electric vehicle. The comparison of the EV specific performance targets is shown in Appendix B. However, the requirements were developed at different points in time and the assumptions were not constant [32].

The current major battery technologies used in EVs are Li-ion and NiMH [35].The specific energy targets for HEVs are quite low and within the capability of lead-acid batteries. The power capability required by most HEVs, however, is around 600 W/kg, which is within the capability of high-power NiMH and Li-ion batteries [32]. Many HEVs available in the market were produced with NiMH batteries, although today LIBs are increasingly substituting NiMHs in these vehicles [35].

The suitable batteries used in PHEVs are nickel-metal hydride (NiMH) and lithium-ion but the current technology for PHEVs is based on the latter. The reason is that, despite the fact that NiMH can be more durable and can sustain higher number of lifetime cycles for deep discharging up to 80% than LIB, the specific energy requirements for PHEVs are more challenging than for HEVs. Additionally, NiMH have lower electric travelling range and lower maximum vehicle speed and acceleration performance due to their inferior energy and power densities compared to LIB [32, 35]

The key difference between the specific performance requirements for HEV and FEV applications is the power-to-energy ratio. In FEV there is no ICE, which means that these vehicles need to operate their battery across the whole range of vehicles speeds. Besides, the battery energy potential must be high enough to guarantee at least a minimum driving range sufficient to cover a daily routine driving [35].

These requirements provide the need for a battery packs with high-power and high-energy, which would be able to withstand high discharging and charging levels while being reasonably light, resulting in larger batteries. However, an increased battery energy density would significantly increase the charging times. Such features are only available through either NiMH or Li-ion batteries, which come at a higher cost. In fact, nowadays the cost of the batteries is the most significant parameter contributing to the high cost of FEVs and it is the most important obstacle to overcome for a full commercialization of these vehicles [35].

2.4. Expected LIB growth in the market demand and need for recycling

Lithium is the lightest known metal and is highly demanded worldwide, specially to produce rechargeable LIBs, due to its very high energy density by weight and high electrochemical potential (3.045 V). The annual global Li metal demand for all industrial applications was forecast to grow from around 44140 metric tons of lithium in 2017 to 79451 metric tons of Li in 2025, as shown in Figure 16 [42]. This issue becomes particularly critical has Li has no foreseen substitute[3] [43].

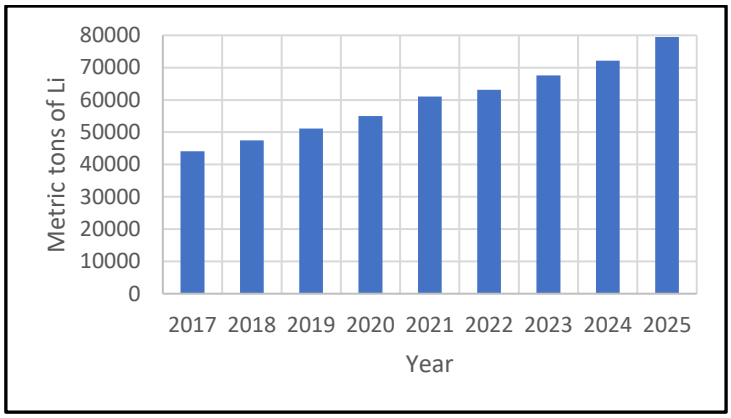

Figure 16 – Projection of total worldwide Li demand from 2017 to 2025. Based on [42].

This increase will be mainly driven by the rechargeable battery sector, which accounts for about 80% of the total Li consumption, as shown in Figure 17. Annual global demand was forecast to grow from 197,200 tonnes in 2016 to 1,008,900 tonnes in 2026 and 2,231,000 tonnes in 2031 [44].

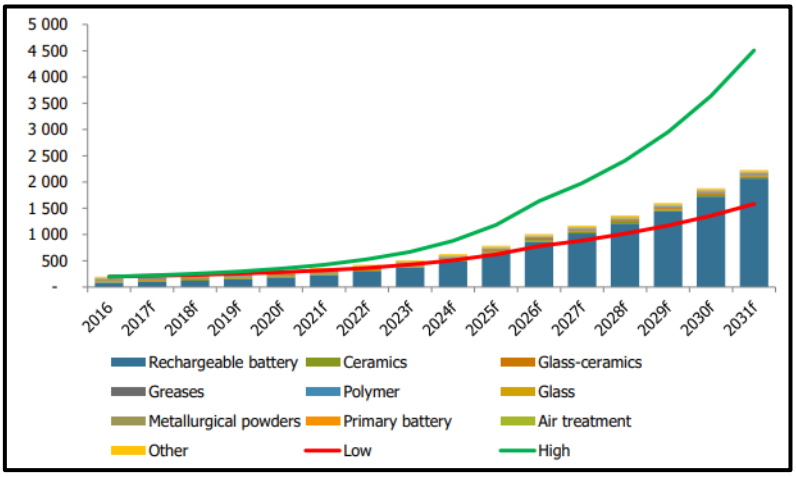

Figure 17 – Forecast consumption of lithium by first use, 2016-2031 (000t LCE) [44].

Particularly, it is expected a growth of about 28% from 2018 to 2020 in the market size LIBs used in electric vehicles, as shown in Figure 18 [45].

[3] There are lithium substitutes in other applications apart from electric vehicles. However, there is little incentive to use them instead of lithium because of the relatively inexpensive price of lithium and the stability of its supply, which might be the reason for the current and foreseen lack of lithium substitutes in EVs [42].

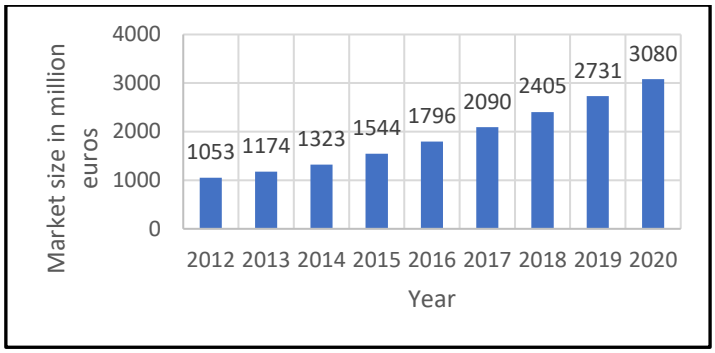

Figure 18 – Projected market for LIB used in EV from 2012 to 2020. Based on [45].

It is forecast that the amount of spent LIBs in 2020 will be higher than $500x10^6$ tonnes due to the enormous growth of production of EVs, corresponding to around 25×10^9 units that must be disposed or recycled. Therefore, the development of efficient recycling technologies of spent LIBs is a challenge that must be overcome [46]. Specifically, for EOL vehicles, the reuse and recovery rates have to be increased to at least 85% with regard to the weight per vehicle and year to meet the foreseen increase of batteries in their EOL [7].

2.5. Review of LIB

There are three battery categories (see Figure 19):

1. Chemical batteries that convert chemical energy into electrical energy through a controlled thermodynamically favourable chemical reaction inside the battery. They can be divided into:
   - Primary battery, which are the generic name for non-rechargeable, single-use batteries.
   - Secondary battery, which are the generic name for reusable, rechargeable batteries.
   - Fuel cell batteries, where the electrical energy comes from an electrochemical reaction between a fuel (hydrogen) and oxygen, but they are still in development for practical use.
2. Physical batteries that convert physical changes in heat and light energy into electricity.
3. Biological batteries that generate electricity through the organic activity of enzymes and microorganisms.

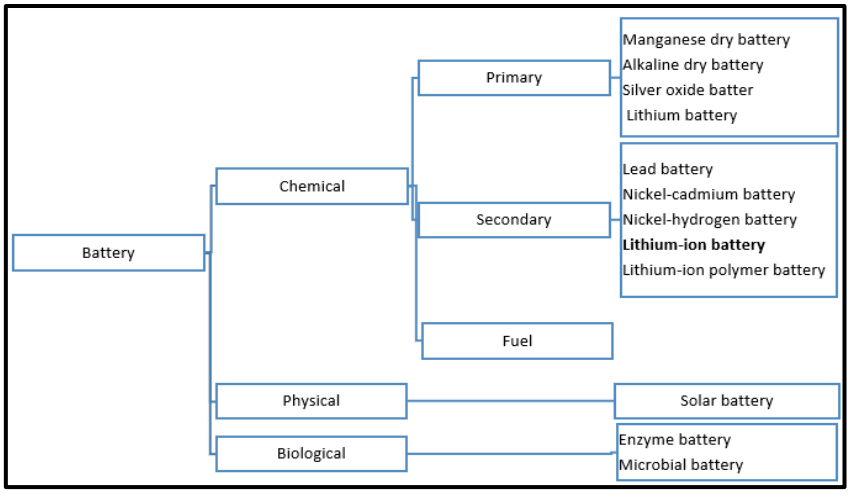

Figure 19 - Types of batteries and classification of the LIBs as secondary batteries. Based on [47].

LIBs are the most suitable existing technology for EVs since they can output high energy and power per unit of battery mass, allowing them to be smaller and lighter compared to other rechargeable batteries (see Figure 20). Furthermore, LIBs have high-energy efficiency, a relatively longer cycle than other rechargeable batteries and no memory effects. These memory effects refer to a decrease in energy capacity after the battery has been discharged shallowly – the Ni-Cd batteries remember the smaller capacity and can no longer fully charge. This effect does not happen in LIBs, so the battery can always be recharged even before its stored energy has been depleted [3].

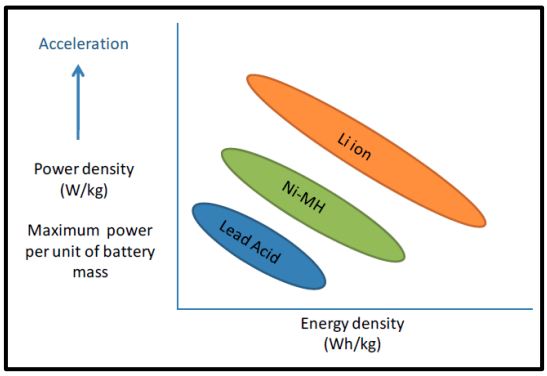

Figure 20 - Power (acceleration) and energy (range) by battery type [3].

2.5.1. Basic operation in a Li-ion rechargeable battery

A LIB is a rechargeable battery in which lithium ions move between the negative and positive electrode, creating electricity flow. It is important to note that for reasons of simplicity the negative and positive electrodes are often referred to as anodes and cathodes respectively in literature, which is only applicable to a battery in the discharging mode i.e., when the battery delivers energy. This simplified representation is followed in this thesis and so, by convention, oxidation (loss of electrons and Li ions) occurs at the anode, whereas reduction (gain of electrons and Li ions) occurs at the cathode during a discharge reaction [3, 48]

When a LIB is fully charged, most of the lithium ions are present at the anode of the battery. The discharging process is initiated when an external circuit connecting the two electrodes is completed. As the battery discharges, the lithium ions migrate from the intercalation sites in the negative electrode with a higher potential energy (anode) in the form of Li^+, go through a porous plastic separator and insert atomic-sized holes in the cathode (lower potential energy), as represented in equation (2) [7, 48, 49, 50].

Negative: $$C + \mathrm{y}\, Li^+ + \mathrm{y}\, e^- \underset{Charge}{\overset{Discharge}{\rightleftharpoons}} Li_y\mathrm{C} \quad (2)$$

Simultaneously, electrons are conducted from the anode (oxidation), transferred through an external circuit, which creates current to power a device; and enter the cathode (reduction), as represented in equation (3). The discharge process continues until the potential difference between the two electrodes becomes too low, at which point the cell is fully discharged. This process is reversed during charging,

which means that when the battery is connected to an external power source, the lithium ions and electrons can be forced to move from the cathode back to the anode [7, 48, 49, 50].

Positive:
$$LiMO_2 \underset{Charge}{\overset{Discharge}{\rightleftharpoons}} Li_{1-x}MO_2 + xLi^+ + \mathrm{x}\, e^- \quad (3)$$

The complete reaction for the LIB in both the discharging and charging mode is represented in equation (4), in which x and y are selected based on the molar capacities of the electrode materials [50].

Overall:
$$LiMO_2 + \frac{x}{y}C \underset{Charge}{\overset{Discharge}{\rightleftharpoons}} \frac{x}{y}Li_yC + Li_{1-x}MO_2 \quad (4)$$

In order to control the rate of electron transfer, the anode must be physically and electrically isolated from the cathode. For that, a separator, which is a permeable membrane electrically insulating that is soaked with an electrolyte (ionically conductive but electrically insulating medium) is used [7, 48, 49].

During the initial battery cycle, a thin film that is usually electrically insulating but ionically conductive, known as the solid electrolyte interphase (SEI) spontaneously forms on the surface of the electrodes due to the decomposition of the electrolyte. The formation of the layer occurs predominantly at the graphitic anode, which operates at potentials at which the electrolyte is thermodynamically unstable - less than 600 mV. The formation of the layer creates a complex heterogeneous collection of phases and layers having many secondary interfaces. The composition, behaviour and properties of the SEI depend on the electrode/electrolyte system and operating conditions – the SEI of a stable electrode system must act as a passivating protective layer that does not interrupt Li diffusion or reversible Li insertion reactions over repeated charge/discharge cycles [48].

This layer is essential to allow Li^+ transport while blocking electrons to prevent further electrolyte decomposition as well as to ensure continued electrochemical reactions, protecting the anode from corrosion and the highly reactive electrolyte from further reduction. However, due to its brittle properties, this layer can be cracked due to stress caused during the normal cycling of the battery, leading to corrosion of the anode [11]. The operational principle of a typical LIB is illustrated in Figure 21 [7].

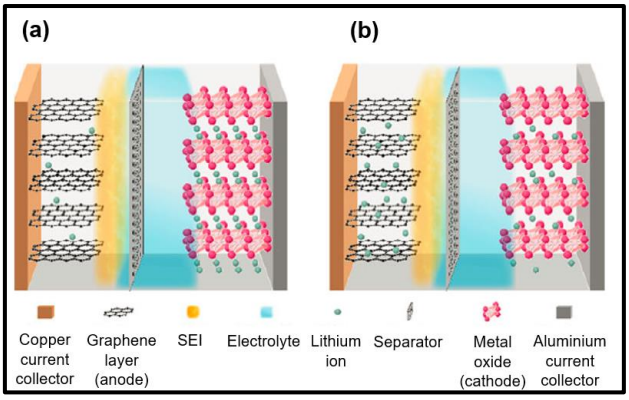

Figure 21 - Schematic illustration of the fundamental operating principle of a LIB in the discharged (a) and in the charged state (b) [7].

For high-power applications such as EVs, several requirements must be satisfied simultaneously [51]:

1. The electrolyte must have a high ionic conductivity, typically larger than 10^{-3} S/cm.
2. Most batteries commercialized today have a graphite anode that interacts with the electrolytes, forming a SEI layer. The stabilization and control of the SEI is crucial, not only to improve the cyclability and the performance of the cell, but also to make it safer, since flammable gas can be generated during SEI formation, and the SEI can be resistive, thus increasing locally the temperature.
3. The thermal stability of the Li salt against the organic electrolyte solvents must be assured.
4. The cathode material should not dissolve in the electrolyte.
5. Tolerance on abuse (resistance to incidents, measured through mechanical and thermal tests).

2.5.2. Constitution of LIB

A LIB cell is composed of four main components: cathode, anode, electrolyte solution and a separator, as shown in Figure 22 [47, 49].In addition to these essentials, the LIB also has a protective metal casing, covering plastic and an electronic control unit [52].

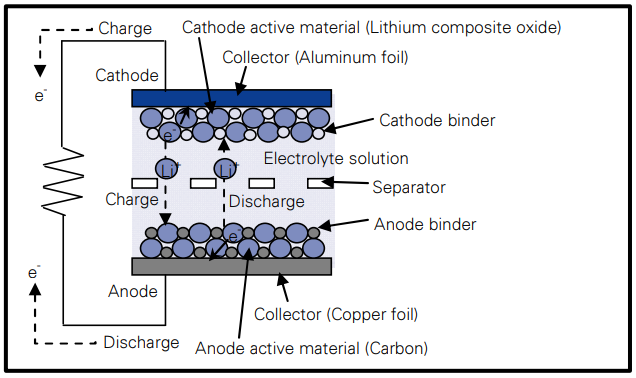

Figure 22 – Schematic illustration of inside a typical LIB [47].

The electrodes consist of four parts, which are:

- Current collector (Al in the case of the positive electrode since it is a light abundantly available metal that forms a passivation layer to inhibit oxidative corrosion and it alloys with lithium at low potentials, excluding its use as an anode current collector, for which Cu is used instead);
- Particulate active material;
- Polymer binder;
- Carbon conductive additive (such as carbon black, carbon fibres, carbon spheres and carbon tubes) to provide sufficient electron transport to the site of lithium intercalation in electrode.

The summarized function description of the lithium-ion battery cell components is given in Table 4 [3, 46, 49].

Table 4 – Lithium-ion battery cell components and respective functions. Based on [3, 46, 49].

Component	Functions	Examples
Cathode	1) Emit lithium-ion to anode during charging. 2) Receive lithium-ion during discharging.	- $LiCO_2$ (LCO) - $Li(Ni_{1/3}Mn_{1/3}Co_{1/3})O_2$ (NMC) - $Li(Ni_{0.8}Co_{0.15}Al_{0.05})O_2$ (NCA) - $LiMn_2O_4$ (LMO) - $LiFePO_4$ (LFP)
Anode	1) Receive lithium-ion from anode during charging. 2) Emit lithium-ion during discharging.	- Carbon materials - $Li_4Ti_5O_{12}$
Binder	Adhesive agent that links the anode and cathode with the current collector sheets (Cu, Al)	Polyvinylidene fluoride (PVDF)
Electrolyte	Pass lithium-ions between cathode and anode. It should conduct Li-ions efficiently while preventing electron conduction.	Li salt (e.g. $LiPF_6$) dissolved in a solvent that is usually a mixture of linear and/or cyclic carbonates (e.g. ethylene carbonate (EC), propylene carbonate (PC))
Separator	1) Prevent short circuit between cathode and anode by preventing physical contact of the electrodes. 2) Pass lithium ions through pores in separator	Micro-porous polypropylene or polyethylene

The composition of a typical LIB, in percentage of the total battery cell weight, for EVs is represented in Figure 23 [46, 49].

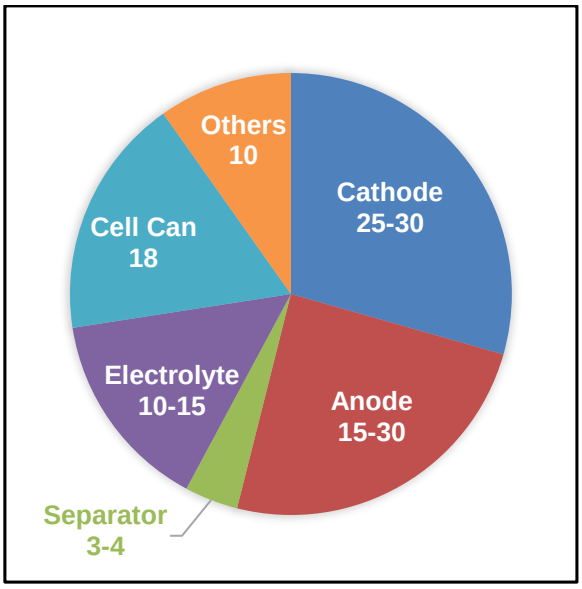

Figure 23 – Composition of a typical LIB, in weight percentage of the total battery cell. Based on [46, 49].

2.5.2.1. Chemically active compounds of LIBs

The generic term “lithium-ion” is referent to a broad range of different chemistries, which have been adjusted for the specific applications. The introduction of new cell designs and chemistries as a consequence of the scientific progress regarding LIB, increases the complexity of its recycling process. An overview of past, current and expected battery cell chemistries in the market is given in Figure 24 [7].

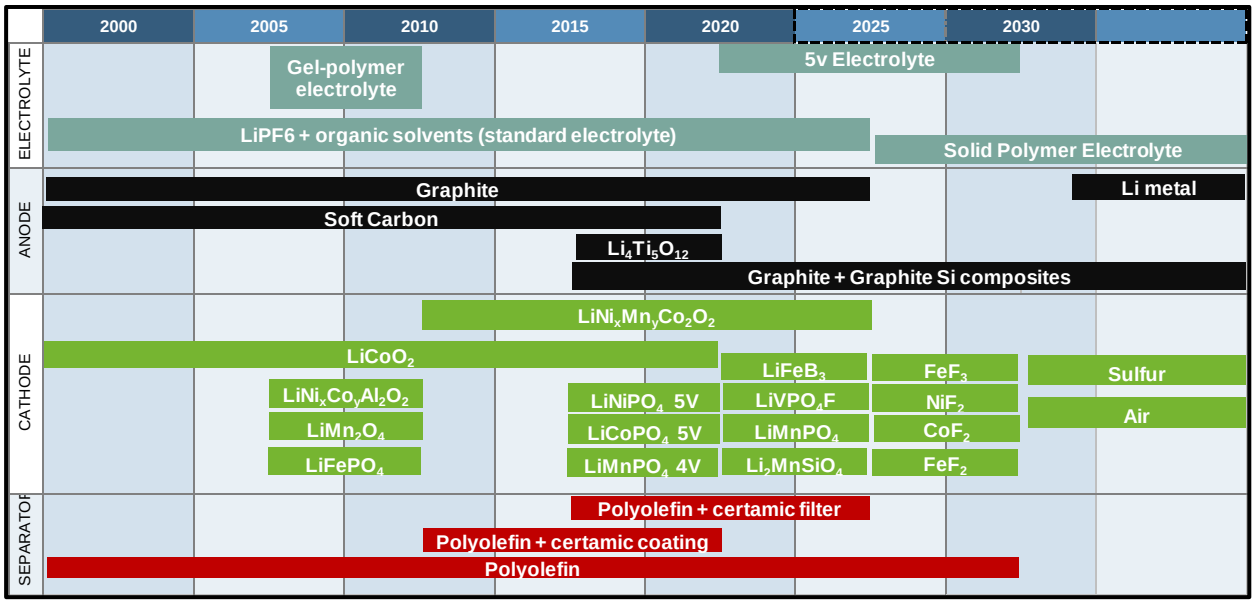

Figure 24 - Major innovations in material technology: past, existing and expected battery chemistries. Based on [7].

A) Cathodic active material

The cathode is composed of an aluminum foil coated with an electrochemically active material. In the beginning of the 2000s, most LIBs used lithium cobalt oxide (LCO or $LiCoO_2$) compounds as the cathode material, which is generally considered unsuitable for automotive applications due to its inherent safety risks. In fact, the use of Co in the cathodic active material has been reduced due to the safety concerns, high toxicity and cost of this element through a partial substitution of Co with Ni, Mn or Al, often referred as a lithium-transition-metal-oxide $LiMO_2$ (M stands for metals such as Co, Ni, Mn, Al or their combinations) cathode [7, 53, 54]. It is worthwhile to mention that the exchange of Co by only Ni results in an unstable isostructural $LiNiO_2$ due to the tendency of Ni^{2+} ions substituting Li^{+} ions, leading to a conductivity loss and therefore a partial substitution of Ni with Mn or even Ni with Al was the solution found to this problem [7, 11].

In fact, LIBs are usually classified according to their cathodic active compound [11]. Currently, the most prominent technologies for automotive technologies are lithium-nickel-cobalt-aluminum (NCA), lithium nickel-manganese-cobalt oxide (NMC), lithium-manganese oxide spinel (LMO) and and lithium-iron phosphate (LFP). Each combination of the anode and cathode material has distinct advantages and disadvantages, from the business point of view, where the high costs remain the major problem and from the technical perspective, which includes five main dimensions [53]:

1. Specific energy – the capacity of the battery to store energy per kilogram of weight, which limits the EV driving range;
2. Specific power – the amount of power that batteries can deliver per kilogram of mass. It is particularly important in HEVs since they discharge a small amount of energy quickly;
3. Safety – it is the most important criterion for EV batteries. The main concern in this area is to avoid thermal runway – a positive feedback loop whereby chemical reactions triggered in the cell intensify heat release, potentially resulting in a fire. This phenomenon can be caused by an overcharged battery, a short-circuit or discharged-rates that are too high. The batteries that are prone to thermal runaway, such as NCA, NMC and LMO must be used with system-level safety measures that either contain the cells or monitor their behavior.
4. Performance – peak power at low temperatures, SOC measurement and thermal management;
5. Life span - measured in terms of both the number of charge-discharge cycles and overall battery age.

The challenge from the business point of view is to reduce manufacturing costs through scale and experience effects as market volumes expand [53].

Ideally, the batteries of a given type would be standardized as soon as the next best generation battery chemistry is established. However, currently, there is no single technology that wins all dimensions as shown is [53].

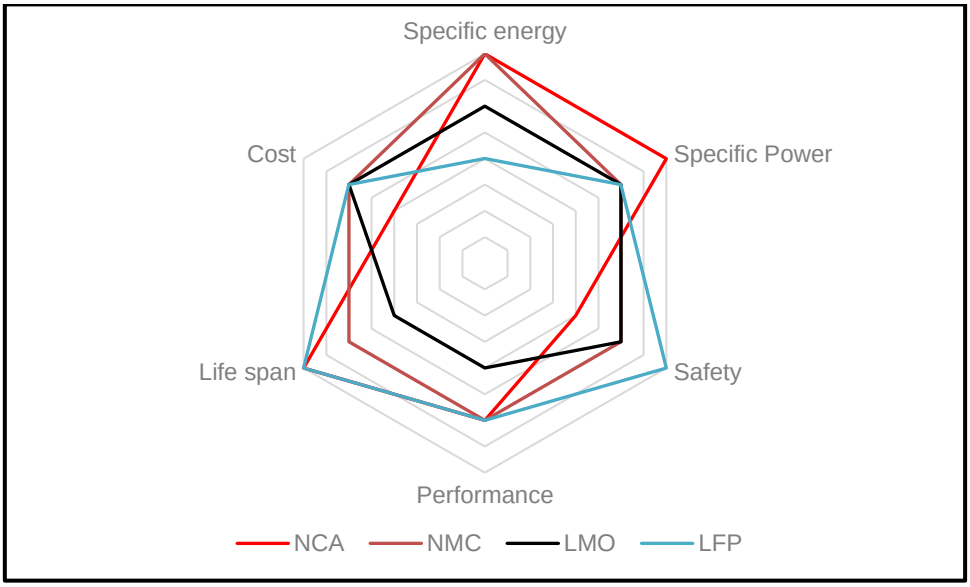

Figure 25 - Comparison of the dimensions among the four principal LIB technologies for EVs. Based on [53].

Additionally, another factor that can be consider which is both a technical challenge and a commercial barrier is the long charging time that is currently only overcome by fast charging methods which employ more sophisticated charging terminals but increase the cost and weight as they require enhanced cooling systems on board the vehicle [53].

B) Anodic active material

The anode material should be able to conduct electrons and enable the efficient flow of Li-ions without excessive structural and volume changes. The most common anode active material is graphite since its layered structure provides a good basis for Li-ion intercalation. During charging, lithium ions become stored within the graphite, embedded between the sheets. The capacity of the battery depends on how many lithium ions can be stored in a given amount of anode material and the theoretical storage capacity of graphite is relatively low (32 mA h per g). Another commercial option is LTO ($Li_4Ti_5O_{12}$) due to its claimed combination of stability, long cycle life and inferior energy density. Additionally, silicon can be used as additive to graphite to improve its specific capacity. The anode is connected to the copper foil to enable the conduction of electric current from the cell [11, 49].

Metallic nanoparticles, carbon nanotubes and tin compounds are among the latest technologies in development to enhance anode performance. These new chemistries could increase the recycling value of the anode, which is currently mainly recycled for its copper current collector [49].

2.5.2.2. Elements present in a typical LIB

The results from multiple studies for the composition of typical spent LIB cells were summarized in Table 18 (see Appendix C). The typical spent LIB cells are usually composed of Co, Li, Cu, Al, Fe and Ni metals, organic chemicals and plastics. Zeng and Li dismantled several spent LIB cells and conclude that the Cu, Al and Fe metals were in their elemental state while the Co, Li and Ni metals were in a combined state [52].The range of values of Co, Li, Cu, Al, Fe and Ni (weight %) present in a typical spent LIB cell are shown in Figure 26. Most of the spent cells generated nowadays are essentially coming from discarded communication/information equipment and so are of the LCO type, reason why the cobalt composition is always high.

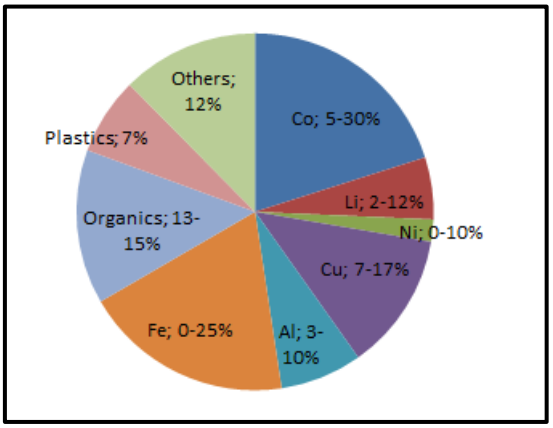

Figure 26 – LIB cell composition range, in weight %.

The mass concentrations of materials in different types of LIB modules are summarized in Table 19 (see Appendix C) as reported from multiple studies. The compositions depend on the types of materials used for the cathode, anode, separator and casing as well as the intended application [49]. The range of values of Al, Co, Cu, iron/steel, Mn, Ni and others (weight %) present in a typical LIB module, considering the most important batteries in the market (LCO, NMC, NCA and LFP) are shown in Figure 27.

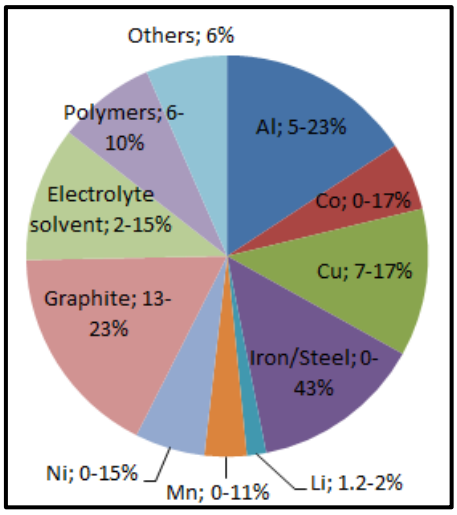

Figure 27 – Typical LIB module composition range, in weight %.

The economic importance and supply risk results of critically assessments of the metallic elements (2017) of LIBs are presented in Figure 28 [43, 55].

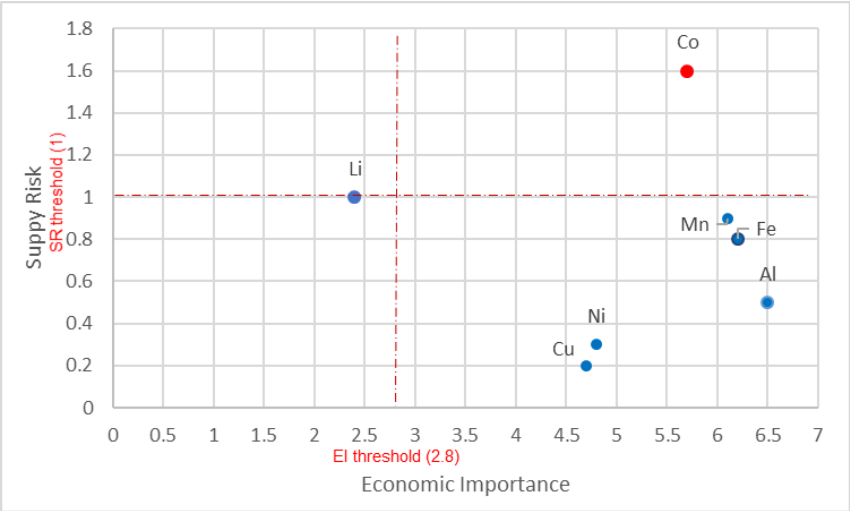

Figure 28 – Economic importance and supply risk of 2017 criticality assessment of Li, Ni, Cu, Al, Mn, Fe (non-critical raw materials represented by the blue dots) and Co (critical raw material represented by the red dot). Adapted from [43, 55]

The criticality assessment presented is based on two parameters. The economic importance (EI) and the supply risk (SR). The first one is calculated based on the importance of a given material in the EU end-use applications and performance of available substitutes in these applications, i.e., it relates to the potential consequences in the event on an inadequate supply of the raw material. The supply risk (SR) measures the risk of inadequate supply of a raw material to meet industry demand, which can be reduced by recycling and substitution [56].

If a given material has both parameters above the thresholds established by the European Commission, it is considered critical [55, 56]. In the constituting metallic elements of LIBs, Co is the only one considered critical while the others have a high EI (above the EI threshold) but a low SR, with the only

exception being Li, which has an EI below the EI threshold (although it is not far from the value and may increase with the rise in the LIBs demand) but a relatively high SR (equal to the SR threshold).

2.6. Recycling techniques for LIBs

The world has developed remarkably both from a technical and economical perspective since the launching of LIBs in the beginning of 1990's. However, this has also resulted in an accelerated exploitation of natural resources, which leads to the conclusion that the Earth cannot bear the linear economy of expendable goods. Instead, circulating goods and materials in use for longer periods of times and several rounds should be favored, changing towards a circular economy [11].

An important part in the implementation of targets of a circular economy model is recycling, which refers to the processing of constituent materials of an end-of-life (EOL) product and incorporating them back to the material value chain. The concept of a circular economy is schematized in Figure 29 [11].

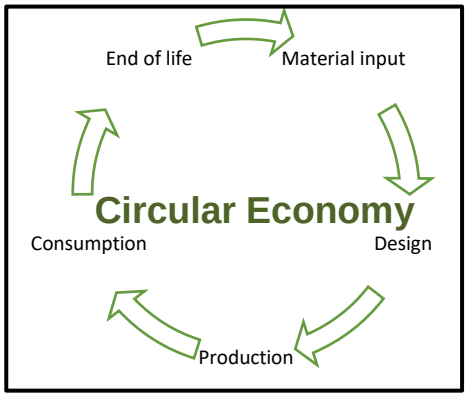

Figure 29 - Schematic presentation of the circular economy. Based on [11].

However, recycling has environmental and economic consequences and several possibly contradictory objectives have to be considered when designing economically and environmentally sustainable recycling process to close the loop for resource circulation [11].

Currently, there are three main points of destination for EOL LIBs, which are municipal solid waste landfills, waste-to-energy facilities and specialized recycling facilities. The first two should be avoided since the valuable materials are lost. The possible pathways and outcomes for LIB waste stream is presented in Figure 30 [11].

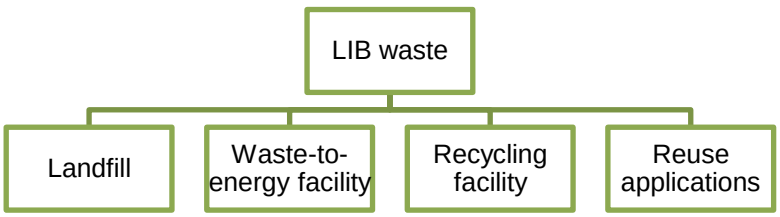

Figure 30 - Possible destinations for LIB waste. Based on [49].

The major recycling challenge of LIBs is to develop economic ways to extract and process the valuable metals within these batteries [49]. Considering this pathway, the value chain of EV batteries comprises

seven steps: component production (including raw materials), cell production, module production, assembly of modules into the battery pack (including an electronic control unit and a cooling system), integration of the battery pack into the vehicle, use during the life of the vehicle and reuse and recycling, where the latter is the focus of this chapter (see Figure 31) [53].

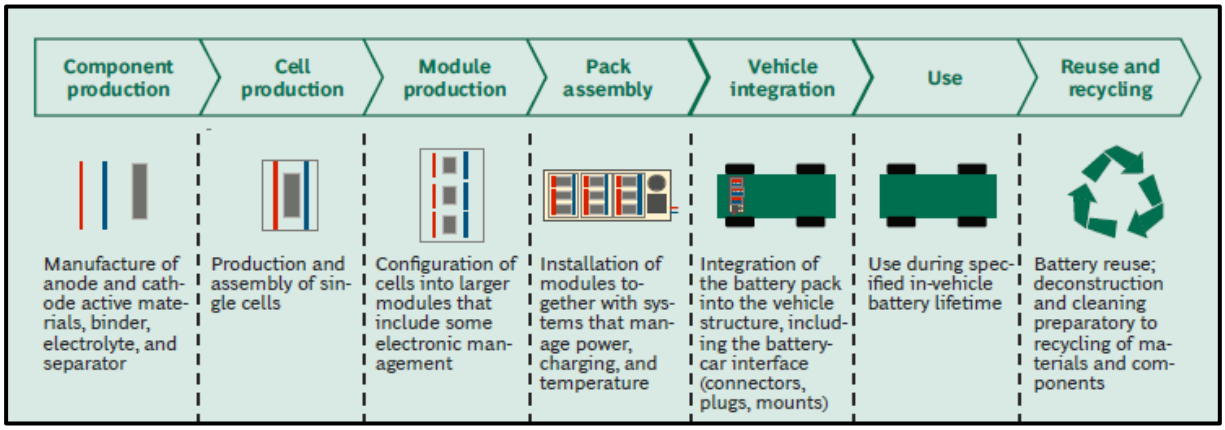

Figure 31 – Value chain for electric vehicle batteries [53].

Recycling processes for LIBs are combinations of different unit operations. At first, a deactivation of the battery should be done to minimize the possibility of a thermal runaway, and other chemical reactions as the electrochemically stored energy is reduced. There are three ways of deactivating the LIB [57]:

1. Discharge (with or without a conductive liquid) – reduces the stored energy, which could otherwise activate further reactions and therefore reduces the hazard level;
2. Thermal pre-treatment – the electrolyte is volatized or even all organic compounds of the battery cells are decomposed;
3. Freezing of the electrolyte – the electrolyte is frozen to prevent electrochemical reactions and short circuits during a subsequent crushing process.

The following unit operations can be divided into three types of treatments [57]:

1. Mechanical treatments – imply crushing to open the battery cells or modules, followed by the liberation of the materials that are considered valuable, which is accompanied by classifying and sorting processes to separate Al foil, Cu foil, separator and the electrode active materials. The casing of the battery cells, modules and connecting components can also be recovered.
2. Pyrometallurgical treatments - several components of battery cells, sometimes including the battery cells themselves, are melted. In this process, the lithium and aluminium remain in the slag while the transition metals nickel, cobalt and copper can be recycled from the cast. It is necessary further treatment to recover lithium, which could be a hydrometallurgical process.
3. Hydrometallurgical treatments – used to recover pure metals, like lithium, from slag derived from pyrometallurgical processes or from the separated electrode active materials derived from mechanical processes. This process includes leaching of the targeted metals, extraction and separation, and finally recovery of products from separated streams by crystallization, precipitation or electrowinning.

Figure 32 summarizes possible process options for the involved unit operations and depicts the advantages of combining different unit operations to obtain high recovery rates.

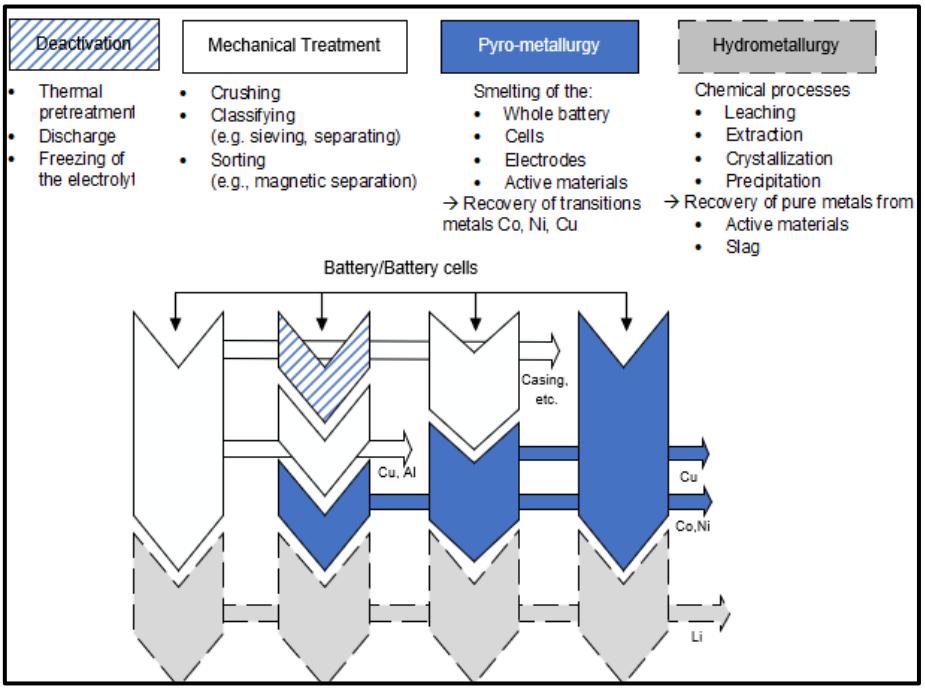

Figure 32 – Unit operations in battery recycling and their possible combinations to establish efficient recycling process routes. Based on [57].

2.6.1. Deactivation

The deactivation of the LIBs is necessary either for EOL transport of damaged LIBs or as a pre-treatment step before recycling. There are several possible ways to deactivate the LIBs [57].

2.6.1.1. Discharge

The charge/discharge operations during the life span of a LIB in an EV or HEV are usually controlled by a battery management unit (BMU). This unit controls the current flow during charging and discharging, monitors the voltage of each battery cell or module, detects temperatures, controls the end-of-charge and end-of-discharge voltage (the prescribed voltage at which the charge and discharge, respectively, of a battery may be considered complete) and takes suitable countermeasures in case of malfunctions. Charging and discharging by the BMU is only possible in a specific voltage range specified for each battery chemistry. A complete discharge of the energy stored is preferable for a secure disassembly of the battery systems or battery modules and the following steps [57].

However, to accomplish this complete discharge, voltages beyond the default end-of-discharge voltages are needed, which are often prevented by the BMU as such a deep discharge could be accompanied by a polarity reversal (as the battery is discharged, the cell that goes down to zero volts first will continue to have current forced through it by the other cells - when this occurs, the voltage across the fully-discharged cell is reversed) and formation of flammable gases in the cell. To avoid the rise of inner pressure within a battery cell due to gas formation, specific discharge techniques can be applied. As the probability of a voltage increase after a deep discharge is very high, it is advisable to direct short-

circuiting the battery system, module or cell after the discharge because it decreases the probability of exothermal reactions of a damaged or overheated battery cell [57].

A) Discharge in conductive liquid

The LIBs can be discharged by electrolysis of a conductive liquid medium either for transport or as a pre-treatment step. The battery system is placed in a solution (an aqueous sodium chloride with a concentration of 0.3 % by weight is recommended) inside a nonconductive container. To prevent leakage, a second container should be placed around the first one. The discharge and the storage of the battery system must be controlled for a minimum of 24 h regarding the voltage and the temperature. During the electrolysis, there is a formation of a gas due to the reactions of ions within the solution as shown in Figure 33 [54].

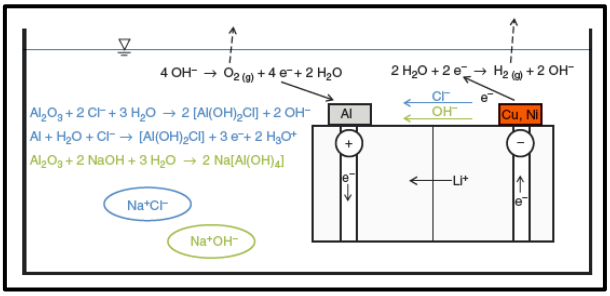

Figure 33 - Reactions and gas formation during electrolysis of a sodium chloride and a sodium hydroxide dissolution [57].

Additionally, there can be reactions between the ions within the solution and the battery casing, which could lead to corrosion followed by a release of electrolyte and a reaction between the conducting salt and the saline solution, causing the opening of the cell casing and the formation of reactive and acidic compounds such as hydrogen fluoride, see equation (5). To neutralize the acid compounds, a sodium hydroxide dissolution can be used instead of sodium chloride [9, 57].

$$LiPF_6 + H_2O \rightarrow LiF + POF_3 + 2HF \uparrow \quad (5)$$

2.6.1.2. Thermal pre-treatment

The thermal deactivation can be used as a first step in the recycling of LIBs. In the Belgian company Umicore, in a preheating section, the battery cells are slowly heated in a furnace up to 300ºC, at which chemical reactions occur inside the cell and the solvents of the electrolyte evaporate, reducing to a minimum the risk of explosions. Additionally, the cells vent and the gaseous compounds exhaust and are inflamed due to the rise in the inner pressure. After this treatment, the battery cells are electrochemically inactivated and free of inflammable solvents, however, an exhaust after-treatment is needed due to the gaseous combustion products [7, 54].

On the other hand, in the German battery recycler Accurec, a thermal deactivation process is used in a vacuum chamber up to 250ºC and approximately 700 mbar. The electrolyte evaporates and condenses in a downstream condenser. In this treatment, the battery cells are deactivated, and the electrolyte is recovered, however, this product still contains impurities due to the decomposition products [54].

2.6.1.3. Freezing of the electrolyte

The damaged LIBs can be transported using the freezing of the electrolyte treatment since it decreases the potential of exothermal reactions due to the rise of temperature as the damaged or defective LIB cells are frozen (it is recommended to freeze the battery systems, modules or cells down to -65ºC). The low temperature avoids chemical reactions. During transport, a maximum of -60ºC must be ensured and the interfaces have to be secured [54].

Additionally, this method can be used as a pre-treatment for mechanical recycling processes such as crushing because it suppresses the heat generation by mechanical strain, lowers the reaction potential and achieves an embrittlement for a more efficient crushing and separation process [54].

It is important to mention that the enhanced safety can only be achieved if the materials are continuously kept at low temperatures and that is why a combination with another deactivation method should be provided [54].

2.6.2. Dismantling and mechanical treatment

When portable batteries are recycled they are usually crushed directly without any previous special handling, however, car batteries require manual dismantling and the battery cells are transported to a battery recycling facility while the other components go to non-specific recycling facilities.

2.6.2.1. Disassembly

EVs contain LIB cells, assembled in battery modules (subunit of the battery system), BMUs and further electronics (e.g. temperature sensors, casing and connecting elements) as depicted in Figure 34 [54].

The electronic elements and the system casing can be separated and recycled in existing processes for consumer electronics, which decreases the size and the electrochemically stored energy content of the starting material for crushing or melting processes, for example. Therefore, it reduces the safety issues and impurities in the following recycling process. The main purpose is to recover all components, including the materials of the battery cells [54].

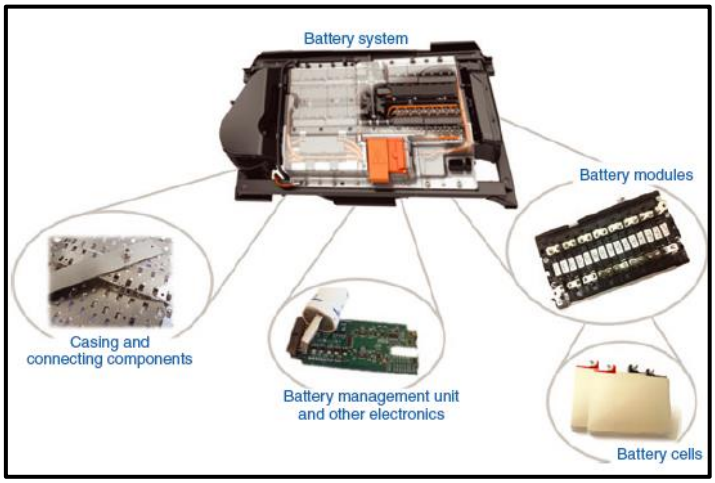

Figure 34 - Components of a battery system [54].

At present, a high input of manual disassembly steps is needed due to the lack of standardization in terms of the battery system designs. From an economic point of view, it is beneficial to discharge the battery before the disassembly process as only electricians are allowed to handle charged systems, which significantly impacts labor costs. In the future, it is expected that an automation of the disassembly will decrease the costs of the process, particularly labor costs, as the standardization of the battery system structure and the total number of systems to be recycle increases. Regarding this scenario, several studies have been done to combine manual and automated process steps [54].

2.6.2.2. Mechanical treatment

The purpose of mechanical processing is to liberate and separate materials to a point where subsequent processing steps are economically and technologically feasible as well as to remove hazardous components or contaminants. These objectives are usually achieved with a combination of processing stages including crushing, classification and sorting processes [11, 10].

A) Crushing

In most cases, after the disassembly of LIB systems into smaller subunits, the next step of the recycling process is crushing. In this step, the cells are opened, and their valuable components are released. Additionally, the battery packs are converted into a product flow that could be stored as bulk material, transported or processed. There are two main types of specific crushing methods [54].

1. Wet crushing

An automated shredding process especially designed for LIBs by the company Retriev Technologies Inc. is used. A hammer mill is operated in a brine solution (electrochemical discharge in which the cell is immersed in salt water) for crushing. This dissolution neutralizes acid and other emissions of chemical reactions that occur during crushing. After this treatment, solids and liquids can be separated [54].

2. Inert/dry crushing

According to a study made by Zhang et al., dry crushing shows advantages over wet crushing because of fewer impurities in the fine fraction and since a better separation of metal electrode substrates and the particulate coating components can be achieved. However, several characteristics of LIBs must be considered when it comes to dry crushing, such as [54]:

I. The electrolyte has flammable organic which can form an explosive mixture with aerial oxygen;
II. There are other components, such as the commonly used PVDF binder and the lithium-based conducting salts containing fluorine, which decompose at elevated temperatures. Consequently, they form acid gas compounds such as hydrogen fluoride and other gaseous products.

Therefore, an ignition of the atmosphere inside a shredding must be avoided. Regarding this issue, a gastight shredder for dry inert crushing of LIB modules was developed by the company Hosokawa Alpine AG. This shredder is equipped with a discharge grate that allows upper particle size limitation and

thereby an adjustable degree of liberation. The oxygen content inside the shredder is reduced, establishing inert conditions, to avoid formation of explosive mixtures previously mentioned. Additionally, to avoid exothermal chemical reactions, dry crushing processes should be fed with completely discharged battery modules or cells [54].

B) Classifying and sorting

A combination of sorting and sieving steps can be used after crushing fragments of electrodes to separate the case, the separator and the powder fraction, consisting of coating agglomerates, for further recycling [54].

Firstly, the sorting step can be done by using a magnetic separator to separate ferromagnetic parts. Secondly, the sieving step can be applied to separate the lasting heavy fraction by air separation methods such as zigzag sifting where the mixed materials are fed to the zigzag tube at a certain height in a zigzag sifter. The materials are uplifted to the top of the sifter by an adjustable airstream to the bottom by gravity, allowing a multistage cross-flow separation – with one cross-flow separation in each zig and zag. This results in a heavy fraction, which contains Al and Cu foils still partly coated with active material, at the bottom of the sifter and a lightweight fraction, which consists of separator, smaller foil fragments and already detached coating agglomerates, at the top. Figure 35 shows a schematic of the zigzag air classification process and the gained fractions [54].

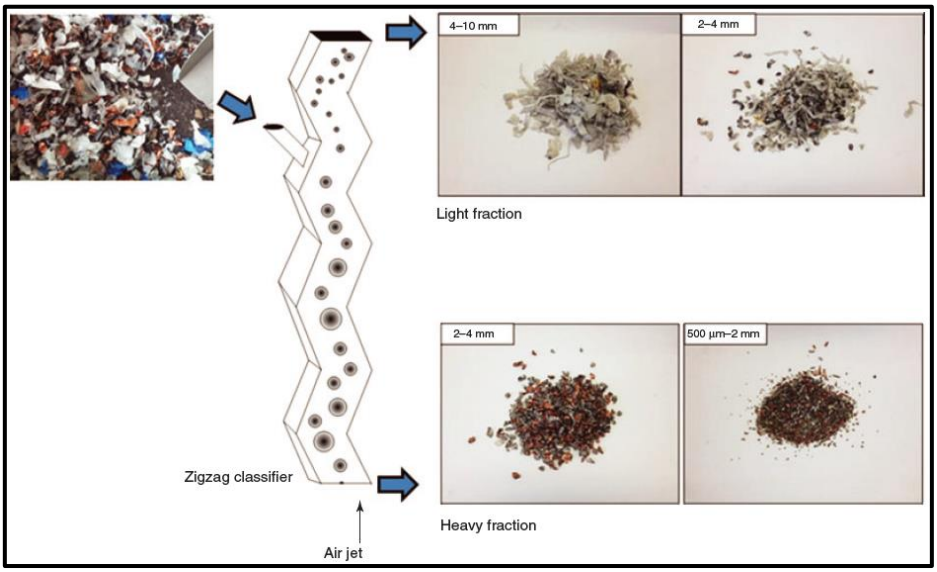

Figure 35 - Air classification in recycling processes for LIBs using a zigzag classifier; typical light and heavyweight fractions are shown [54].

After some classification steps, a second milling step can be applied to remove the remaining particulate coating from the current collector foil to increase the yield of coating fragments and foil with less impurities in each of the fractions. An alternative mechanism to separate the current collector and the particulate coating could be the dissolution of the binder in a solvent or the decomposition of the binder under high temperatures. To improve the purity of the light- and heavy powder fractions, additional sieving steps with a smaller mesh size need to be applied. The finer the mesh size, the smaller the scraps that pass the sieve and therefore, the lower the impurities of each fraction [54].

2.6.2.3. Problems with deactivation and dismantling of LIB

Waste LIBs exhibit many hazardous characteristics, such as the ability to spontaneously ignite and/or release hazardous chemicals under landfill conditions. In fact, LIBs have been known to catch fire when crushed, overheated or when there is a manufacturing defect. When the batteries are completely discharged, the risk of fire decreases since the potential energy within the battery is smaller than a charged battery.

However, when a charged or partially charged battery is improperly handled, it may catch fire or explode, which has been the cause of fire in garbage and recycling trucks that compact the waste they collect, leading to the explosion of LIB and fire in the truck's waste [49].

Therefore, the discharging of the battery for recycling purposes must be handled with care. Particularly, discharging in brine must be done in a ventilated area as it produces oxygen gas. On the other hand, if a resistor is used instead to discharge the battery, the temperature of the battery should be monitored and not exceed 90ºC. Additionally, even after discharging to zero volts, the battery must be dismantled in a well-ventilated area to minimize exposure to toxic gases from the electrolyte [49].

Another issue that can have serious implications for LIBs that are sent to a waste-to-energy facility is the fact that fire or explosion can be initiated when the temperature within the cell reaches certain thresholds as these facilities use high temperatures to treat the waste. As explained in chapter 2.5.1, at normal operating temperatures, a SEI film covers the graphite anode, protecting it from unwanted side reactions with the liquid electrolyte [11, 49].However, at temperatures above 90ºC, the SEI film will begin to exothermically decompose, resulting in a further temperature increase within the battery. After the temperature exceeds 120ºC, the SEI film can no longer protect the anode from reacting with the electrolyte and consequently combustible gases are produced [49].

Oxygen gas will be produced above a certain threshold temperature as the metal oxide layer starts to degrade as this threshold will depend on the cathode material (which is 310ºC for $LiFePO_4$ and 150ºC for $LiCoO_2$ cathodes, for example). Additionally, these high temperatures cause the decomposition of the electrolyte, which creates additional combustible gases. It is the interaction between the combustible gases and the oxygen generated that can lead to a violent reaction, which can cause a thermal runaway effect. A solution found for this problem is to use a separator that deforms when temperatures reaches a certain point, impeding the movement of lithium ions [49].

2.6.3. Pyrometallurgical processes

Pyrometallurgy involves thermal treatment to decompose the components of spent LIB modules. The process involves two steps. Firstly, spent LIBs are provided a low temperature in a furnace to reduce the danger of explosion and evaporation of the electrolyte. Secondly, all plastics and solvents are burned at a higher temperature to supply some of the energy for the smelting, followed by formation of slag and the reduction of valuable metals to an alloy of copper, cobalt, nickel and iron. These metals are then recovered from the alloy by leaching (a hydrometallurgical process). The slag is constituted by lithium,

aluminum, silicon, calcium, iron and any manganese that was present in the cathode material. However, recycling aluminum or lithium from the slag is neither energy or economically efficient [8, 46]

Currently, pyrometallurgical technologies have been combined effectively with hydrometallurgical processes by some companies such as Umicore, Accurec and Sony. Copper, nickel and cobalt can be recycled effectively, resulting in purified and gathered alloys, with the advantage of treating many spent LIBs at the same time and thus reducing the large-scale production costs and simplifying the operation. However, this process has several disadvantages, such as [46]:

1. It has a high energy-consumption due to the high temperature operation associated to extra instruments for the control of toxic gases;
2. All organic electrolytes, binders, acetylene black, and some others are mostly burned off;
3. Li and Mn cannot be recycled as they are trapped in the slag of complex materials.

Therefore, the recycling of LIBs that do not contain Ni or Co metals with pyrometallurgical processes is not economically beneficial [46].

2.6.4. Hydrometallurgical processes

Hydrometallurgical methods can be applied for the direct recovery of valuable transition metals such as Co, Ni, Mn and Li from the mechanical separated coating materials as well as the extraction of Al and Li from slag of pyrometallurgical processes. Moreover, products of the hydrometallurgical processes can be used to resynthesize the battery active materials [10, 54]

2.6.4.1. Leaching

The first step of a hydrometallurgical treatment is leaching of the regained powder fractions including the active material fraction, which dissolves the metallic fraction and recycled metal solutions for subsequent separation and recovery. The lithium-transition metal compounds are leached in inorganic or organic acids. The purpose of the leaching process step is to reduce the impurities and organic residues as well as to separate the different product metals, as purely as possible [54, 58].

In the alkaline leaching method, the cathodes are immersed in sodium hydroxide (NaOH) solution to dissolve aluminium foils into solution. The reaction of Al foils in NaOH is described in equation (6). After washing with water and filtration, Al foils and active materials are effectively separated [46].

$$2Al + 2NaOH + 2H_2O \rightarrow 2NaAlO_2 + 3H_2 \quad (6)$$

In recent years, acid leaching is the most widely used method in both industrial application and academic research since it benefits the chemical properties of metals in aqueous solution to isolate and recover a marketable product. The valuable metals from cathode materials are leached out, using either inorganic acids (e.g. H_2SO_4, HNO_3, HCl) or organic acids (e.g. succinic, ascorbic, citric) as leaching agents, often supported by reducing agents (e.g. H_2O_2, $NaHSO_3$, Na_2SO_3) which make the metal-forms easily dissolve in the acid solutions by oxidizing them to higher oxidation states [46]. The leaching efficiency depends

on several factors such as the nature of the cathode, the acid and reducing agent used and its concentration, the leaching time and temperature, stirring speed and the liquid/solid (L/S) ratio [59].

2.6.4.2. Impurities and purification

There are very high-quality battery requirements in the industry, especially for traction batteries and therefore these specifications need to be met after the recycling processes, which should be designed to gain raw materials with high quality to be reused for synthesize battery materials. For this reason, it is crucial to reduce to a minimum the impurities, which come from the mixture of materials and electrochemical reactions that occur during the battery's life as well as the recycling process itself. Regarding this subject, several proposes have been done, which can be found in literature [54].

2.6.4.3. Electrochemical processes

To regain high quality raw materials for a LCO battery active material synthesis, an electrochemical process called *Etoile-Rebatt* technology was used by Ra and Han (2006), in which separated $LiCoO_2$ was leached in a solution of LiOH and KOH, co-deposited on a platinum working electrode and precipitated again [54].

2.6.4.4. Solvent extraction

Cobalt can be regained by well-established solvent extraction technologies and manganese can be preliminarily removed using bis-2- ethylhexylphosporic acid [54].

Chapter 3. Experimental Methodology

The methodology followed in the experimental work was divided in several steps, using three spent lithium-ion battery modules from a hybrid electric vehicle provided by ValorCar (EPR) as a case study. The LIB modules were first discharged and manually dismantled. Afterwards, a physical and chemical characterization of the electrode material of one of the batteries was done, and a leaching step was completed to recover the metals included in the electrode material as stated in Figure 36.

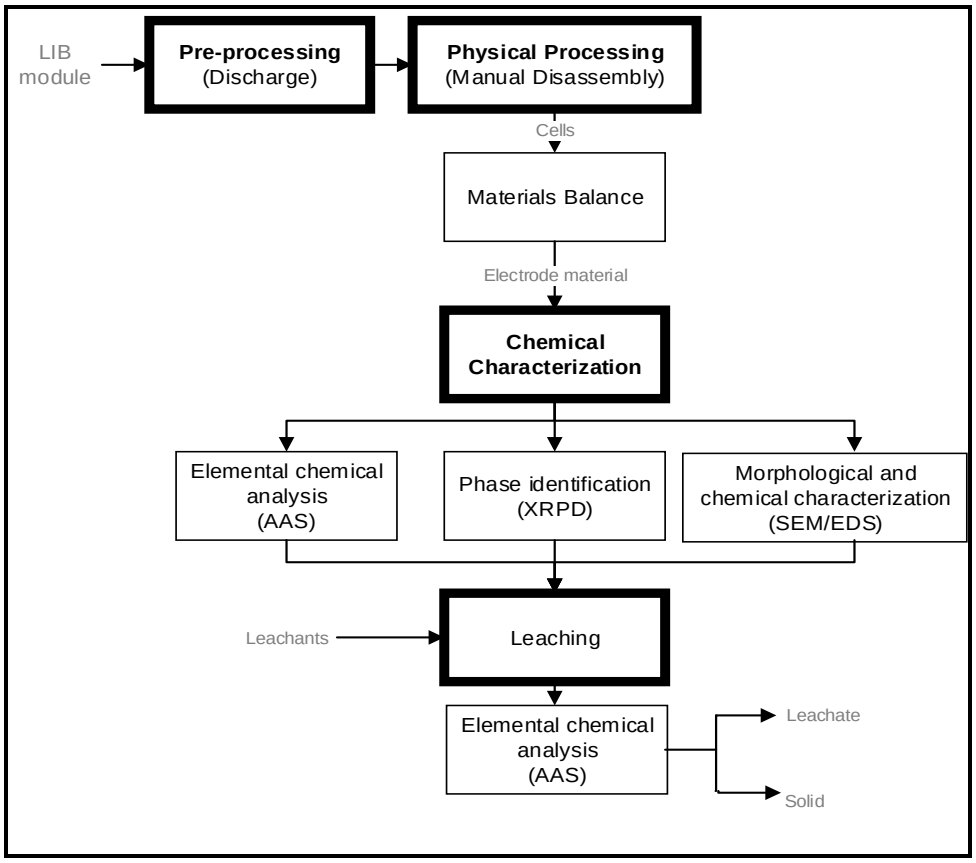

Figure 36 - Experimental methodology.

Table 5 shows the reference voltage of the LIB used and its nominal battery energy per unit mass (specific energy) which determines the battery weight required to achieve a given electric range along the energy consumption of the vehicle. Additionally, the capacity, which is the total Ah available when the battery is discharged at a certain discharged current from 100% state-of-charge (maximum capacity) to the cut-off voltage (minimum allowable voltage; it is the voltage that defines the “empty” state of the battery) and the weight and number of cells per module are also indicated. [60].

Table 5 – Specifications of the lithium-ion batteries modules used.

	Module	Cell
Voltage [V]	126	3.5
Specific energy [Wh/kg]	37	22.8
Capacity [Ah]	6.5	
Weight [kg]	21.9	
Number of cells inside	35	

The battery modules used, respective dimensions and projection view are shown in Figure 37.

Figure 37 – Projection view of the LIB module used.

3.1. LIB discharge

One of the first steps of every battery recycling process is the disassembly. However, when a charged or partially charged battery is improperly handled it may catch fire or explode. For that reason, it is preferable to discharge the energy stored in the battery before the disassembly [49, 61, 62].

This experimental step, besides the need of battery dismantling for characterization purposes, can also provide important information on the development of a procedure for safe discharge and disassembly of a LIB used in a HEV.

The 35 cells of the LIB module from a HEV were discharged using a domestic oil heater as a resistor in order to create a simple circuit represented in Figure 38.

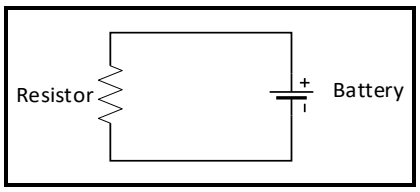

Figure 38 – Representation of the used electric circuit in the discharging of the LIB.

The discharge method used in this project was the (almost) constant resistance discharge since the resistance varies with the temperature and therefore it is never 100% constant. In alternative, either the constant current discharge method or a discharge by electrolysis of a conductive liquid medium could have been used to discharge the LIBs [54, 63].

During the discharging process, the current and voltage were measured to guarantee that the corresponding values would tend to zero. The measurements were done at 3 different oil heater powers for the first LIB (2 kW, 1.25 kW and 0.75 kW) as a test. However, since the temperature of the cells did not increase (being always under 55ºC, which is far below the 90ºC threshold necessary for the SEI layer to decompose), for the other two LIBs, the measurements were made with the highest discharge

power. The resistance measured for the LIB 1 was 26 Ω, 39 Ω and 42 Ω for three different powers tested in the oil heater, respectively 2 kW, 1.25 kW and 0.75 kW. For the LIB 2 and LIB 3, the (almost) constant resistance applied was around 19 Ω and 26 Ω, respectively

The following procedure, shown in Figure 39 was repeated for 3 different lithium-ion modules and the temperature of the weld was constantly measured using an infrared temperature tester thermometer. All the windows and the door of the laboratory were kept open while discharging the LIBs to guarantee a well-ventilated area to minimize exposure to toxic gases from the electrolyte.

Figure 39 – Followed discharging procedure.

3.2. LIB disassembly

After the discharge, the batteries were disassembled. The purpose of the disassembly is to allow the separation of the battery cells from other structural and connecting components for the subsequent processes and it is desirable to maintain the high quality of the recovered raw materials. The disassembly is carried out completely manually with the help of hand tools, as described in Figure 40. The process started with the opening of the battery system, i.e. removal of the cover, and ended with the removal of the mechanical connections between the system components and the base. The separation of the battery cells from the cells base (see the nomenclature explanation in Table 8) is explained in the section 4.2 and the disassembly of the LIB cells themselves is explained in section 3.3.

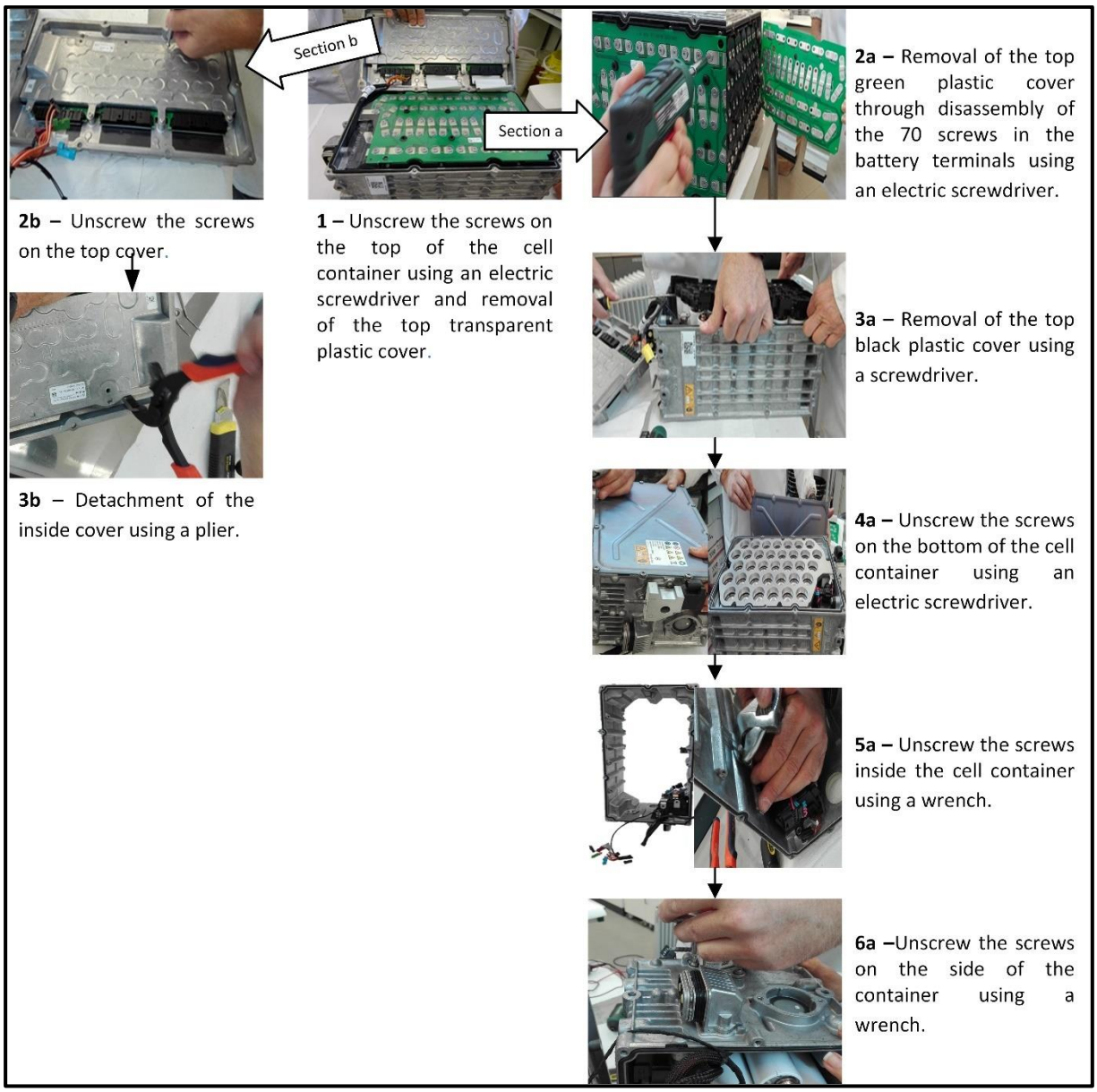

Figure 40 - Followed disassembly process.

3.3. Materials balance of components

The aim of this experimental step is to determine the average weight of each cell component of a spent LIB of a HEV, thus performing a complete mass balance in order to contribute to a better definition of the recycling process of these spent products. Three cells were subsequently disassembled and characterized.

First, the plastic protection of the cells was cut using a cutter and then the top cap was opened with a cutting disk – this part of the process took 2 minutes per cell and was done without damaging the cells. Afterwards, the separators, the cathode, the anode and the insulation film were unrolled and then carefully split to avoid any contamination (see Figure 41). The different parts were weighed and measured, including the electrodes, the cell can and the separator

Figure 41 - Disassembly of the battery cells.

3.4. Chemical characterization

The present section aims at explaining the chemical characterization methods used on the electrode materials of a LIB since they are constituted by several metals with economic value and therefore are major components to be considered in the recycling process of LIBs.

3.4.1. Phase identification (XRPD)

The phase analysis of the active electrode materials was conducted by X-ray powder diffraction (XRPD, PANanalytical X'PERT-PRO diffractometer). The preparation of the cathodic and anodic active materials samples is described in Figure 42. XRPD analysis was carried out using CuK_{α} radiation and a scan step size of 0.050° (2θ), a step time of 75 s, and generator settings of 35 mA and 40 kV.

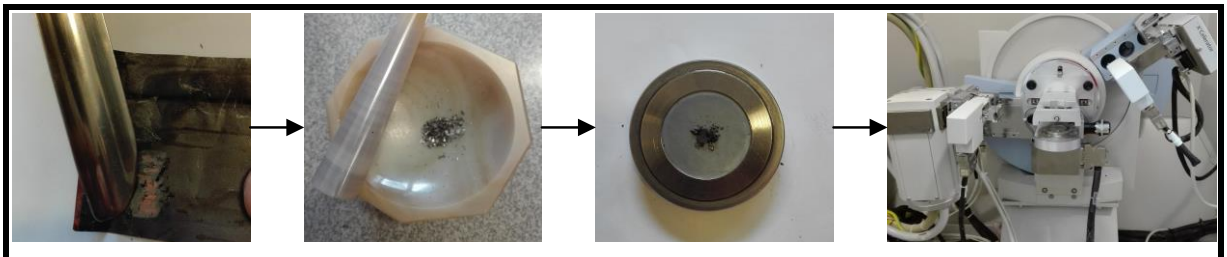

1) The active electrode materials were separated from the current collector using a spatula

2) The samples were transferred into the mortar and grounded using the pestle.

3) The samples were transferred into the sample-holder.

4) The samples were placed in the diffractogram from an XRPD analysis.

Figure 42 – XRPD sample preparation followed procedure.

Phases identification was made by comparing the interplanar distances and intensities observed in the diffraction patterns obtained using the X'PERT HIGHSCORE PLUS software with the phases present in the PDF2 database.

3.4.2. Elemental chemical analysis (AAS)

The elemental chemical composition was quantified by flame atomic absorption spectrometry (AAS) (thermoelemental 969AA) by analysing different metals in solution. A previous digestion procedure of the solid samples was therefore necessary, using strong and concentrated acid mixtures. Two different attacks were attempted: one with HCl/HNO_3 and another with HCl/H_2O_2. The final purpose of this procedure is to determine the concentration weight % of the Li, Ni, Co, Al and Mn elements on the electrode materials and therefore know the LIB type. The followed methodology is represented in Figure 43.

The flame AAS analytical technique is based on the principle that ground state metals absorb light at a specific wavelength, corresponding to the necessary energy to make electrons jump to a higher energy level, emitting a photon of light. The samples are atomised, i.e. the metal ions in a solution are converted into ground state free atoms by means of a flame and the radiation from the specific light source is focused on the atomic vapor in the flame and enters a monochromator. The amount of light absorbed by the sample, that is measured by reading the spectra produced when the sample is excited by radiation, is directly proportional to the number of the atoms of the chosen element, i.e., the absorbance is directly proportional to the concentration of the analyte absorbed for the existing set of conditions. The concentration is calculated based on the Beer-Lambert law, equation (7) [64].

$$A = \varepsilon . b . c \tag{7}$$

Where A is the measured absorbance;

ε is wavelength-dependent molar absorptivity coefficient;

b is the path length;

c is the analyte concentration.

The concentration is determined from a calibration curve, obtained using standards of known concentration because the Beer-Lambert is only linear under specific conditions. For instance, at high concentrations it makes inaccurate measurements due to the stronger interatomic and electrostatics interactions in the atoms of the analyte that happen because of the reduced amount of space between atoms, which can change the molar absorptivity of the analyte. Besides, high concentrations also change the refractive index of the solution causing deviations from the Beer-Lambert law. The wavelengths and the standard concentration ranges used of each element are represented in Table 6.

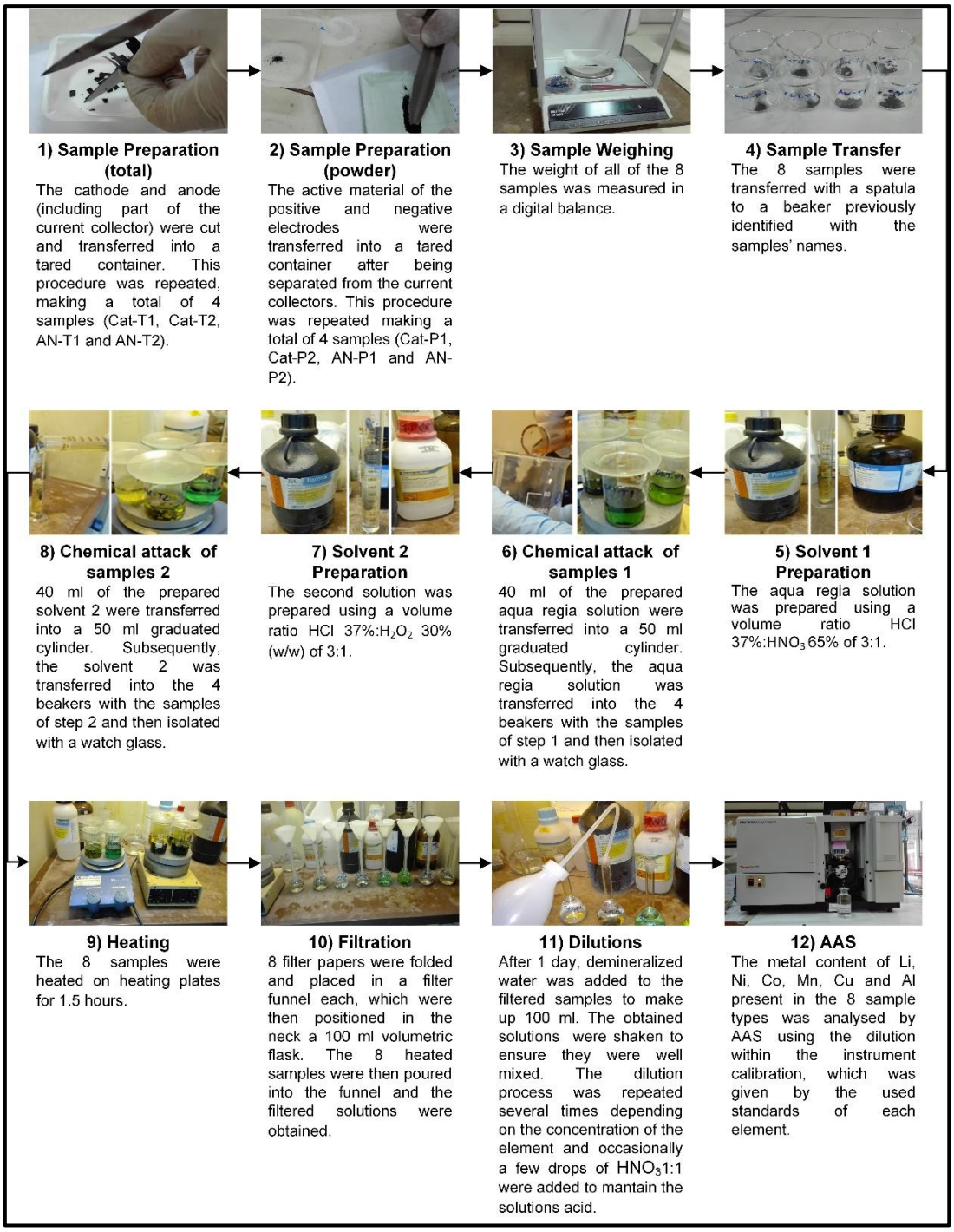

Figure 43 - Followed spectroanalytical procedure.

Table 6 – Wavelength and standards concentration used in AAS for Li, Ni, Co, Cu, Al and Mn.

	Li	Ni	Co	Cu	Al	Mn
Wavelength (nm)	670.8	2.32	240.7	324.6	396.2	279.5
Concentration range of calibration curves (mg/L)	0,2-1,5	0,5-6	0,2-5	0,5-3,5	10-60	0.5-3

3.4.3. Morphological and chemical characterization (SEM/EDS)

Scanning electron microscopy (SEM) (JEOL JSM 700 1F microscope) was used for studying the surface morphology of the electrode materials (the active electrode material) by detecting secondary electron image (SEI) and backscattered electrons (BSE). Additionally, the SEM used was equipped with an EDS analyser to perform compositional analysis on the samples, i.e., to identify materials and contaminants, as well as to estimate their relative concentrations on a specific area within the area of interest at the surface of the specimen.

The contrast in the images given by the BSE are a result of the contrast in the atomic number between different elements with atomic number differences of at least 4 (it does not detect Li) as heavier elements scatter electron more efficiently and therefore show up brighter in the images. On the other hand, the topographic contrast is given by the SEI as the brighter regions in the images correspond to hills on the surface of the sample [65].

For this analysis, 4 different samples were used (2 with only the active electrode material – either cathodic or anodic – identified as “P” samples and 2 also with the current collector for the cathode and the anode identified as “T” samples). Figure 44 shows the analysed samples.

Figure 44 – Cathodic and anodic samples (“P” and “T”) analysed by SEM.

3.5. Leaching tests

The leaching tests were performed on the electrode materials (cathode and anode, mixed in proportional weights), including the metal current collector sheets. The aim of these experiments was to evaluate the leaching behaviour of the valuable metals contained in the electrodes as well as the contamination resulting from the collector sheets. Hydrochloric and sulphuric acid solutions were tested, with or without different reducing agents. The followed methodology is represented in Figure 45.

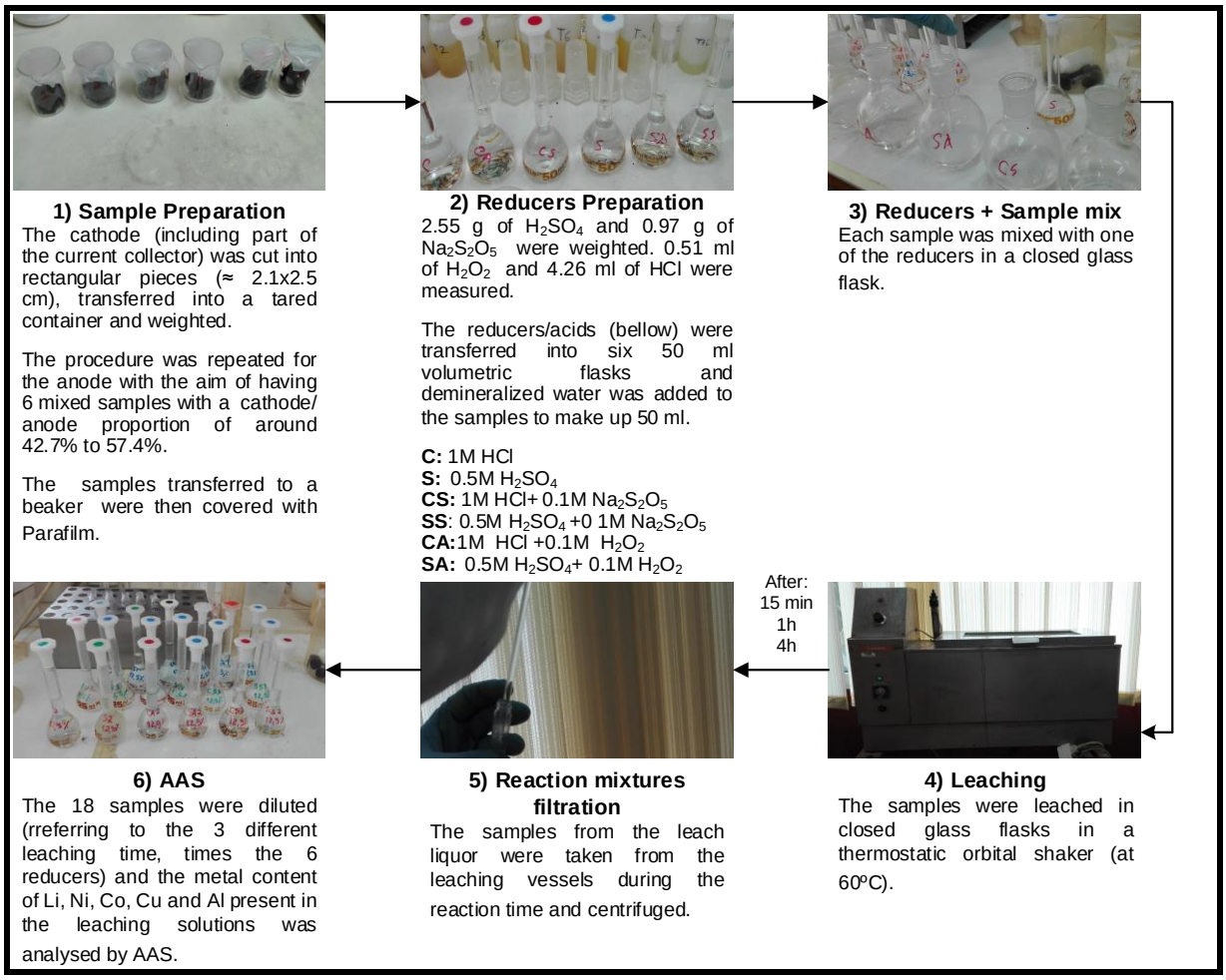

Figure 45 - Followed leaching procedure.

In order to calculate the necessary mass to obtain 0.5M H_2SO_4 and 0.1M $Na_2S_2O_5$, as expressed in step 2 of the leaching procedure, equation (8) was used.

$$mass = desired\ molarity \times volume \times Mw \times purity \quad (8)$$

Where *desired molarity* is 0.5, 0.1, 1 and 0.1 for H_2SO_4, $Na_2S_2O_5$, HCl and H_2O_2, respectively [mol/L];
volume is 0.05 l, corresponding to the volume of the volumetric flask [L];
Mw is the molecular weight [g/mol];
Purity is 0.96, 0.98, 0.37 and 0.30 for H_2SO_4, $Na_2S_2O_5$, HCl and H_2O_2, respectively [w/w].

In order to calculate the necessary volume to obtain 1M HCl and 0.1M H_2O_2, the mass was divided by the density of the solution.

Page intentionally left blank

Chapter 4. Results and Discussion

4.1. Discharge

The current intensity in the wire and the open circuit voltage (total and individual) were measured directly using a multimeter for a given oil heater power. The internal resistance of the oil heater was calculated using Ohm's law as expressed in equation (9) assuming a constant resistance (R), which is not absolutely accurate since the resistance changes with the temperature.

$$R = \frac{V}{I} \tag{9}$$

Where V is the operating voltage and I is the current.

The open circuit voltage was measured before the battery was submitted to any charge and its value should be identical to the average individual open circuit voltage multiplied by the 35 cells since the cells were in series. The applied power (P) was calculated as expressed in equation (10).

$$P = V.I \tag{10}$$

Where V is the operating voltage and I is the current in the wire.

The results obtained are summarized in Table 7. All the batteries were initially charged since the V_{oc} was above zero volts. The battery was considered discharged when the operating voltage was below 200 mV. This result was achieved after less than 4:46 hours for the LIB 3, however, for safety reasons, all the batteries continued discharging for 24 hours.

Table 7 - Measured current in the wire and operating voltage for a given oil heater power and time and comparison between the measured open circuit voltage and the calculated open circuit voltage.

LIB	I (A)	V (V)	Time (h)	Calculated P (W)	Calculated R (Ω)	V_{oc} (V)	Calculated V_{oc} (V)	V_{oc} error (%)	Individual V_{oc} (V)
1	2.97	126.2	NA	374.81	42	128	128.1	0.078	3,660 ±0.01
	3.20	126.1	NA	403.52	39				
	4.90	125.9	NA	616.91	26				
2	6.30	121	00:00	762.30	19	121	119.0	1.624	3.401±0.02
	0.17	2.958	01:45	0.50	17				
	0.04	1.484	02:29	0.06	37				
	0.03	0.595	03:19	0.02	20				
3	5.00	127.8	00:00	639.00	26	129	129.4	0.256	3.697±0.03
	4.84	124.8	00:17	604.03	26				
	0.05	1.205	03:59	0.06	24				
	0.07	0.03	04:46	0.002	0				

NA means not analysed. The dismantling of the LIB1 was only exploratory and therefore the times were only measured for LIB2 and LIB3.

From the results of the individual $V_{oc,}$ it is possible to observe that the voltage in each cell was identical, as expected since they have a series connection. This shows that the cells were not damaged and therefore it is safe to proceed to the next step (disassembly) after the discharge. The aim of this experimental step was successfully achieved as the discharge procedure for a HEV was done.

4.2. Disassembly

The main components of the EV battery system used are shown in Figure 46, labelled with a number later used for reference.

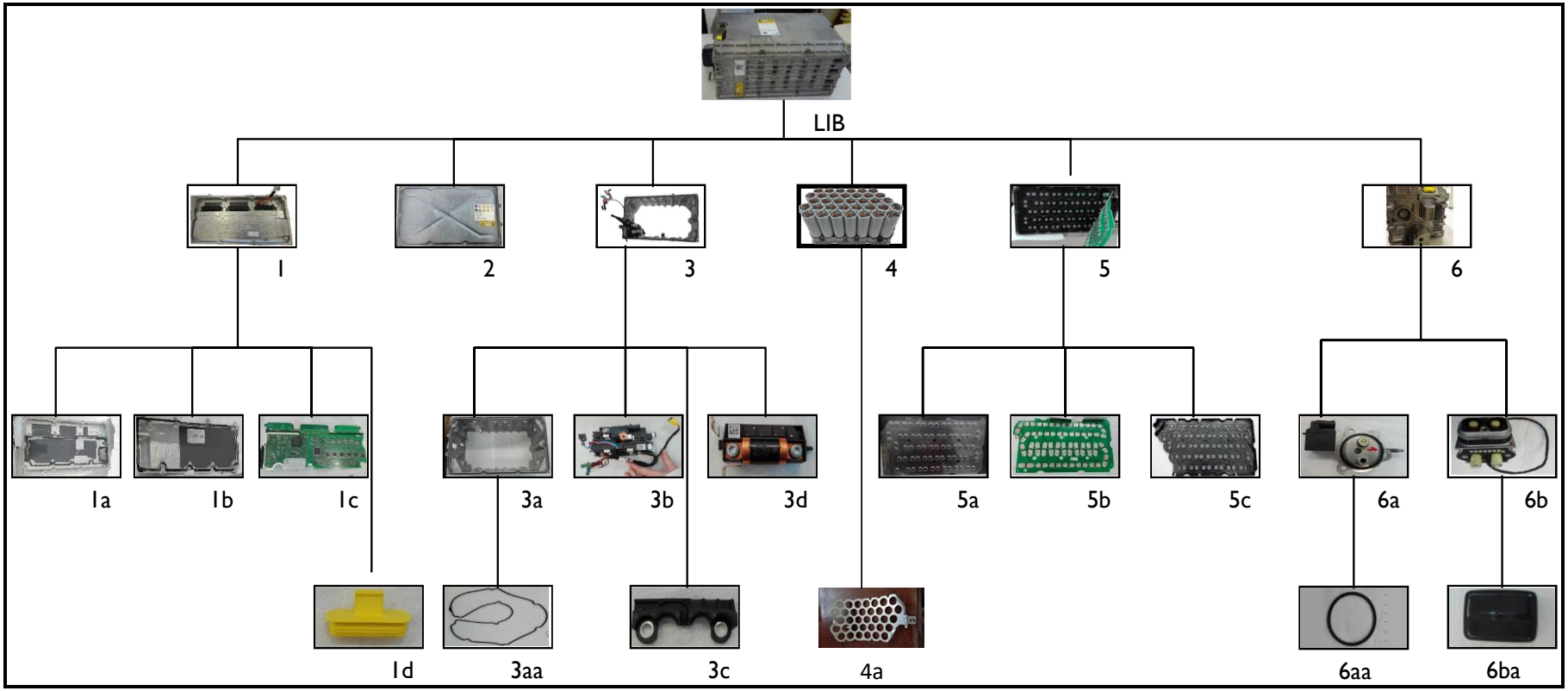

Figure 46 - Main components of the HEV battery system used after disassembly.

In order to plan the disassembly process, it is important to consider that there is a wide variety of lithium-ion battery designs, flexible components like cables and the dangerous substances as the gases from the electrolyte contained in the battery cells. All these factors contribute to a complex disassembly of LIB systems in automotive applications and therefore it is a cost and time-consuming process.

The descriptions of names and numbers used according to Figure 46 are shown in Table 8.

Table 8 –Identification of the main components of the HEV battery system used.

Component		**Sub-component**	
Number	**Name**	**Number**	**Name**
1	Top cover	1a	Outside cover
		1b	Inside cover
		1c	Battery management system (BMS) – electronic boards
		1d	External plastic lid
2	Metallic base	----------	----------
3	Metallic container	3a	Container
		3aa	Rubber insulator strip
		3b	Box
		3c	Connector 3b/3d
		3d	Service Battery
4	Battery cells	4a	Cells base
5	Top cell terminals plastic protections	5a	Transparent insulator
		5b	Green insulator/ cell terminal protection
		5c	Black insulator
6	Right part of the LIB module	6a	Valve
		6aa	O-ring
		6b	Connector terminal
		6ba	Lid 2

During the disassembly process, there was no need to use specialized tools. Instead, only a small number of different tools were used. However, to use this process in industry one difficulty arises from the screws that have different measures and heads and therefore require different types of screwdrivers for the disassembly, which also increases the time for the disassembly since a certain amount of time

will be spent for changing the tool. Moreover, not all screws are accessible from the same direction, requiring several orientation changes of the tool and even a turn-over of the whole battery.

Nevertheless, the main difficulty was the disassembly of the battery cells (4) since they are connected to the cells base (4a) through a polymer. This polymer is possibly a thermoset with flame retardant because when in contact with a flame, the flame disappears almost instantaneously, which is most likely a security measure to prevent the battery from catching fire.

To separate the components (4) and (4a), 24 different solvents (see Table 9) were tested in contact with a sample from the polymer.

Table 9 – Identification of the solvents used in an attempt to dissolve the polymer.

Nr	Name	**Nr**	Name	**Nr**	Name	**Nr**	Name	**Nr**	**Name**	**Nr**	Name
1	CH_2Cl_2	5	$CHCl_3$	**9**	C_3H_6O	**13**	$C_2H_4Cl_2$	**17**	C_7H_8	**21**	HCl 27%
2	C_6H_{14}	**6**	CH_3OH	**10**	C_3H_7NO	**14**	C_3H_8O	**18**	C_3H_8O	**22**	NH_3 25%
3	CH_3CN	**7**	C_2H_6OH	**11**	$C_4H_8O_2$	**15**	EGDME	**19**	HNO_3 65%	**23**	HF 25%
4	$C_4H_8O_2$	**8**	$(C_2H_5)_2O$	**12**	C_2H_6OS	**16**	$C_2H_5NO_3$	**20**	H_2SO_4 35%	**24**	Aqua Regia

However, as shown in Figure 47, it was not possible to dissolve the polymer using the referred solvents and for that reason, a mechanical approach was chosen instead to separate the components (4) and (4a).

Figure 47 – Solvents in contact with the polymer.

A mechanical lathe was successfully used to separate the components (4) and (4a) as shown in Figure 48. However, this process was time-consuming and required physical strength from the operator and therefore it is not the best option for the disassembly of these components. This problem shows that the initial product design could be improved, for example, by following the guidelines of design for disassembly as proposed in [66], in which a three-pronged strategy involving technology, methodology and human factors is discussed, acknowledging the need for a systematic disassembly sequence, a method for “one-to-many” disassembly and finally the importance of human factors involved in manual disassembly.

Figure 48 – Mechanical lathe used to separate the components (4) and (4a).

It is important to notice that the batteries were manually dismantled as it is the general case in the industry due to the many types of products, the non-existent standards in battery design and the fact that the detailed designs of the batteries are not usually available to the recycler. This leads to a higher labour cost, however, for the same reasons a fully automated disassembly may not be the best approach. Instead, a robot-assisted disassembly could be a suitable option for an industrial process, in which the unscrewing task could be mainly done by the robot as it is a simple technique that has been automated previously and has widespread application in the disassembly of EV batteries [67, 68].

4.3. Materials balance of components

The cylindrical cells of the spent LIB are composed of several components. A schematic drawing of the main parts of a sealed cylindrical Li-ion cell battery similar to the one worked with in this project is shown in Figure 49. The material of the exterior case is aluminium, which is covered with a plastic label.

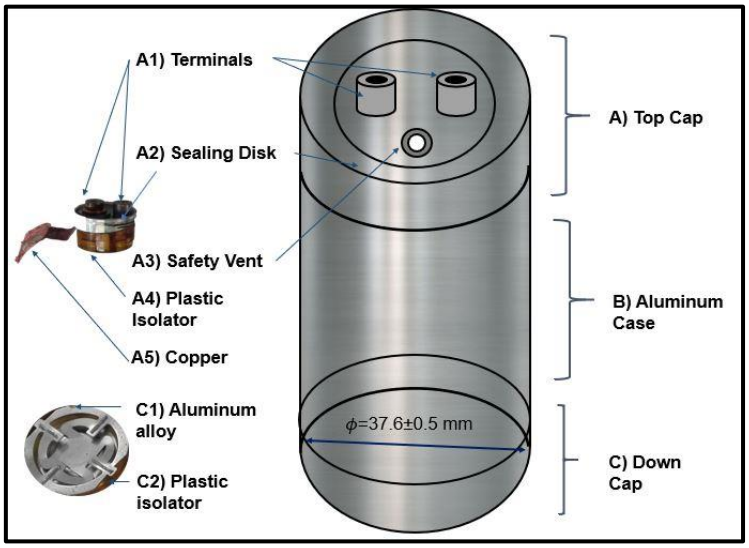

Figure 49 - Schematic drawing of the Li-ion battery cell constitution.

The dismantling of cylindrical Li-ion cells showed that the electrode structure is jelly-roll type, in which the electrodes are separated by a polymer sheet impregnated with an electrolyte. There are two separating sheets and the components of the cells are arranged in layers of separator-anode-separator-cathode as shown in Figure 50.

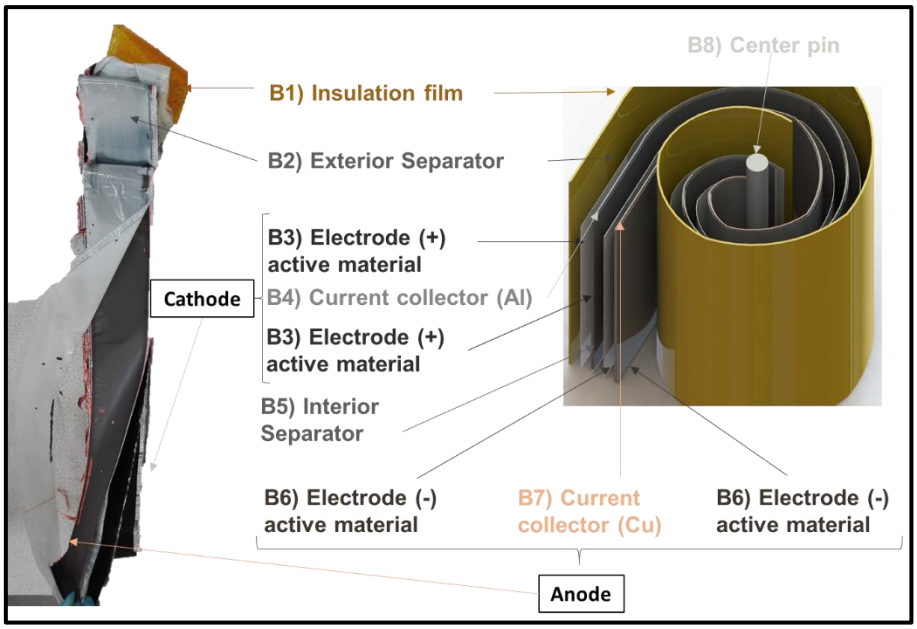

Figure 50 - Components arrangement and details of the electrodes in the cylindrical cells.

The cathode is constituted by an aluminium current collector with an electrode powder on both sides and the anode is composed of a copper current collector with an electrode powder on both sides. It was possible to observe that the electrode power both in the cathode and in the anode were compacted and its separation from the respective current collector was not viable.

For that reason, the mass of the aluminium and copper foil in each cell was calculated using equation (11).

$$M_{metal\_foil} = W_{metal\_foil} \times L_{metal\_foil} \times \delta_{metal\_foil} \times \rho_{metal\_foil} \quad (11)$$

Where M_{metal_foil} is the mass of the metal (aluminium or copper) foil [g];
W_{metal_foil} is the width of the metal (aluminium or copper) foil [cm];
L_{metal_foil} is the length of the metal (aluminium or copper) foil [cm];
δ_{metal_foil} is the thickness of the aluminium foil (0.0034 cm) or copper foil (0.0021 cm);
ρ_{metal_foil} is the density of the aluminium (2.7 g/cm^3) or copper (8.96 g/cm^3).

The measured dimensions are represented in Figure 51. The components are (from left to the right) the insulation film, the exterior separator, the cathode, the interior separator, and finally the anode. The electrodes and the separators have more than 4 m of length but since the sheets are all very thin (in the order of micrometres), they fit inside the cell can which has a diameter of 37.6 ±0.5 mm. The current collectors have a higher width compared to the one of the corresponding active material

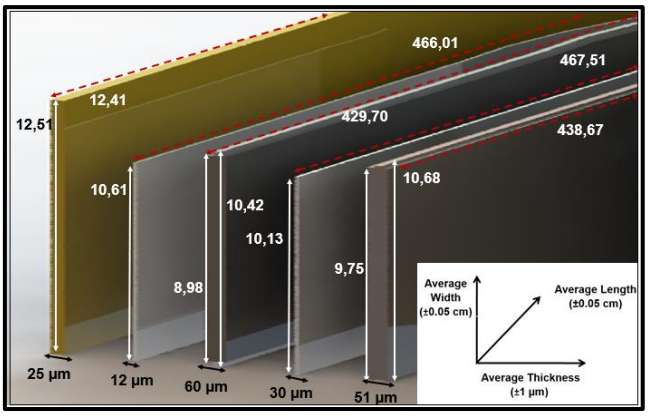

Figure 51 – Average measured dimensions of the cell components B1 to B7.

The mass balance for the 3 cells was performed as presented in Table 10, in which the average values correspond to the dismantling of those cells (C, X and Z).

Table 10 - Materials mass balance of the main components of the cells of lithium-ion batteries.

		Weight									
		C Cell		X Cell		Z Cell		Average			Total for 35 cells
Material/Component		(±0,05 g)	(%)	(±0,05 g)	(%)	(±0,05 g)	(%)	(±0,05 g)	(%)	DESVPAD	(±0,05 g)
Anode *	B7	58.9	18.6	104.2	32.0	105.3	32.6	89.5	27.8	26.5	3132.6
	B6	48.6	15.3	7.0	2.1	6.0	1.8	20.5	6.4	24.3	717.4
	Sub-total	107.5	33.9	111.2	34.1	111.3	34.5	110.0	34.2	2.2	3850.0
Cathode *	B4	34.6	10.9	41.1	12.6	48.4	15.0	41.4	12.9	6.9	1448.1
	B3)	48.3	15.2	42.1	12.9	31.5	9.8	40.6	12.6	8.5	1421.9
	Sub-total	82.9	26.1	83.2	25.5	79.9	24.7	82.0	25.5	1.8	2870.0
Polymers	A4	6.2	2.0	6.1	1.9	6.2	1.9	6.2	1.9		215.8
	External plastic isolator	4.2	1.3	3.8	1.2	4.1	1.3	4.0	1.3	0.2	141.2
	B1	0.7	0.2	0.8	0.2	0.8	0.2	0.8	0.2	0.1	26.8
	B2	10.9	3.4	10.6	3.3	10.5	3.3	10.7	3.3	0.2	373.3
	B5	10.0	3.2	10.9	3.3	15.2	4.7	12.0	3.7	2.8	421.2
	C2	0.7	0.2					0.7	0.2		24.5
	Sub-total	32.7	10.3	32.2	9.9	36.8	11.4	33.9	10.5	2.5	1186.5
Metals	A1 + A2+A3	27.3	8.6	27.2	8.3	27.0	8.4	27.2	8.4	0.2	950.8
	A5	5.2	1.6	5.1	1.6	5.2	1.6	5.2	1.6	0.1	180.8
	Lateral Cell can	19.9	6.3	25,4 **	7.8	25,5 **	7.9	23.6	7.3	3.2	826.0
	B8	8.9	2.8	9.2	2.8	9.2	2.8	9.1	2.8	0.2	318.5
	C1	4.3	1.4					4.3	1.3		150.5
	Sub-total	65.6	20.7	66.9	20.5	66.9	20.7	66.5	20.6	0.8	2326.3
Cell (without dismantling)	Total***	317.1	100	325.8	100	322.9	100	321.9	100	4.4	11260.2
	Calculated total	288.7		293.5		294.9		292.4		3.3	7362.8
	Mass lost (%)		9.0		9.9		8.7		9.2	0.7	34.6

* The uncertainty of the cathode and anode weight is ±0.05 g. This calculus can be found in Appendix D.
**With component C
***Total weight of the cell before dismantling

The mass lost (9%) is most likely the mass of the electrolyte and some of the metal in the top cap due to the cutting process. Approximately 34% of the cell weight is the anode and 26% is the cathode (both including electrode powders and collector foils). The cell can (lateral, top and bottom) contributes to 17% of the cell weight while the separator is around 7% of the cell. Other polymers, essentially insulating parts, weigh near 4%. Another distribution exercise can be made in terms of metals and compounds: about 27% is aluminium (from case materials and collector foil), 28% is copper (essentially from collector foil), 6% is graphite and 13% is the lithium-transition metals oxide.

The comparison between these values with the bibliography (see Figure 23) is presented in Figure 52. The major discrepancy is in the anode which may be related with the fact that the values in the literature refer mainly to the LIBs used in consumer electronics.

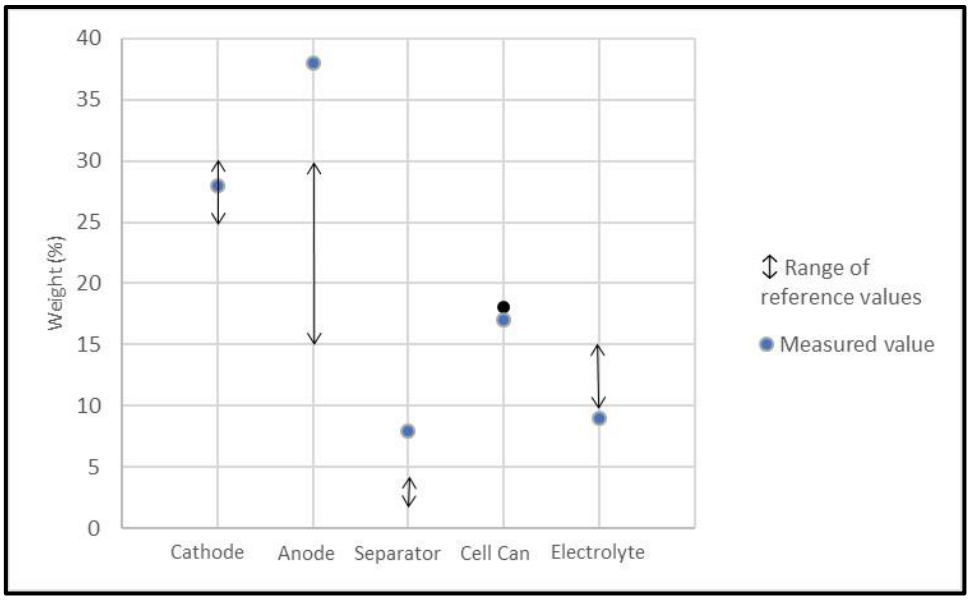

Figure 52 - Comparison between the obtained values of weight (%) of the cell components with the referenced values.

4.4. Phase and chemical characterization

4.4.1. Phase identification (XRPD)

Phase identification of anodic and cathodic active materials was carried out by X-ray powder diffraction (XRPD). The patterns obtained, presented in Figure 53, show the presence of diffraction lines corresponding to graphite and copper (JCPDS files nrs. 00-008-0415 and 00-004-0836) in the anode and $LiNiO_2$ (JCPS file nr. 00-009-0063) in the cathode. In the cathode pattern, a fluorescence effect was detected (not shown in Figure 53), which indicates the presence of Fe, Ni or Co, and corrected.

The graphite and $LiNiO_2$ identified correspond to the active anode and cathode materials of the batteries, respectively. These results are compatible with the common battery composition, graphite in the case of the anode and for the cathode it is in the composition comprised of $LiMO_2$, where M represents a transition metal like Ni, Co, Mn and Al, at different atomic ratios Generally, the XRD patterns do not differ significantly between the different compositions (besides small deviations in some reflexions) and so the patterns obtained in the sample can be any kind of the above referred species. The copper

detected in the anodic sample is probably an impurity due to an insufficient separation of the active material from the current collector.

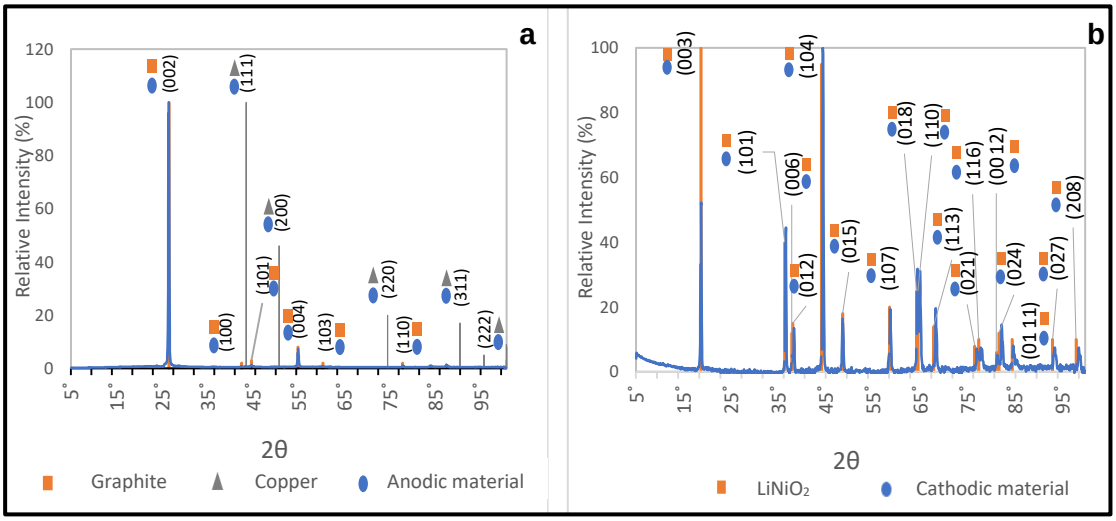

Figure 53 - XRPD patterns (CuKα radiation without filter) of electrodic material and phase identification: a – anode; b – cathode

The diffraction lines corresponding to the graphite (in the anode) and $LiNiO_2$ – type (in the cathode) phases are narrow revealing well crystallized materials. In addition, some peak deviations were found in the pure $LiNiO_2$ alloy phase, probably related to a solid solution where Ni is replaced by Mn and/or Co (according to section 2.5.2.1) in the active cathodic material.

4.4.2. Elemental chemical analysis (AAS)

Quantitative elemental chemical analysis of the battery electrodes was performed by AAS after complete solubilisation of the electrode materials, using either aqua regia (identified with solvent 1) or $HCl:H_2O_2$ (identified with solvent 2). The analysed samples were the electrode material, including the current collector (identified with the letter T as in "total") or only the active material (identified with the letter P as in "powder"). The (%w/w) of the elements was calculated according to equation (*12*).

$$(\%w/w) = \frac{concentration\ [mg/L] \times dilutionfactor \times initial\ volme\ [L]}{weight\ [mg]} \qquad (12)$$

Elemental chemical composition of electrodes is presented in Table 11.

Table 11 shows that there is not much difference in the obtained concentration of the elements using either solvent 1 or 2. The cathode is very rich in nickel, with the cobalt and lithium content much lower. Most of the aluminium content seems to be in the current collector, however, there is still some aluminium in the active cathodic material. The copper content is almost non-existent and is probably due to a contamination from the anode. Concerning the anode, the copper content is very high in the "T" samples since the current collector is indeed copper, however, neither aluminium or cobalt were detected. Nickel's concentration is almost non-existent as well as lithium, but its content can be explained by the presence of some lithium ions in the anode during the charging process that were not all transferred to the cathode in the discharging process.

In the active anodic material, around 98% of its constitution was not evaluated by AAS but it is probably referent to the graphite phase, as it was reported in the XRPD. For the cathode, there is a difference of around 26% of unidentified elements, which may be related with the presence of the electrolyte, binder, carbon conductive powder and other unidentified elements/compounds. This last explanation is based on the fact that in the samples with active cathodic material, the powder remained at the surface of the beaker after being mixed with the solvents (see steps 6 and 8 of the Figure 43), which did not happen for the active anodic powder, which was uniformly dispersed in the beaker.

Table 11 - Elemental chemical composition (%w/w) of the electrode materials.

Electrode material	ID	% Li	% Ni	% Co	% Cu	% Al	%Mn	% O*	SUM	Balance
Cathode	T1	4.0	22.3	4.0	1.8	23.6	n.d.	18.6	74.4	25.6
	T2	4.0	22.1	3.9	0.4	24.0		18.4	72.8	27.2
	P1	5.4	35.6	7.0	0.5	1.1		24.7	74.3	25.7
	P2	5.5	34.1	7.4	0.5	1.1		25.5	74.1	25.9
Anode	T1	0.2	0.1	n.d.	50.6	n.d.			50.8	49.2
	T2	0.1	0.1		47.9				48.2	51.8
	P1	0.0	0.2		1.6				1.9	98.1
	P2	0.2	0.2		1.7				2.2	97.8

n.d. – not detected (below determination limit)

* The oxygen (%w/w) was calculated assuming a 1Li:2O stoichiometry

Considering that the cathode and anode constitute 28% and 37.6% of the battery cell weight respectively, each cell contains approximately the chemical composition presented in Table 12. Taking into account that the 35 cells weight 11.2602 kg and that the total weight of the battery module is 21.9 kg, the cells represent 51.4% of the module and therefore it is possible to estimate the metal composition of batteries. However, aluminium's content is not possible to estimate since it is present in many other components, e.g. 1, 2, 3, 6, C1 and B, and the copper value will be inferior to the real one since it is also present in other components like A1 and A5.

Comparing the experimental data with those determined by other authors (see Figure 26 and Figure 27) most of the elements are within the reported values. The major difference seems to be in the lithium content, which is lower considering both the reports for the cell and module. However, the available data shall be consulted with precaution as they are referent to the broad range of LIB chemistries. In particular, in the case of the cobalt, in some reports there is no cobalt content (for the module) and for the cell the minimum content found was 5%, meaning that data found for the cells cannot be from NCA batteries.

Table 12 – Chemical composition (%w/w) per cell and per lithium-ion battery module and its comparison with the reported values (see Figure 26 and Figure 27).

Chemical composition (%w/w)		Li	Ni	Co	Cu	Al
Per cell	Experimental*	1.1	5.7	1.0	17.1	6.1
	Reported	2-12	0-10	5-30	7-17	3-10
	Comparison	Slightly below the reported results	Within the reported values	Significantly below the reported results	Within the reported values	Within the reported values
Per module	Experimental*	0.6	2.9	0.5	> 8.8	
	Reported	1.2-2	0-15	0-17	7-17	
	Comparison	Slightly below the reported results	Within the reported values	Within the reported values	Possibly within the reported values	

*The experimental results are the average of 3 samples.

A summary of the constitution in %w/w of the LIB studied is presented in Figure 54.

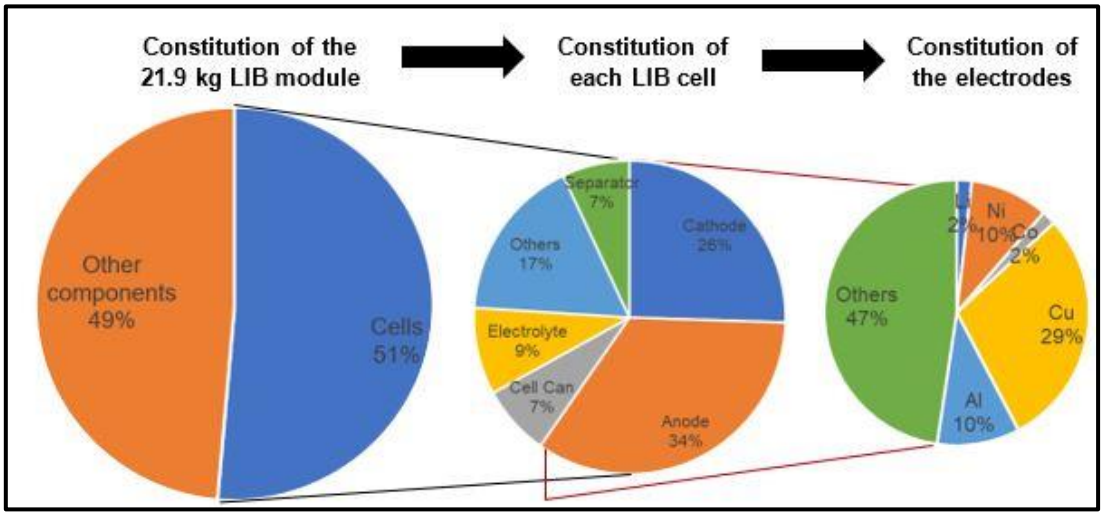

Figure 54 – Constitution of the studied LIB module, cell and electrodes (%w/w).

Finally, to identify the active cathodic material composition, the obtained weight of the Li, Ni, Co and Al for the "P" samples was standardized by dividing the average weight of the P1 and P2 samples for each element by the atomic weight of the element and then converted to make lithium correspond to 1 as in the stoichiometry $LiMO_2$, as indicated in Table 13.

Table 13 – Experimental standardized weight of Li, Ni, Co and Al elements and its conversion.

Element	Standardized weight	Converted weight
Li	0.78	1.00
Ni	0.59	0.76
Co	0.12	0.16
Al	0.04	0.05

With the results presented in Table 13, the most likely composition for the active cathodic material is $Li(Ni_{0.8}Co_{0.15}Al_{0.05})O_2$ and therefore the battery analysed is presumably a NCA battery type.

4.4.3. Morphological and chemical characterization (SEM/EDS)

The SEM analysis of the surface of the anodic materials of lithium-ion batteries showed particles with euedric morphology. Figure 55 shows a SEM micrograph of the anodic material for the "T" sample, as well as two EDS spectra obtained in different phases of the sample.

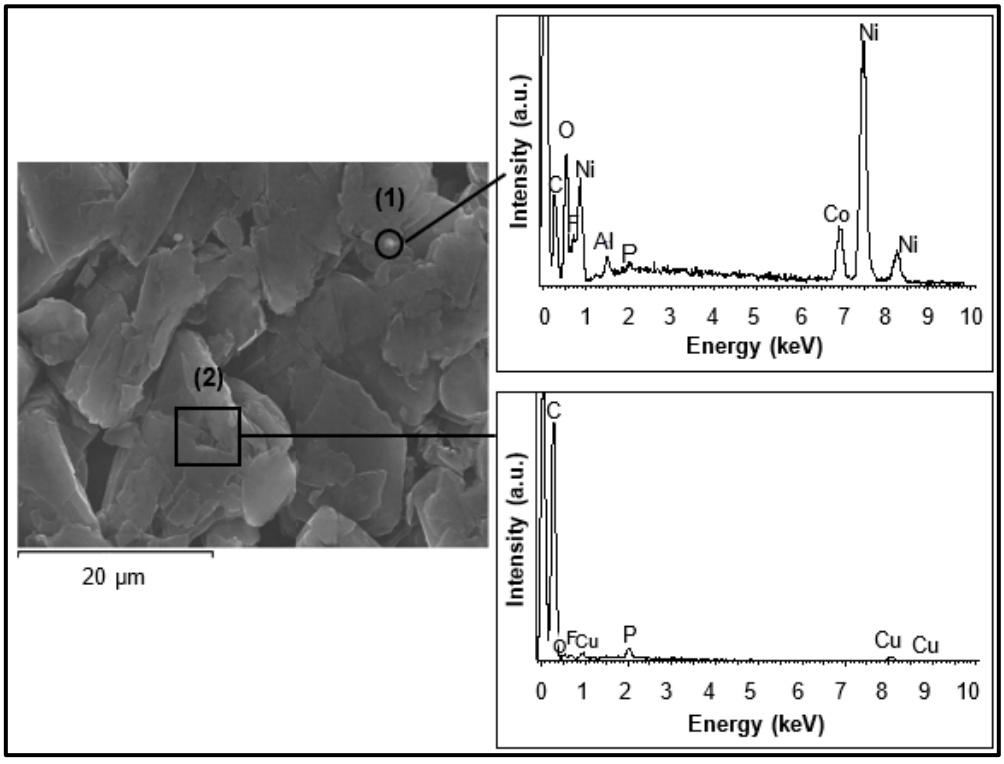

Figure 55 - SEM micrograph of anodic material ("T" sample type) of spent LIB, and EDS spectra of two different phases.

The spectra of area 2 revealed the presence of Cu, which was attributed to the current collector that was exposed at the surface, and the C peak identified in both anodic areas corresponds to the graphite phase of the active anodic material, as expected. The small P and F peaks identified can be related with the contamination of the electrolyte $LiPF_6$ and the O peak might also be due to the organic solvent that the $LiPF_6$ is dissolved into. In the area 1, Al, Ni and Co were identified as a contaminant of the $Li(Ni_{0.8}Co_{0.15}Al_{0.05})O_2$ phase present in the active cathodic material, which also explains the spherical morphology observed. The “P” sample had a homogeneous composition since the spectra obtained for the different areas were all similar to the one of area 2 in the “T” sample.

Figure 56 shows a SEM micrograph of the anodic material for the “P” sample.

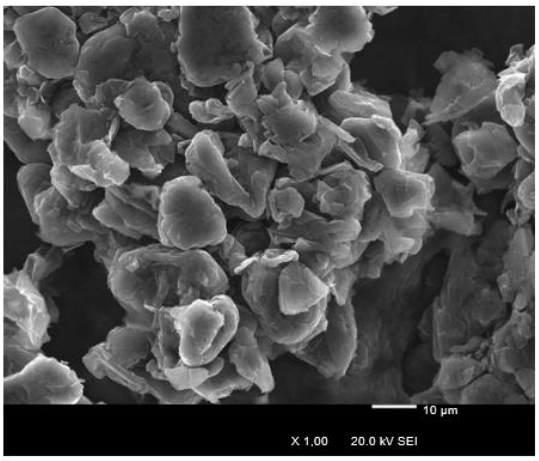

Figure 56 - SEM micrograph of anodic material (“P” sample type) of spent LIB.

SEM analysis of the surface of the cathodic materials of lithium-ion batteries showed particles with a spherical morphology. Figure 57 shows a SEM micrograph of the cathodic material for the “T” sample, as well as two EDS spectra obtained in different phases of the sample.

The spectra of the three different areas reveals the presence of Al, Co, Ni and O, which are the expected elements to be present in the black mass of the cathode due to the reported results by AAS. The main difference between area 3 and the other two areas is the identified F and P peaks which are attributed to a contamination of the electrolyte $LiPF_6$. The spectra of both area 1 and 2 reveals the same peaks but with different intensities as area 1 has two Ni peaks with more intensity and the C peak has less intensity compared to area 2. The observed C peak can be attributed either due to a carbon conductive additive or to a contamination from the graphite present in the anode or from the organic solvents present in the electrolyte solution. The observed colour difference between the areas, where area 1 is brighter than the others, is related with the topography and due to the presence of a hill in that zone.

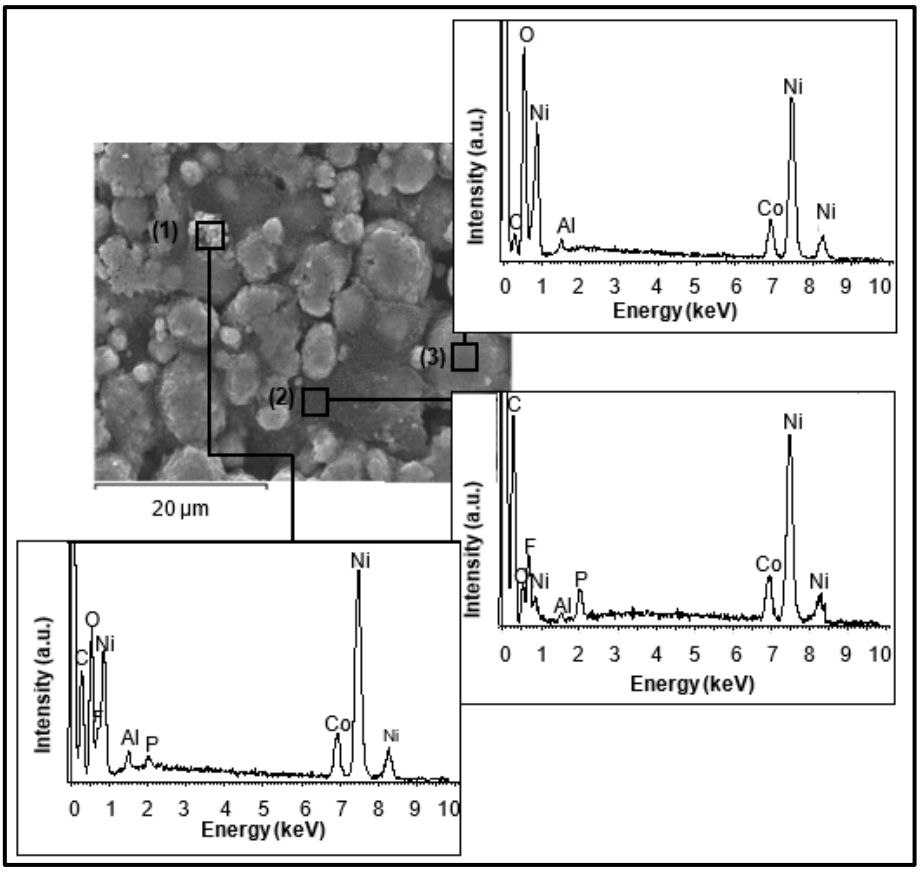

Figure 57 - SEM micrograph of cathodic material ("T" sample type) of spent LIB, and EDS spectra of three different phases.

The "P" sample presented similar differences in the composition as the "T" sample, where two main areas can be distinguished due to the absence of F and P – brighter areas - or presence of F, P and Cu (apart from the cathodic elements O, Al, Ni and Co), which are present in the darker areas. The Cu element is the main difference compared to the "T" sample and it is probably related with a contamination from the copper foil of the anode. The SEM micrograph of the cathodic material using BSE is presented in Figure 58.

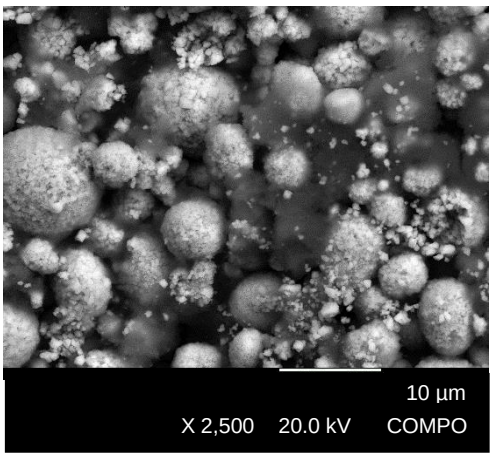

Figure 58 - SEM micrograph of cathodic material ("P" sample type) of spent LIB using BSE.

4.5. Leaching tests

The recycling of spent lithium-ion batteries generally involves deactivation, mechanical treatment, hydrometallurgical treatment, or pyrometallurgical treatment. It was decided to study hydrometallurgical treatments since, from an environmental and health point of view, they are considered to be more suitable as they have low energy consumption, higher recovery of elements with high purity grade and do not have air emissions [5].

In the hydrometallurgical treatments applied after a mechanical treatment for the recycling of spent lithium-ion batteries, the metals from the black mass are dissolved in aqueous solutions containing reagents. These reagents are usually acids, either inorganic such as HCl, H_2SO_4 or HNO_3 or, more recently, organic acids, for example citric or succinic acid. In most studies, the acids are then combined with hydrogen peroxide, which is used as a reducer to promote the reduction of some elements present in the composition of the spent batteries that are more easily dissolved when they are in a more reduced form [69].

However, hydrogen peroxide easily decomposes and therefore its efficiency is usually low [5]. Based on this, the purpose of this part is to compare the effect on the leaching yield of the $Na_2S_2O_5$ reducer with that of H_2O_2 and also to compare the difference in the leaching yield for the acids HCl and H_2SO_4 in the case of a $Li(Ni_{0.8}Co_{0.15}Al_{0.05})O_2$ battery, aiming at contributing for complementing the characterization of these materials.

It is worthwhile to mention that there are other important variables that can affect the metals dissolution such as acid and reducer concentrations, leaching temperature, liquid to solid ratio and the leaching time. However, the only variable studied was the leaching time as the others were fixed [5, 59].

The resulting metal rich solution can be treated by solvent extraction, precipitation or ion exchange to recover metals but it is not the purpose of this thesis [5].

The leaching experiments were conducted using electrode material samples with approximately 42.7% of cathode and 57.4% of anode as calculated in the mass balance. The percentage of each element in the initial sample was calculated using the results from the initial elemental chemical analysis by AAS using the equation (13).

$$\%\ element\ in\ the\ initial\ sample = \frac{m_{cathode} * x_{\ element\ in\ the\ cathode} + m_{anode} * x_{\ element\ in\ the\ anode}}{m_{cathode} + m_{anode}} \quad (13)$$

Where $m_{cathode}$ is the weighted mass of the cathodic material (aluminium foil included) [g];
$x_{\ element\ in\ the\ cathode}$ is the percentage of the element in the cathode in the initial sample [%];
m_{anode} is the weighted mass of the anodic material (copper foil included) [g];
$x_{\ element\ in\ the\ anode}$ is the percentage of the element in the anode in the initial sample [%].

The resulting initial concentrations of metals in the solid electrode samples used in the leaching tests were 1.8% Li, 9.6% Ni, 1.7% Co, 28.5% Cu and 10.2% Al.

Metals leaching yields ($\eta_{element}$) were determined from the leachant concentrations, referring to the initial solids content, using equation (14).

$$\eta_{element} = \frac{c_{element} \times V_{solution}}{m_{initial} \times \%\ element\ in\ the\ initial\ sample} \quad (14)$$

Where $c_{element}$ is the obtained element concentration by AAS times the dilution factor [mg/L];
$V_{solution}$ is the initial volume of the leaching solution, corresponding to 0.05 L [L];
$m_{initial}$ is the total initial mass of the electrodes (cathode plus anode) [g].

Tests using different reducers were performed and the results are shown in Figure 59. Different scales of the ordinates axis were used to show in more detail the metals behaviour. The reducers tested were 0.1 M $Na_2S_2O_5$ and 0.1 M H_2O_2 and the acids tested were 1 M HCl and 0.5 M H_2SO_4. The L/S ratio was fixed at 20 L/kg and the leaching temperature at 60ºC. A test using only acid solutions (without reducer) was carried out to evaluate the acid influence (C and S samples).

The dissolution of Li, Ni and Co (metals present in the cathode material), was generally quick and efficient: after 1 hour, leaching yields attained were near 80% or higher. Values attained for Li are always higher than the other two metals, being recoveries practically total, and the variations found with time and with the type of leachant are negligible and can be explained by the experimental errors. In most conditions, Ni and Co yields stabilized after 1 h of reaction, except for the leachants H_2SO_4 alone and with H_2O_2, where a continuous increase was found, from 60% for 15 min to ~100% for 4 h. The mixture of H_2SO_4/$Na_2S_2O_5$ reveals the higher reaction rates. Sulphuric acid mixtures seemed more effective for cobalt than those with hydrochloric acid, leading to final recoveries near 100% for the first one, while only 85% for the second one. The reason of this behaviour can be related with the total acid consumption for dissolving other metals, as it will be discussed later.

The dissolution of Cu shows different behaviour when using H_2SO_4 or HCl and leachants, the first one leading to substantially lower leaching efficiencies. In some tests it is observed an increase until 1 h of leaching and then decreased when H_2SO_4 or HCl and H_2O_2 were used but it was practically null when H_2SO_4 was used with either reducer. This behaviour can be explained by changes in the oxidation state as initially part of the copper dissolves in acid media but the reductive conditions of the reaction do not allow to achieve high concentration in the leachate and part of the Cu(II) is reduced again to the metallic form as suggested in previous studies [5].

In HCl media, with acid alone or mixed with H_2O_2, Cu leaching increases suddenly until 1 h and stabilizes at 41% (a slight decrease is even observed with H_2O_2). The mixture HCl/$Na_2S_2O_5$ reveals substantially lower yields increasing almost linearly until 4 h but the maximum dissolution was 10%. This behaviour relates with the electrochemical character of the dissulfite agent, clearly being more reducer than the peroxide. If this metal is considered a contaminant, it is positive that its dissolution is low as it can hinder the purification of the leaching solution for obtaining the metals of interest that are present in the cathode. In this sense, the use of H_2SO_4 mixtures seemed appropriate. However, it is worthwhile to mention that copper recovery from batteries should be an aim in terms of a global recycling process, but leaching is not the optimized process for its recovery and instead, copper separation can be achieved by

mechanical treatment or pyrometallurgy, which makes the copper remaining in the active material a contaminant that should be minimized in the leachate [5].

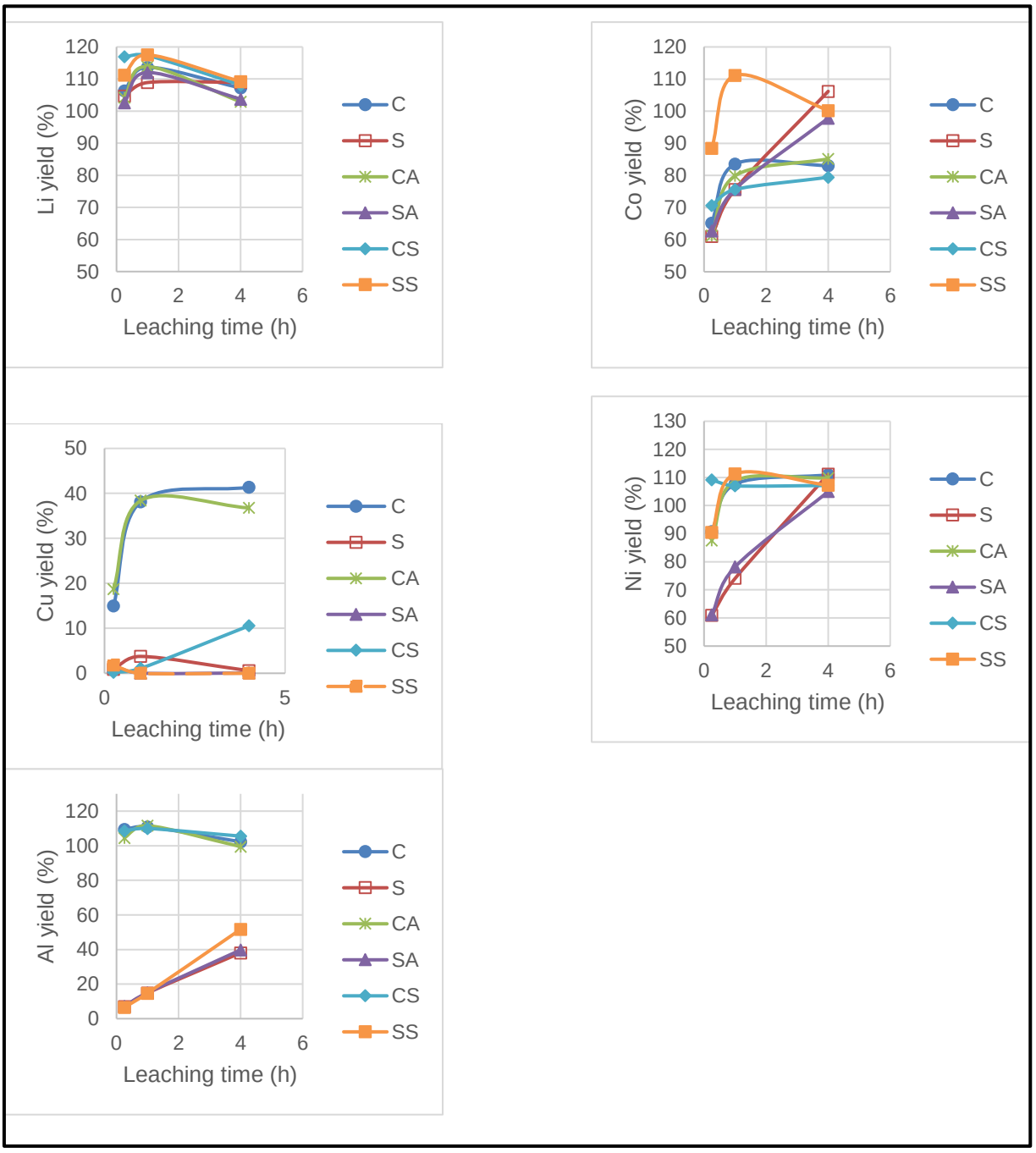

Figure 59 - Dissolution of different metals from spent LIBs with the leaching time using different additives. Leaching conditions: L/S: 20 L/kg; leaching temperature: 60ºC. The meaning of the defined nomenclature can be found on Figure 45.

Relatively to aluminium leaching behaviour, its high corrosion resistance due to the formation of a resistive oxide layer, limits the leaching efficiency. However, despite aluminium's high resistance in oxidizing environments, it has been shown that the presence of aggressive anions, like chloride, creates localized attacks [59]. This could explain why the leaching efficiency of Al is much higher when the HCl (around 100%) is used compared to H_2SO_4 (bellow 60%). When HCl (with or without reducer) was used,

the aluminium dissolution was practically total for the first time tested (15 min). A slight decrease for the 4 h of reaction can be attributed to the acid consumption and subsequent increase in the pH for which precipitation of hydroxides could be expected as suggested in previous studies - [5]. However, experimental errors can eventually also explain those variations. The higher Al dissolutions achieved with HCl mixtures can be responsible for the correspondent decrease in the leaching of cobalt, above discussed. Considering the high Al content in the initial solid (10%) the sudden consumption of a substantial acid amount in the first period of the reaction can hinder the leaching of other species.

When H_2SO_4 (with or without reducer) was used, the Al leaching efficiency was lower and it increased almost linearly until 4 h of leaching. The lowest dissolution was observed from 0.25 to 1 h when only H_2SO_4 (without reducer) was used, which can be considered the best result since the aluminium dissolution is not desired from the leachate purification point of view.

Figure 60 shows the effect of acid and/or reducer nature on the leaching for 4 h, at 60ºC. The results indicate that the most efficient acid to leach the electrode material in general is the sulfuric acid. This is not in agreement with previous studies about the cathodic material of a NCA LIB [59] which state that the most efficient acid to leach the cathodic elements Li, Ni and Co is the hydrochloride acid due to the presence of chloride ions that promote the dissolution by destabilizing the formation of a surface layer. However, the leaching time studied was 18 h instead of 4 h, which may explain the discrepancy in the derived conclusions.

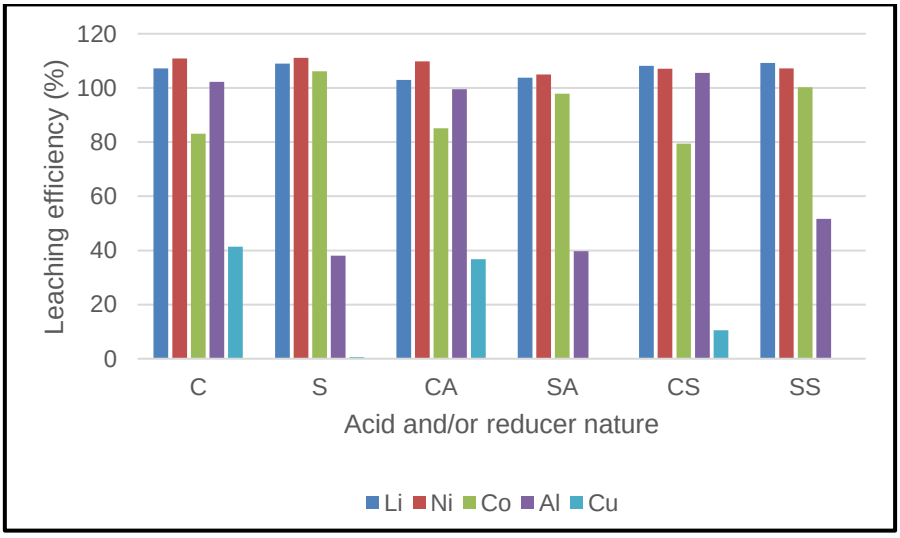

Figure 60 – Acid and/or reducer nature effect on the leaching efficiency of the cathodic and anodic material. Leaching conditions: L/S: 20 L/kg; leaching time: 4 h; leaching temperature: 60ºC.

Lower lithium dissolution was reached when only H_2O_2 was added to both acids while when only acid (without the reducers) or H_2SO_4 with $Na_2S_2O_5$ were used, the highest lithium extraction was achieved, which indicated that, under the tested conditions, the lithium does not need to be reduced. However, when compared with the other reducers, the addition of $Na_2S_2O_5$ seems to favour its extraction as previously reported for a NMC LIB [5].

Based on the results obtained by the comparison of the use of the different reducers, if the leaching time is 4 h, the optimized option would be to use only H_2SO_4 as it maximizes the lithium, nickel and cobalt

yields, corresponding to about 100% and minimizes the aluminium and copper yield, corresponding to about 38% and 0.6% respectively. However, if the leaching time is 1h, the optimized option would be to use H_2SO_4 with $Na_2S_2O_5$ since it maximizes the lithium, nickel and cobalt yields, corresponding also to about 100% and minimizes the aluminium and copper yield, corresponding to about 15% and 0.005% respectively.

Finally, it is worthwhile to mention that the leaching efficiencies above 100% can be interpreted as a total, or almost-total recovery of the metals. These results can result from a variety of causes such as small variations in the volume, in fact, part of the leaching solution might have been evaporated but that effect was not accounted for in the leaching yield calculations and therefore the obtained value was superior to reality. Another factor to consider is the errors in the sample analysis as the samples were tested at different times and to test the first sample (after 15 min) part of the acid was removed and therefore will not be present in the second sample (after 1 h) and the same logic can be applied for the third sample (after 4 h).

4.6. LIB recycling profitability critical analysis

LIBs used in EVs are projected to have a lifespan of around 10 years while LIBs used in most portable electronics have a lifespan of less than 3 years, causing a rapidly growing LIB waste stream (expected to be higher than 500 thousand tonnes by 2020) [46]. From a recycling firm's perspective it is essential to predict the economic feasibility of LIB recycling. Traditionally, recycling offers economic opportunities to recover valuable materials used in battery production, namely cobalt, which is widely used in LIBs due to its high energy density [70]. However, as cobalt is a critical raw material and also expensive, manufacturers are moving towards low-cost cathode materials, as the NCA option studied in this thesis, to reduce the battery manufacturing costs. The transition from expensive cathodic materials to less expensive options reduces the economic incentives to recycle those batteries at their end of life.

A study developed by Wang et al. predicted that the minimum amount of spent LIBs (T) necessary for a recycling facility, which only recycled LIBs, to start being profitable would be 170 000 kg/year. This value was obtained based on an average variable cost (2420 €/tonne) with a standard deviation of 1045 €/tonne, an assumed fixed cost based on data from battery recycling facilities and the revenue calculated (R), assuming all metallic materials contained in LIBs could be recovered at an average recycling efficiency using data prior to 2011 and that only LCO batteries were recycled in that facility. As state in equation (15), annual revenue would be equal to the sum of fixed (FC) and variable costs (VC) [70].

$$R \times T = FC + VC \times T \tag{15}$$

The fixed costs do not depend on the volume of batteries being recycled, including management salaries, rents of office and processing areas, while the variable costs are referent to the expenses that scale proportionally with the volume of outputs, which change according to the type, size and purity of the cathode, geographic location, recycling technology, collection, transportation and processing cost [70].

As pointed out by the author, as LIBs come in many different sizes, form factors, pack configurations and cathode chemistries, LIB recycling facilities would likely be commingled, which was not considered in the calculation. Additionally, the variable costs assumed in the paper are not based on industrial batteries [70]. The definition of an industrial battery, according to the European Portable Battery Association (EPBA) is a battery "designed exclusively for industrial or professional uses or is used in any type of electric vehicle" and therefore the LIBs used in EVs fit into this category, which means the used variable costs to do the calculation of the break-even point lacks a major percentage of the LIBs which are and will be in their end-of-life [71]. Due to these factors, it is not reasonable to predict if the recycling of LIBs would be profitable based solely on the results obtained from this thesis.

From all the aspects related to the variability of the cathode types, however, the form factors may not be considered in the calculations as it was demonstrated by Richa et al. that the total volume and basic material breakdown of an EOL waste stream will not significantly change with the form factor, particularly for LIBs in EVs [72].

In order to calculate the theoretical expected revenue, one could consider the proportion (α_i) of each one of the 5 cathode chemistry types (NCA, NMC, LMO, LFP and LCO). For each battery type, the unit revenue could be calculated by multiplying the price of the scrap value P_j (which would depend on the purity of the metal obtained) by the average material composition $Ava_{i,j}$ (in kg of metal per 1000 kg of module) and the recycling efficiency RE_j as stated in equation (16), which is an adaptation of the equation proposed by Wang et al..

$$\sum_{i=1}^{6}\left(\alpha_i \times \sum_{j=1}^{7}(P_j \times Ava_{i,j} \times RE_j)\right) \quad (16)$$

The indices referred to in equation (16) are shown in Table 14.

Table 14 – Indices information.

Variables	Indices	Battery type	Variables	Indices	Element
i	1	NCA	j	1	Li
	2	NMC		2	Ni
	3	LMO		3	Co
	4	LFP		4	Cu
	5	LCO		5	Al
				6	Mn
				7	Iron/Steel

The theoretical expected revenue from the NCA battery used as a case study can be calculated and used as a reference in a future study to calculate the revenue of a recycling facility. For that, the values from Table 12 regarding the %w/w of the different elements, per cell were used to calculate the weight (in kg of element per 1000 kg of module) of each element j considering that the 35 cells weight 11.2602 kg and that each LIB module has 21.9 kg.

Table 15 shows the price per element that the total of the cells of the studied lithium-ion battery module would have, the mass per each element and the recycling efficiency considering the leaching efficiency obtained from two leaching scenarios analysed in the LNEG laboratory with a 20 L/kg L/S ratio, a leaching temperature of 60ºC and that the concentration of the sulphuric acid is 0.5 M: scenario 1 assumes that the leaching was done using only H_2SO_4 with a leaching time of 4 h while scenario 2 assumes that the $Na_2S_2O_5$ reducer was added with a leaching time of 1 h.

Table 15 – Revenue estimation of the recycling of a NCA battery based on the commodity market prices of the elements, the mass of each element per tonne of LIB module and the recycling efficiencies obtained from scenario 1 and 2. The prices were taken from [73, 74, 75].

	P ($/kg)	Ava (kg/ tonne)	RE 1	RE 2	R 1	R 2
Li	16.50	6.00	1	1	99	99
Ni	12.39	29.00	1	1	359.31	359.31
Co	56.50	5.00	1	1	282.5	282.5
Cu	6.20	88.00	0.006	0.00005	3.274	0.0273
Al	2.14	31.00	0.38	0.15	25.20	9.95
Mn	2.10	0	NA	NA	NA	NA
Iron/Steel	0.15	NA	NA	NA	NA	NA
R ($/tonne module)					769.3	750.8
R (€/tonne module)					677.6	661.3

NA means not analysed.

Before any conclusions can be taken, some considerations must be made. First, the prices shown are estimates only as they can easily change based on region, supplier or various other factors. Additionally, they come from different sources and only around 96% of the cell constitution was studied. It is worthwhile to mention that it was assumed that the scrap value was the same as the commodity market price but in reality, it would depend on the purity obtained from the recycling process compared the one attained from the raw material. Secondly, despite the revenue regarding scenario 2 is higher, it does not mean that it would be more beneficial to use the leaching conditions correspondent to that scenario as it is not efficient to try to recover Cu or Al from leaching and another recycling method should be used instead, which would increase the recycling efficiency regarding those metals. Moreover, the recycling efficiency was assumed to be the same as the leaching efficiency, which may not correspond exactly to reality as the crystallization and precipitation steps were not studied in this thesis.

It can be concluded that the LIB studied has considerable economic value, however, that is mainly due to the Co content, which is the most valuable metal, even though in this case the Ni content is much higher. This result is not surprising. In fact, Wang et al. predicted that for a recycling facility to be

profitable, the proportion of LCO cathode batteries in the waste stream would need to be at least 21% [70].

Although there is not enough data to confirm, it can be assumed that currently commingle recycling LIBs is not profitable due to the complexity of the available processes partially due to the variability of specific materials contained in the spent batteries, the related recycling costs and the growing non-cobalt chemistries in the market. These factors may explain part of the reason why only 5% of the lithium-ion batteries out on the European market currently reach recycling facilities [76].

At present, the potential economic value of recycling LIBs is associated with a number of uncertainties, such as:

1. How many batteries will reach their EOL per year?
2. How many of those batteries will be from EVs?
3. What is the proportion of batteries that should be recycled (instead of reused)?
4. What is the proportion of each cathode type (α_i) in the waste stream and the specific materials comprising each cell within the battery waste stream?
5. What are the recycling costs (fixed and variable) assuming a commingled recycling?
6. How many individual lithium-ion cells are present in the EV battery packs and in the consumer products?

However, waiting until such questions are answered presents a risk of not allowing sufficient time for the LIB production industry to react to the emergence of a full scale LIB waste stream. To overcome potential economic constraints of LIB recycling, particularly for less valuable, non-cobalt chemistries, the recovery process and industry may require policy intervention to reach economies of scale. In fact, the EU has set a mandatory target that 45% of batteries in portable electronics in EU Member States shall be recycled by 2016 [43].

From the economic point of view, it is also important to mention that many of the materials used in the cells are coming from geopolitical unstable countries, which may lead to a shortage of those materials and ultimately to a price increase that would make recycling of LIBs profitable.

Chapter 5. Conclusions and Future Work

The safe discharge procedure of spent LIBs was successfully proposed, meeting the first objective. The safety measures found in the bibliography such as the fact that the discharging must be done in a well-ventilated area to minimize exposure to toxic gases from the electrolyte and that the temperature should monitored not to exceed 90ºC (temperature at which the SEI films starts to exothermically decompose) were considered in the procedure proposed (research question 1a) by monitoring the temperature of the weld, which was always under 50ºC, and opening all the windows and the door of the laboratory (research question 1b). The proposed discharge procedure has the potential of being applied in the industry with some adaptation to the number of resistors used to discharge the LIBs at the same time considering that the discharge time (3 to 4 hours) should be used in an efficient way. The manual dismantling of these batteries was successfully done. However, part of the procedure used is not the best approach at an industrial scale because it was not possible to separate the battery cells from the cells base in a seamless way as it required physical strength from the operator and it was a time-consuming process to use a mechanical lathe to separate these components (research question 1c).

The physical, chemical and morphological characterization of spent LIBs was carried out to evaluate their recycling potential. The complete disassembly of the battery components allowed to perform a mass balance, which verified that the electrode materials weighed 60% of the cell weight, with the anodes having the highest contribution (34%) while the metallic components contribute to about 21% of the balance. Plastic materials account for around 11% to the cells weight and the 9% of the mass lost from the cell was attributed to the electrolyte (research question 2a).

Concerning chemical characterization, the main phases were identified by XRPD being graphite the active anodic material and the structure of the cathodic active material was identified as being $LiMO_2$ (research question 2b). The AAS allowed concluding that the metals present in the anode are Li (0.2%), Ni (0.1%) and Cu (49%) and that the type of battery is NCA as the cathode is essentially made of Al, Ni, O, Co and Li, corresponding to 24%, 22%, 19%, 4% and 4% respectively (research questions 2c and 2d).

Morphology of the electrode materials was assessed by SEM analysis, which allowed observing the euedric morphology of particles in the anodic material and the spherical morphology in the cathodic material (research question 2e).

The leaching behaviour of the electrodes of the NCA LIB, with 1 M hydrochloric acid or 0.5 M sulphuric acid at 60ºC and with a 20L/kg L/S ratio, allowed for assessing the reactivity of metal-bearing phases. The best leaching conditions were achieve using H_2SO_4 as the acid since the leaching yield of the Li, Co and Ni were very high (corresponding to 100%) when H_2SO_4 was used (with or without the reducer $Na_2S_2O_5$) after either 1 or 4 hours of leaching. On the other hand, the Al and Cu leaching yields were minimum, corresponding to 38% and 0.6% after 4 h of leaching with H_2SO_4 respectively and 15% and 0.005% respectively after 1 h of leaching with H_2SO_4 with $Na_2S_2O_5$ (research question 3a). This demonstrates that hydrometallurgical processing can be an adequate approach for recycling end-of-life LIBs for recover Li, Ni and Co metals but not for Al and Cu recovery.

The economic feasibility of LIB recycling was analysed considering the revenue of recycling 1 tonne of the LIB studied through discharge, disassembly and leaching, based on the commodity price of each element, their mass and the leaching efficiency, making a total of around 678 €. However, it is more likely that a recycling facility would be commingled due to the variety of cathode chemistries and therefore the result obtained would only contribute to a percentage of the revenue, with the LCO batteries having a higher inherent revenue due to their higher cobalt content, increasing the total revenue. Although there is not enough data to confirm it, currently, commingle recycling LIBs is probably not profitable but waiting until the recycling uncertainties regarding the recycling costs and the estimation of future waste flows are refined may not allow sufficient time for the industry to adapt and react to the emergence of a full scale LIB waste stream. There are EU policies that demand the recycling of 45% of batteries in portable electronics, which might extend to the industrial batteries such as LIB in the future. Additionally, it is important to consider that many of the materials contained in the LIB come from politically unstable countries, increasing the recycling importance and possibly the profit associated (research question 4a).

5.1. Recommendations for future developments

Following this thesis, some future studies can be proposed. The disassembly methodology proposed could be improved, particularly regarding the separation of the battery cells from the cells base possibly using an alternative solvent to dissolve only the polymer. In addition, the initial LIB design for disassembly should also be enhanced not only to facilitate the separation of all the components but also to possibly do it in an automatic way.

The recovery of graphite from LIBs was not considered in this study and it is also not addressed in the literature. In most processes, the heat treatment steps adopted during the treatment of LIBs lead to the loss of graphite. As LIBs represent an important source of this material, its recovery from them should be investigated in additional works.

The best process to recover the Al and Cu metals (mechanical treatment or pyrometallurgy) from the electrodes should be investigated in order to complement the recovery by leaching of the remaining metals from the cathodic and anodic materials.

Moreover, the subsequent operations of leaching of LIB materials, for purification and recovery of metals (e.g. precipitation and solvent extraction) should also be addressed in further investigations to establish a complete diagram for the treatment of these wastes.

Finally, a further investigation regarding the economical feasibility of recycling LIBs at an industrial scale should be done by investigating the recycling costs (fixed and variable) regarding different recycling processes. The revenue from the LIB studied in this thesis could be used as reference to calculate the potential overall commingled LIB recycling revenue.

It is expected that this thesis can contribute to the development of the integrated and sustainable management of spent LIB, considering the principles of a circular economy.

References

[1] B. Scrosati and J. Garche, "Lithium batteries: Status, prospects and future," *Journal of Power Sources,* vol. 195, no. 9, 2009.

[2] European Commission, "Road transport: Reducing CO2 emissions from vehicles," European Commission: Energy, Climate change, Environment, [Online]. Available: https://ec.europa.eu/clima/policies/transport/vehicles/cars_en. [Accessed 03 10 2018].

[3] M. Lowe, S. Tokuoka and T. Trigg, "Lithium-ion batteries for electric vehicles: The U.S. value chain," *Environmental Defense Fund,* pp. 12-20, 2010.

[4] J. L. Xianlai ZENG, "Spent rechargeable lithium batteries in e-waste: composition and its implications," *Journal of Environmental Science and Engineering,* vol. 8, no. 5, pp. 792-796, 2014.

[5] N. Vieceli, C. A. Nogueira, C. Guimarães, M. F. Pereira, F. O. Durão and F. Margarido, "Hydrometallurgical recycling of lithium-ion batteries by reductive leaching with sodium metabisulphite," *Waste Management,* no. 71, pp. 350-361, 2018.

[6] Elibama, "European Li-Ion Battery Advanced Manufacturing for Electric Vehicles," 2014. [Online]. Available: https://elibama.files.wordpress.com/2014/10/v-d-batteries-recycling1.pdf. [Accessed 03 10 2018].

[7] A. Kwade and J. Diekmann, Eds., "Recycling of Lithium-ion Batteries: The LithoRec Way," in *Sustainable Production, Life Cycle Engineering and Management*, Springer International Publishing, 2018, pp. 10-25; 33-40.

[8] L. Gaines, "The future of automotive lithium-ion battery recycling: Charting a sustainable course," *Sustainable Materials and Technologies,* pp. 2-7, 2014.

[9] Z. W. C. S. Z. S. Weiguang Lv, "A Critical Review and Analysis on the Recycling of Spent Lithium-Ion," *ACS Sustainable Chemistry & Engineering,* no. 6, pp. 1504-1521, 2018.

[10] C. H. L. F. G. S. T. L. A.-S. F. A. K. Jan Diekmann, "Ecological Recycling of Lithium-Ion Batteries from Electric Vehicles with Focus on Mechanical Processes," *Journal of The Electrochemical Society,* vol. 1, no. 164, pp. A6184-A6191, 2017.

[11] J. Valio, "CRITICAL REVIEW ON LITHIUM ION BATTERY RECYCLING TECHNOLOGIES," Aalto Univerity School of Chemical Engineering, 2017.

[12] R. B. Gupta, Gasoline, diesel, and ethanol biofuels from grasses and plants, Cambridge University Press, 2010.

[13] A. Emadi, M. Ehsani and Y. Gao, Modern Electric, Hybrid Electric and Fuel Cell Vehicles: Fundamentals, Theory and Design, CRC Press, 2009.

[14] C. Schwarz, G. P. Merker and R. Teichmann, Eds., Combustion Engines Development: Mixture Formation, Combustion, Emissions and Simulation, Springer, Berlin, Heidelberg, 2012, p. 35.

[15] M. G. Babu and K. Subramanian, "Conventional Fuels for Land Transportation," in *Alternative Transportation Fuels: Utilisation in Combustion Engines*, 1st ed., CRC Press, 2013.

[16] B. G. Miller, Combustion Engineering Issues for Solid Fuel Systems, Academic Press, 2008, pp. 11-40.

[17] Committee on the Assessment of Technologies for Improving Light-Duty Vehicle Fuel Economy and National, Assessment of Fuel Economy Technologies for Light-Duty Vehicles, National Academies Press, 2011, pp. 12-15.

[18] E. Johnson, "Cars and ground-level ozone: how do fuels compare?," *European Transport Research Review,* vol. 9, no. 4, 2017.

[19] D. Kushnir, "Lithium Ion Battery Recycling Technology 2015: Current State and Future Prospects," ESA REPORT #2015:18, Göteborg, Sweden, 2015.

[20] F. Soares, P. R. Almeida, J. A. P. Lopes, R. Garcia-Valle and F. Marra, "State of the Art on Different Types of Electric Vehicles," in *Electric Vehicle Integration into Modern Power Networks*, R. Garcia-Valle and J. A. P. Lopes, Eds., New York, Springer International Publishing, 2013.

[21] OPEC Secretariat, "Oil demand and transportation: an overview," *OPEC energy review,* vol. 39, no. 4, pp. 349-375, 2015.

[22] N. Abas, A. Kalair and N. Khan, "Review of fossil fuels and future energy technologies," *Futures : the journal of policy, planning and futures studies,* vol. 69, pp. 31-49, 2015.

[23] "BP Statistical Review of World Energy," June 2016.

[24] Working Group III Contribution to the Fifth Assessment Report of the Intergovernmental Panel on Climate Change, "Climate Change 2014: Mitigation of Climate Change," Cambridge University Press, 2014.

[25] T. Boden, G. Marland and R. Andres, "Global, Regional, and National Fossil-Fuel CO2 Emissions," *Carbon Dioxide Information Analysis Center, Oak Ridge National Laboratory, U.S. Department of Energy, Oak Ridge, Tenn., U.S.A.,* 2017.

[26] T. Kizildeniz, "Effects of climate change including elevated CO2 concentration, temperature and water deficit on growth, water status, and yield quality of grapevine (Vitis vinifera L.) cultivars," *Agricultural water management,* vol. 159, pp. 155-164, 2015.

[27] K. Skalska, "Trends in NOx abatement: A review," *The Science of the total environment,* vol. 408, no. 19, pp. 3976-3989, 2010.

[28] "A Study on Oil Dependency in the EU: A report for Transport and Environment," Cambridge Econometrics, UK, July 2016.

[29] H.-W. Schiffer, "World Energy Resources," World Energy Council, 2016.

[30] K. Young, C. Wang, L. Y. Wang and K. Strunz, "Electric Vehicle Battery Technologies," in *Electric Vehicle Integration into Modern Power Networks*, New York, Springer International Publishing, 2013.

[31] X. X, W. C, L. G, Y. CP and S. W, "Development of a plug-in hybrid electric vehicle educational demonstration," in *Proceedings of 2009 North American power symposium*, Starkville,MS, USA, 2009.

[32] D. A. Corrigan and A. Masias, "Batteries for Electric and Hybrid Vehicles," in *Liden's Handbook of Batteries*, 4th ed., McGraw-Hill, 2011.

[33] J. Larminie and J. Lowry, "Types of Electric Vehicles — EV Architecture," in *Electric Vehicle Technology Explained*, Wiley, 2012.

[34] B. M. Al-Alawi and T. H. Bradley, "Review of hybrid,plug-in hybrid, and electric vehicle market modeling Studies," *Renewable and Sustainable Energy Reviews,* vol. 21, pp. 190 - 203, 2013.

[35] A. Poullikkas, "Sustainable options for electric vehicle technologies," *Renewable and Sustainable Energy Reviews,* vol. 41, p. 1277–1287, 2015.

[36] EUROBAT, Association of European Automotive and Industrial Battery Manufacturers, "EUROBAT E-Mobility: Battery R&D Roadmap 2030 - Battery Technology for Vehicle Applications".

[37] G. Duarte, R. Varella, G. Gonçalves and T. Farias, "Effect of battery state of charge on fuel use and pollutant emissions of a full hybrid electric light duty vehicle," *Journal of Power Sources,* no. 246, pp. 377-386, 2014.

[38] P. Pisu, "Merging mobility and energy vision with hybrid electric vehicles and vehicle infrastructure integration," *Energy policy,* vol. 41, p. 599, 2012.

[39] B. G. Pollet, I. Staffell and J. L. Shangc, "Current status of hybrid, battery and fuel cell electric vehicles: From electrochemistry to market prospects," *Electrochimica Acta,* no. 84, pp. 235-249, 2012.

[40] Mitsubishi Motors, "The Plug-in Hybrid EV System," [Online]. Available: https://www.mitsubishi-motors.com/en/innovation/technology/library/phev.html.

[41] Florida Energy Systems Consortium, "Batteries for Vehicles," 2017. [Online]. Available: http://www.myfloridahomeenergy.com/help/library/transportation/batteries-for-vehicles/#sthash.MjlerRfa.tgwyMioX.dpbs. [Accessed 15 05 2018].

[42] Statista, "Chemical & Resources, Mining, metals & minerals: Global projection of total lithium demand 2017-2025," [Online]. Available: https://www.statista.com/statistics/452025/projected-total-demand-for-lithium-globally/. [Accessed 21 05 2018].

[43] Europeon Commission , "Study on the review of the list of Critical Raw Materials: Non-critical Raw Materials Factsheets," Brussels, 2017.

[44] Roskill Consulting Group Ltd, "Lithium: Global Industry, Markets & Outlook," 2017.

[45] Statistica, "Metals&Electronics, Electronics: Market estimates for lithium-ion battery use in EVs 2012-2020," [Online]. Available: https://www.statista.com/statistics/309570/lithium-ion-battery-market-in-electric-vehicles/. [Accessed 21 05 2018].

[46] L. Yun, D. Linh, L. Shui, X. Peng, A. Garg, M. L. P. L. S. Asghari and J. Sandoval, "Metallurgical and mechanical methods for recycling of lithium-ion battery pack for electric vehicles," *Resources, Conservation & Recycling,* no. 136, pp. 198-208, 2018.

[47] T. Watabe and M. Mori, "Global Markets Research: LiB materials industry," 2011.

[48] C. M. Hayner, X. Zhao and H. H. Kung, "Materials for Rechargeable Lithium-Ion Batteries," *Annual review of chemical and biomolecular engineering,* vol. 3, no. 1, pp. 445-471, 2012.

[49] K. M. Winslow, S. J. Laux and T. G. Townsend, "A review on the growing concern and potential management strategies of waste lithium-ion batteries," *Resources, Conservation & Recycling,* vol. 129, pp. 263-277, 2018.

[50] The McGraw-Hill Companies, Linden's Handbook of Batteries, 4th ed., T. B. Reddy and D. Linden, Eds., 2011.

[51] K. Zaghib, J. Dubé, A. Dallaire, K. Galoustov, A. Guerfi, M. Ramanathan, A. Benmayza, J. Prakash, A. Mauger and C. M. Julien, "Lithium-ion Cell Components and their Effect on High-Power Battery Safety," in *Lithium-Ion Batteries: Advances and Applications*, Elsevier, 2014, pp. 437-460.

[52] X. Zeng, J. Li and N. Singh, "Recycling of Spent Lithium-Ion Battery: A Critical Review," *Critical Reviews in Environmental Science and Technology,* vol. 44, no. 10, pp. 1547-6537, 2013.

[53] The Boston Consulting Group, "Batteries for Electric Cars: Challenges, Oportunities and the Outlook to 2020," The Boston Consulting Group, Boston, 2010.

[54] J. D. S. H. A. K. Christian Hanisch, "Recycling of Lithium-Ion Batteries," in *Handbook of clean energy systems*, John Wiley & Sons, Ltd., 2015.

[55] Europeon Commission, "Study on the review of the list of Critical Raw Materials: Criticality Assessments," Brussels, 2017.

[56] G. B. D. D. J. T. d. M. C. N. V. V.-L. B. L. C. K. Y. T. P. L. B. C. M. S. M. L. N. P. M. A. A.-D. P. P. C. T. E. M. Blengini, "Assessment of the Methodology for Establishing the EU List of Critical Raw Materials," Publications Office of the European Union, Luxemburg, 2017.

[57] C. Hanisch, J. Diekmann, A. Stieger, W. Haselrieder and A. Kwade, "Recycling of Lithium-Ion Batteries," in *Handbook of Clean Energy Systems*, 2015.

[58] Z. Z. X. L. Y. Z. Y. H. H. C. Z. S. Xiaohong Zheng, "A Mini-Review on Metal Recycling from Spent Lithium Ion Batteries," *Engineering,* no. 4, pp. 361-370, 2018.

[59] M. Joulié, R. Laucournet and E. Billy, "Hydrometallurgical process for the recovery of high value metals from spent lithium nickel cobalt aluminum oxide based lithium-ion batteries," *Journal of Power Sources,* no. 247, pp. 551-555, 2014.

[60] MIT Electric Vehicle Team, "A Guide to Understanding Battery Specifications," 2008.

[61] M. J. Lain, "Recycling of lithium ion cells and batteries," *Journal of Power Sources,* no. 97-98, pp. 736-738, 2001.

[62] K. Wegener, S. Andrew, A. Raatz, K. Dröder and C. Herrmann, "Disassembly of Electric Vehicle Batteries Using the Example of the Audi Q5 Hybrid System," *CIRP Conference on Assembly Technologies and Systems,* no. 23, pp. 155-160, 2014.

[63] H. A. Kiehne, Ed., Battery Technology Handbook, MARCEL DEKKER, INC, 2003.

[64] R. García and A. P. Báez, Atomic Absorption Spectrometry, Centro de Ciencias de la Atmósfera, Universidad Nacional Autónoma de México: InTech, 2012.

[65] P. D. L. Reimer, Scanning Electron Microscopy: Physics of Image Formation and Microanalysis, 2nd ed., vol. 45, Springer Series in Optical Science, 1998.

[66] S. Soh, S. Ong and A. Nee, "Design for Disassembly for Remanufacturing: Methodology and Technology," *Elsevier,* no. 15, pp. 407-412, 2014.

[67] S. Vongbunyong, S. Kara and M. Pagnucco, "Application of cognitive robotics in disassembly of products," *CIRP Annals - Manufacturing Technology,* no. 62, pp. 31-34, 2013.

[68] F. Torres, S. Puente and C. Dı´az, "Automatic cooperative disassembly robotic system: Task planner to distribute tasks among robots," *Control Engineering Practice,* no. 17, pp. 112-121, 2009.

[69] Y. Guo, F. Li, H. Zhu, G. Li, J. Huang and W. He, "Leaching lithium from the anode electrode materials of spent lithium-ion batteries by hydrochloric acid (HCl)," *Waste Management,* no. 51, pp. 227-233, 2016.

[70] G. G. C. W. B. K. R. Xue Wang, "Economies of scale for future lithium-ion battery recycling infrastructure," *Resources, Conservation and Recycling,* no. 83, pp. 53-62, 2014.

[71] Perchards SagisEPR, "The collection of waste portable batteries in Europe in view of the achievability of the collection targets set by Batteries Directive 2006/66/EC," 2017.

[72] C. W. B. G. G. X. W. Kirti Richa, "A future perspective on lithium-ion battery waste flows from electric vehicles," *Resources, Conservation and Recycling,* no. 83, pp. 63-76, 2014.

[73] "Metalary," 2018. [Online]. Available: https://www.metalary.com/lithium-price/. [Accessed 09 10 2018].

[74] Trading Economics, 05 10 2018. [Online]. Available: https://tradingeconomics.com/commodities. [Accessed 09 10 2018].

[75] "Pooraka Bottle and Can Recycling Depot: bottles, cans, scrap and more," 04 10 2018. [Online]. Available: https://www.recyclingdepotadelaide.com.au/scrap-metal-prices-adelaide. [Accessed 09 10 2018].

[76] B. S. John Hyland, "Lithium Factsheet," GLOBAL 2000 Verlagsges, Vienna, 2013.

[77] J. Li, P. Shi, Z. Wang, Y. Chen and C.-C. Chang, "A combined recovery process of metals in spent lithium-ion batteries," *Chemosphere,* no. 77, p. 1132–1136, 2009.

[78] S. M. Shin, N. H. Kim, J. S. Sohn, D. H. Yang and Y. H. Kim, "Development of a metal recovery process from Li-ion battery wastes," *Hydrometallurgy,* no. 79, p. 172– 181, 2005.

[79] G. Dorella and M. B. Mansur, "A study of the separation of cobalt from spent Li-ion battery residues," *Journal of Power Sources,* no. 170, pp. 210-215, 2007.

[80] C. K. Lee and K.-I. Rhee, "Preparation of LiCoO2 from spent lithium-ion batteries," *Journal of Power Sources,* no. 109, pp. 17-21, 2002.

[81] H. D, *Annual progress report for energy storage R&D, Vehicle Technologies Program, Energy Efficiency and Renewable Energy,* Washington, DC, 2011, pp. v-vii.

[82] X. Wang, G. Gaustad and C. W. Babbitt, "Targeting high value metals in lithium-ion battery recycling via shredding and size-based separation," *Waste Management,* vol. 51, 16 June 2015.

[83] J. Heelan, E. Gratz, Z. Zheng, Q. Wang, M. Chen, D. Apelian and Y. Wang, "Current and Prospective Li-Ion Battery Recycling and Recovery Processes," *The Minerals, Metals & Materials Society,* vol. 68, no. 10, p. 2632–2638, 2018.

[84] S. Shafiee and E. Topal, "When will fossil fuel reserves be diminished?," *Energy Policy,* vol. 37, no. 1, 2009.

[85] Kitco, 24 08 2018. [Online]. Available: http://www.kitcometals.com/charts/nickel.html. [Accessed 25 08 2018].

[86] Metalary, 2018. [Online]. Available: https://www.metalary.com/lithium-price/. [Accessed 25 08 2018].

[87] InvestmentMine, "Mining Markets and Investment," 23 08 2018. [Online]. Available: http://www.infomine.com/investment/metal-prices/cobalt/. [Accessed 2018 08 25].

[88] Kitco, 24 08 2018. [Online]. Available: http://www.kitcometals.com/charts/Copper.html. [Accessed 25 08 2018].

[89] AKM Baltia, [Online]. Available: http://akmlom.lv/en/. [Accessed 25 08 2018].

[90] M. P. Christian Ekberg, "Lithium Batteries Recycling," in *Lithium Process Chemistry: Resources, Extraction, Batteries and Recycling*, Elsevier, 2015, pp. 233-264.

Appendix A

EU Policy measurements

Table 16 shows the key policies that the EU has put in place to reduce the oil import dependency.

Table 16 - EU policy measure and description in the context of oil import dependency [28].

Policy Measure	Policy description in the context of oil import dependency
The Energy Union Framework (2015)	The Energy Union strategy was established to ensure that the EU's energy supply was secure, affordable and sustainable. It includes the ambition to: - Reduce dependence on energy imports and to diversify energy supply in order to reduce exposure to supply shocks from geopolitical risk. - Improve energy efficiency (by at least 27% by 2030). - Decarbonise the economy (to achieve a target of 40% emissions reduction by 2040). - Become a global leader in clean energy technologies.
EU Energy Security Strategy (2014)	Many countries in Europe (particularly in Eastern Europe) are reliant on just one or two sources of oil and gas supply and this over-reliance on few sources creates security of supply vulnerabilities. The EU Energy Security Strategy aims to mitigate the risks associated with high dependence on insecure energy supplies. Longer term measures include a goal to increase domestic energy production and diversify sources of supply by negotiating effectively with current and new trade partners.
The Oil Stocks Directive (2009)	The Directive requires all EU Member States to maintain stocks of crude oil and/or petroleum products equivalent to at least 90 days of net imports or 61 days of consumption (whichever is higher), which can be quickly and easily accessed during periods of supply crisis.
Vehicle Emissions Regulation (2013)	The European Commission introduced a target for 2021 that limits CO_2 emissions from new cars to 95g CO_2/km and emissions from new vans to 147g CO_2/km. The European Commission has also promised new post-2020 efficiency standards. To achieve these targets, EU vehicle manufacturers will need to implement energy-efficient improvements to vehicle technologies and increase the share of low-carbon powertrains (such as electric vehicles) in the sales fleet.

Appendix B

Comparison of specific performance targets for HEV, PHEV and FEV

The comparison of the EV specific performance targets is shown in Table 17.

Table 17 - Comparison of specific performance targets for HEV, PHEV and FEV. Based on [32].

Vehicle Type	Vehicle sub-type	Specific energy (Wh/kg)	Specific power (W/kg)	Power-to-energy ratio
HEV	Stop-start 42 V micro hybrid	25	600	24
	42 V mild hybrid (lower power)	12	520	43
	42 V mild hybrid (higher power)	20	514	26
	Strong hybrid (lower power)	8	625	83
	Strong hybrid (higher power)	8	667	80
PHEV	PHEV (higher power)	57	750	13
	PHEV (higher energy)	97	317	3
FEV	----------	200	400	2

Appendix C

Typical composition of LIB module and cells

The results from multiple studies for the composition of typical spent LIB cells and module were summarized in Table 18 and in Table 19, respectively [49, 52].

Table 18 – Composition of typical spent LIB cells (weight %) [52] .

	Combined state			Elemental state				
Source	Co	Li	Ni	Cu	Al	Fe	Organic chemicals	Plastics
Wang [52]	16	2	----------	10	3	19	----------	----------
Li et al. [77]	16	2	----------	10	3	19	----------	----------
Shin et al. [78]	5-20	5-7	5-10	----------	----------	----------	15	7
Lain [61]	17	2.0	----------	7	4	----------	13	----------
Dorella and Mansur [79]	29	3	0.02	16	8	----------	----------	----------
Zeng et al. [52]	20	12	0.08	----------	10	----------	----------	----------
Lee et al. [80]	28	15		25	14	----------		
Li et al. [52]	22	3	0.40	7	10	----------	----------	----------

----- means not reported or analysed.

Table 19 – Reported elemental and material concentrations (mass %) in LIB modules samples (complete battery) [49].

Cathode		**NCA**	**LMO**	**NMC**	**LCO**	**LFP**
Metals	Al	22	22	23	5.2	6.5
	Co	2	0.0	8	17.3	0
	Cu	13	14	17	7.3	8.2
	Iron/Steel	0.1	0.1	9	16.5	43.2
	Li	1.9	1.4	1.3	2.0	1.2
	Mn	0.0	11	5.9	0	0
	Ni	12	0.0	15	1.2	0
Others	Binder	3.8	3.7	1.4	2.4	0.9
	Carbon (non-graphite)	2.4	2.3	3.5	6.0	2.3
	Electrolyte solvent	12	11.8	1.7	14.0	14.9
	Fluoride	------	---------	4.99	--------	----------
	Graphite	16.5	16.3	----------	23.1	13.0
	Thermal insulation	1.2	1.2	----------	--------	--------
	Oxygen	8.3	12.4	4.54	--------	--------
	Phosphorous	----------	----------	2.04	0	5.4
	Plastics	4.2	4.5	3.29	4.8	4.4

----- means not reported or analysed.

Appendix D

Uncertainty of the calculated weight of the aluminium and copper foil

In order to calculate the uncertainty of the weight of the aluminium and copper foil, it is necessary to first know the uncertainty of the density and volume. In the case of the uncertainty of copper's density, it is assumed that the value is 0 g/ cm^3 since the density found in the bibliography was always the same (8.96 g/cm^3). However, for the aluminium this value differs for each alloy and for that reason its uncertainty is ±0.1 g/cm^3.

Since the volume V can be calculated with equation (17) its variance σ_v^2 is given by equation (18).

$$V = W_{metal\_foil} \times L_{metal\_foil} \times \delta_{metal\_foil} \tag{17}$$

$$\sigma_v^2 = \left(\frac{\partial V}{\partial W}\right)^2 \sigma_W^2 + \left(\frac{\partial V}{\partial L}\right)^2 \sigma_L^2 + \left(\frac{\partial V}{\partial \delta}\right)^2 \sigma_\delta^2 \tag{18}$$

Where $\left(\frac{\partial V}{\partial W}\right)$ is the partial derivate of the volume with respect to the width of the metal foil;
σ_W is the uncertainty of the width of the metal foil [0.05 cm];
$\left(\frac{\partial V}{\partial L}\right)$ is the partial derivate of the volume with respect to the length of the metal foil;
σ_L is the uncertainty of the length of the metal foil [0.05 cm];
$\left(\frac{\partial V}{\partial \delta}\right)$ is the partial derivate of the volume with respect to the thickness of the metal foil;
σ_δ is the uncertainty of the thickness of the metal foil [0.0001 cm].

Replacing the values of equation (18):

$$\sigma_v^2 = 0.05^2(L\delta)^2 + 0.05^2(W\delta)^2 + 0.0001^2(WL)^2$$

$$\Longrightarrow \frac{\sigma_v^2}{V^2} = \frac{0.05^2(L\delta)^2 + 0.05^2(W\delta)^2 + 0.0001^2(WL)^2}{(WL\delta)^2}$$

$$\leftrightarrow \frac{\sigma_v^2}{V^2} = \frac{0.05^2}{W^2} + \frac{0.05^2}{L^2} + \frac{0.0001^2}{\delta^2}$$

Where W is 10.42 cm for the aluminium foil and 10.68 cm for the copper foil;
L is 429.70 cm for the aluminium foil and 438.67 cm for the copper foil;
δ is 0.0034 cm for the aluminium foil and 0.0021 cm for the copper foil.

Replacing the values, $\sqrt{\frac{\sigma_v^2}{V^2}}$ is 0.0298 cm^2 and 0.0478 cm^2 for aluminium and the copper foil, respectively.

Finally, since the mass m can be calculated with equation (19) its variance σ_{m}^2 is given by equation (20).

$$m = \rho V \tag{19}$$

$$\sigma_m^2 = \left(\frac{\partial m}{\partial \rho}\right)^2 \sigma_\rho^2 + \left(\frac{\partial m}{\partial V}\right)^2 \sigma_V^2 \quad (20)$$

Where $\left(\frac{\partial m}{\partial \rho}\right)$ is the partial derivate of the mass with respect to the density of aluminium or copper;

σ_ρ is the uncertainty of the density of aluminium [0.1 g/cm^2] or copper [0 g/cm^2]

$\left(\frac{\partial m}{\partial V}\right)$ is the partial derivate of the mass with respect to the volume of the metal foil;

σ_V is the uncertainty of the volume of the aluminium foil [0.0298 cm] or copper foil [0.0478 cm].

Replacing the values of equation (20) and dividing it by the mass:

$$\sigma_m^2 = V^2\sigma_\rho^2 + \rho^2\sigma_V^2$$

$$\Rightarrow \frac{\sigma_m^2}{m^2} = \frac{\sigma_\rho^2}{\rho^2} + \frac{\sigma_v^2}{V^2}$$

The uncertainty for both metal foils can be then calculated and it is 0.05 cm.